THE CREEP AND RUPTURE BEHAVIOR OF ALUMINUM AS A FUNCTION OF PURITY

By

Italo Salomone Servi

Dott. Università di Milano

1946

S. M. Massachusetts Institute of Technology

1949

Submitted in Partial Fulfillment of the

Requirements for the Degree of

DOCTOR OF SCIENCE

from the

Massachusetts Institute of Technology

1951

Signature of Author
Department of Metallurgy
January 6, 1951

Signature redacted

Signature of Professor
in Charge of Research

Signature redacted

Signature of Chairman
Department Committee
on Graduate Research

Signature redacted

TABLE OF CONTENTS

TABLE OF CONTENTS (CONT.)

LIST OF ILLUSTRATIONS

LIST OF ILLUSTRATIONS (CONT.)

LIST OF ILLUSTRATIONS (CONT).

LIST OF ILLUSTRATIONS (CONT.)

LIST OF ILLUSTRATIONS (CONT.)

LIST OF THE TABLES

ACKNOWLEDGMENTS

The author wishes to express his gratitude:

To Professor N. J. Grant, for suggesting the subject of research, for his assistance and moral encouragement during the course of the investigation; and for his fruitful discussion of the results and of the conclusions.

To the members of the High Temperature Laboratory for their helpful discussions.

To Mr. Edward La Rocca, for machining the creep specimens and part of the apparatus and for his assistance in assembling the creep test units.

To the Bureau of Ships for supporting this investigation.

To The Aluminum Company of America for their fine cooperation in furnishing a variety of materials and their spectrographical analyses.

1. INTRODUCTION

Creep may be defined as the deformation occurring under the combined effects of stress and time. During creep testing, temperature and applied load are generally kept constant. This is done in order to reproduce the conditions existing in many practical cases; as in the case of a gas turbine blade, which is under a centrifugal force at high temperature. Some testing is done at constant stress, to eliminate the effect of increasing stress as the cross section of the specimen decreases. The constant stress tests are more suitable for scientific investigations, the aim of which it is to find the effect of the variables involved in the creep process.

A considerable amount of data has been collected in the last fifty years; most of the data refer to complex alloys, which undergo several types of transformations during creep testing. Relatively little experimental work has been done to support the theories which have been suggested to explain the creep phenomenon. Although the results of these investigations cannot be used directly to develop complex creep-resistant alloys, several fundamental behaviors are established. For example, it was found that an increase in temperature has an effect analogous to a decrease in strain rate. It was also found that the grain boundaries play a very important role in the mechanism of creep at elevated temperatures.

The present investigation was undertaken to gain a better understanding of the creep process, using a set of experimental data which involve a minimum number of variables. To accomplish this purpose high purity aluminum was tested at constant stress over wide ranges of stress and temperature.

Aluminum was chosen because it has a rather low melting point and it

is available in high purity form. At high temperature it does not oxidize much in air since a thin, impervious oxide layer is formed. This layer is transparent and therefore does not hinder the observation of the metallic surface. The main structural instability that is ecountered during creep testing is a change of the grain size.

The aims of this thesis are:

(a) Demonstrate the behavior of simple, high purity aluminum in creep and stress rupture as a function of stress, temperature, strain rate and rupture time.

(b) Study the effect of grain size on the creep behavior of high purity aluminum.

(c) Study the effect of a change in impurity content on the rupture and creep behavior, on the ductility and on the mode of fracture of aluminum.

(d) Study the change in structure during creep and stress rupture tests, such as slip, sub-grain formation, grain growth, and grain boundary flow.

(e) Study the law or laws which govern primary creep.

2. SUMMARY

High purity, commercial 2S and 3S aluminum have been submitted to creep and stress rupture testing at several temperatures between 200° F and 1100° F, at several constant stress levels.

It was found that the primary creep follows Andrade's equation[5] better than Mott's[49] equation of "exhaustion" creep.

There is no linear relation between the applied stress and the logarithm of the minimum creep rate; therefore the Eyring[31] theory of rate process as applied to creep by Kauzman[32] and by Dushman et al[7], does not apply to creep and stress rupture if a wide range of strain rates and rupture times are investigated.

The stress dependence of the minimum creep rate at constant temperature is best expressed by a log-log plot of stress versus minimum creep rate. In the absence of structural instabilities such a plot gives linear relationship. A change in slope occurs at a series of transition points, which are located at lower stress and faster strain rates, the higher the testing temperature. The transition points correspond to the change from the "Low Temperature" to the "High Temperature" behavior of the materials. The slope of the straight lines of the plot Log. stress versus Log. minimum creep rate is greater the smaller the grain size. For constant grain size that slope is greater the higher the temperature.

The dependence of rupture time on stress at constant temperature is quite similar to the dependence of minimum creep rate. A series of transition points are observed in a log-log plot of stress versus rupture time.

As a first approximation the minimum creep rate is inversely proportional to the rupture time. This is especially true under "Low Temperature" conditions of testing.

The minimum creep rate of a fine grain high purity aluminum is smaller than the minimum creep rate of a coarse grain sample tested at the same stress in the "Low Temperature" region. The reverse is true in the "High Temperature" region.

As a first approximation the temperature, stress and strain rate at which the transition from "Low Temperature" to "High Temperature" occurs for high purity aluminum agree with the equation suggested by Mott[35] for the beginning of "grain boundary slip". The same is true for 2S aluminum if different values of the constants are used in Mott's equation.

In the absence of considerable grain growth during testing the relation between minimum creep rate and temperature at constant stress follows Boltzmann's equation:

$$\text{rate} = A\, e^{-Q/RT}$$

where T is the absolute temperature and A, Q, R are constants. The change from "Low Temperature" to "High Temperature" is not associated with a change of the temperature coefficient Q, at least within the limits of accuracy of the data.

The high purity aluminum samples fail in a ductile manner under any testing conditions. A single crystal at very high temperature fails by gliding. 2S and 3S aluminum samples fail in a ductile manner under low temperature testing conditions (below the equi-cohesive temperature.) Under high temperature conditions (above the equi-cohesive temperatures) the failure of 2S and 3S aluminum is brittle (intercrystalline). The transition from ductile

to brittle failure is gradual; the change is more marked for 3S than for 2S aluminum.

Grain boundary migration occurs during creep testing in high purity aluminum at high temperature conditions (above the equi-cohesive temperature).

Slip bands are observed in high purity, coarse grained samples under any testing conditions. As a first approximation, the spacing of the slip bands is inversely proportional to the applied stress. The constant of proportionality is much larger than the constant predicted by Orowan[43] for the minimum slip spacing, but is in better agreement with the experimental results of Yamaguchi[42].

A break-down of the grains into sub-grains was observed in high purity aluminum tested under high temperature conditions. The size of the sub-grains is of the same order of magnitude of the spacing between slip bands. The regularity and the direction of the sub-grain boundaries suggest a relation between the slip process and the formation of sub-grains.

The elongation of the specimen at the beginning of the third stage of creep ("true elongation[26]") is practically constant with decreasing creep rate for ductile specimens. For brittle specimens the true elongation decreases as the rupture time increases. Therefore a marked decrease in true elongation is noticed at the transition from "Low Temperature" to "High Temperature" behavior for 2S and 3S aluminum. This decrease in true elongation is more marked for 3S than for 2S aluminum.

Metallographic observations of the surface of deformed samples confirmed that the transition from low temperature to high temperature corresponds to the beginning of grain boundary flow. Observation of longitudinal sections of deformed samples showed that no cracking occurs at the grain

boundaries of high purity samples tested under any conditions. Cracking at the grain boundaries is noticed in 2S and 3S aluminum samples which were tested at "High Temperature".

"Slipless" flow was observed after high temperature testing only in the case of fine grained specimens, independently of the purity of the material. Observations of high purity aluminum samples indicate that "slipless" flow occurs when the grain size after testing is smaller than the slip spacing which can be observed in coarser grained specimens tested under similar conditions.

The creep and rupture behavior of 2S and 3S aluminum is quite similar to the behavior of the complex cobalt-base alloys which have been investigated by Grant and Bucklin[26]. The main difference consists of the fact that certain instabilities such as overaging and oxidation do not affect the creep and rupture behavior of aluminum even at very high temperatures.

The different behavior of high purity aluminum, as far as ductility and mode of fracture are concerned, clearly shows the effect of impurities on the creep and rupture properties of metals.

It may be assumed that at constant strain rate the strength of the grain boundaries has a temperature coefficient which is different from the temperature coefficient of the grains. Under certain conditions of temperature and strain rate the strength of the grain and the strength of the grain boundaries are the same. These conditions correspond to the transition from low temperature to high temperature behavior. At faster strain rate, or at lower temperature the grain boundary is stronger than the grain. The reverse is true at slower strain rate or higher temperature.

3. PREVIOUS INVESTIGATIONS

Creep and stress rupture tests date back over a century. In 1883 Thurston[1] conducted stress rupture tests on iron at room temperature. He mentioned a similar experiment done by Vicat "half a century ago". Howe[2] first determined the shape of a creep curve in 1885. In 1904 Trouton and Rankine[3] suggested a logarithmic relation between creep relaxation and time. One year later Phillips[4] first mentioned the word "creep". In 1910 Andrade[5] discovered his famous equation for primary creep, which has been recognized valid for pure metals up to now. He was the first to perform constant stress tests.

Engineering interest in the creep phenomenon started much later, when McVetty[6] suggested a method for extrapolation of creep data. Since then, many contributions to the understanding of the creep process have been made, both from the empirical and the theoretical viewpoints. It is impossible to give a detailed summary of the existing literature on this subject. The survey of the previous investigations will be limited to results concerning aluminum, and to the current theories of the mechanism of creep as affected by temperature, strain rate, and purity.

Very few data have been published, concerning creep rates and rupture times of aluminum. Information on creep rates of high purity aluminum at constant stress have been given by Dushman et al[7], who tested wires in a rather limited range of temperatures and strain rates. For 2S aluminum, data have been obtained by Sherby[8], who studied the effect of grain size on the creep rates. Sherby conducted constant load tests from 90° F to 400° F. Dorn and Tietz[9] studied the creep and stress rupture properties of 3S aluminum over a wide range of rupture times: however, the temperature range was limited to 90° F to 400° F.

The limited amount of information reported above cannot be directly compared with the results of this research since the purity, the grain size, the type of sample and the method of testing were different.

Qualitative studies of the mechanism of creep for aluminum have been done at a larger extent. Hanson and Wheeler[10] observed the behavior of 99.6 percent aluminum (2S) at different temperatures and strain rates by microscopical examination of polished samples. According to Hanson and Wheeler, under suitable conditions (high temperature and slow strain rate) no signs of slip bands appear on the surface of the polycrystalline sample. The grain boundaries are developed by straining, although no cracks are opened during the earlier stage of deformation. As the deformation proceeds, cracks open at the grain boundaries and the sample fails by intercrystalline cracking. If the temperature is lower, or the strain rate is faster, the slip bands are visible and the failure is transgranular. Single crystals deform and fail by shear along slip planes at all temperatures.

More recently Wood et al.[11, 12, 13] found that at elevated temperature the grains of aluminum break down into "cells", which slightly change their orientation during deformation. A more detailed report on this subject will be made later (see: Experimental results, Part B).

Creep testing of aluminum by torsion at constant stress was done by Ke[14]. Important results were obtained that are concerned with the viscous behavior of the grain boundaries. However these results cannot be directly compared with the others mentioned above, since they have been obtained at a very low stress level, where the plastic deformation is completely recoverable (anelastic behavior).

Electron microscope research by Heidenreich and Shockley[15] has demonstrated that each "slip band" of deformed aluminum consists of many slip lines. The distance between the slip lines is constant, while the distance between slip bands, and the number of planes in each band is not constant. Brown[16] indicated that this is true up to 500° C, and that the distance between slip bands is a function of the temperature. The specimens observed by Brown were deformed by compression without controlling the amount of deformation and the applied stress. The change in slip band spacing and thickness as a function of the temperature was recognized previously by Crussard[60].

The function of the grain boundaries in high-temperature creep has long been recognized since Jeffries[17] suggested the existance of an "equi-cohesive temperature" at which the strength of the grain is equal to the strength of the grain boundary. Jeffries found that the faster the strain rate, the higher the equi-cohesive temperature. If the Jeffries' theory is correct one should expect that a fine grained material is more creep resistant than a coarse grained material below the equi-cohesive temperature. The reverse should be true above that temperature. The study of the effect of grain size on the creep rates is very limited. The first publication, by Clark and White[18] is still one of the best. Hanffstengel and Hanemann[19] found that when the creep rate is plotted versus the stress for fine grained and coarse grained lead at 25° C, two intersecting curves are obtained. Hanson[20] first suggested the existance of an "optimum grain size" for best creep resistance of tin. Parker and Riisness[21] suggested that the number of grains per cross section and not the absolute grain size determines the creep resistance. A study of the distribution of

stresses between the grains and the grain boundaries was done by Siegfried[22] who found that the Jeffries' theory is correct. Sully[23], working on McKeown[24] data for lead, found that the creep resistance is a function of the ratio "grain boundary surface to grain boundary volume". He concluded that the creep resistance at elevated temperatures increases continuously, as the grain size increases, without passing through a maximum as suggested by Hanson[20] and by Crussard[25].

The contribution of the grain boundaries to the flow of metals at elevated temperatures has also been recognized in complex alloys. It was found that at elevated temperatures a material fails along the grain boundaries with very little ductility; while at lower temperatures the same material deforms and fails in a ductile manner. Grant and Bucklin[26] studied this phenomenon on cobalt-base alloys. They also found that the transition from the "low-temperature" (ductile) to the "high-temperature" (brittle) behavior of those alloys corresponds to a change in slope of the curves obtained by plotting the logarithm of the applied stress versus the logarithm of the minimum creep rate or versus the logarithm of the rupture time. Grant and Bucklin also found a marked decrease in the "true elongation[26]" at the transition points mentioned above.

4. PLAN OF WORK

The plan of work is summarized as follows:

(a) Building the apparatus: An apparatus was designed to perform tensile creep testing from room temperature to 1300° F at constant load or at constant stress up to 100 percent elongation, under a maximum applied load of 300 pounds.

(b) Preparation of the samples: Preliminary heat treatments were planned to develop the most suitable structure. The actual preparation of the samples involved machining, heat treating, and finishing. The dimensions of each sample were determined after the finishing operation.

(c) Creep testing:

(i) Preliminary tests: The purpose of the preliminary tests was to determine the order of magnitude of the stress levels to be investigated; and to test the apparatus. Minor alterations were made on the apparatus after these tests.

(ii) "Standard" tests: creep testing was planned for four types of samples:

1. High purity aluminum (99.995%), coarse grained
2. High purity aluminum, fine grained
3. 2S aluminum (99.3%)
4. 3S aluminum (98.2%)

During the test the elongation was measured as a function of time; and the appearance of the sample was observed through a viewing window.

(iii) Special tests: A few special tests were planned to study the behavior of special types of samples, such as single crystals or samples having mixed grain size.

(d) Examination of the samples: it was planned to examine each sample after creep testing, both on the surface and on a cross or longitudinal section.

(e) Determination of the minimum creep rate and correlation of the data: The minimum creep rate was determined from the creep curves and the following data were correlated and compared with the results of previous investigations: temperature, stress, minimum creep rate, rupture time, total elongation, elongation at the beginning of the third stage of creep ("true elongation"), coefficient of primary creep, temperature coefficient of secondary creep.

5. DESCRIPTION OF APPARATUS AND MATERIALS USED

5.1 Apparatus

The apparatus consisted of two creep testing units which were provided with a loading beam of ratio 3 to 1. A constant stress system was introduced, in this apparatus: a detailed description of the constant stress system appears in Appendix I.

The elongation was recorded by reading a dial gage, having a one inch travel. 1/1000 inch was read directly on the dial, and 2/10000inch was read by interpolation. The main spring was removed from the gage to avoid the effect of non-axial stresses. The gage was fastened to the frame: a balanced arm was secured to the upper specimen holder. One end of this arm held a polished magnet, which was touching the head of the gage shaft. Using this set-up the elongation has been measured without disturbing the specimen at all.

Two tubular furnaces were used: one was platinum wound and was capable to reach very high temperatures; the other was nichrome wound and was used for the lower temperatures. Each furnace was provided with a 1/2 inch viewing window, which permitted the examination of the specimen during testing.

The temperature was controlled by one thermocouple, which was touching the upper part of the specimen. A description of the method of calibration of the controlling thermocouple is shown in Appendix II.

The sequence of the operations is summarized as follows:

(a) The sample was placed in the apparatus and heated.

(b) The sample was loaded about 30 minutes after it came to temperature. The loading time was less then ten seconds for most of the tests. The loading time was increased up to two minutes for very fast tests at the lower temperatures.

(c) The creep curves were determined by reading the dial gage periodically.

(d) After failure the specimen was removed and quenched within two minutes. A few tests were not conducted to completion, but the "third stage" was always reached before interrupting the test.

(e) The final length of the cold specimen was determined. The sample was used for metallographic examination.

The determination of the accuracy of the data cannot be done for sure, but an order of magnitude can be ascertained. The temperature gradient and control were kept within ± 3° F. The minimum weight necessary to unbalance the beam corresponded to an applied stress of 5 psi. The determination of the stress was done within ± 1.5 percent. The absolute measurement of the elongation was probably done within ± 1/100 of an inch, since the elongation on loading includes the yielding of the threads and other foreign factors. However, once an arbitrary "zero" was established after loading, the measurement of the subsequent elongation was done within ± 1/1000 of an inch. This value includes the error due to expansion or contraction of the frame and of the holders as the room temperature changes.

A few experiments were duplicated to test for reproducibility. The reproducibility of the minimum creep rates was within 10 percent. Very fast tests at the lower temperatures showed a poorer reproducibility.

5.2 Materials

Three grades of aluminum were tested:

(a) High Purity (99.995% aluminum)

(b) 2 S (99.3% aluminum)

(c) 3 S (98.2% aluminum)

The spectrographical analyses of these materials is reported in Table I.

TABLE I

Spectrographical Analysis of the Impurities Contained in the Three Grades of Aluminum Used for Creep and Stress Rupture Testing*

Type of Aluminum	Impurities (percent)									
	Cu	Fe	Si	Mn	Mg	Zn	Cr	Ti	Pb, Ni, Bi, B	Na, Ca
High Purity	0.0017	0.002	0.001		0.0002					0.0006
2 S	0.11	0.47	0.12	0.01	0.00	0.01	0.00	0.03	0.00	
	0.10	0.46	0.12	0.01	0.00	0.01	0.00	0.03	0.00	
3 S	0.09	0.37	0.16	1.15	0.00	0.01	0.01	0.01	0.00	
	0.09	0.36	0.16	1.15	0.00	0.01	0.01	0.01	0.00	

* The three grades of aluminum and their spectrographical analyses were furnished by the Aluminum Company of America.

The conditions of the materials both "as received" and after heat treatment are listed in Table II.

The microstructures of the 2S and 2S aluminum after heat treatment are presented in Figure 1, Figure 2, and Figure 3. The samples were machined from the "as received" rods: the gage length of the samples was 1 ± 0.2 inch: the diameter of the straight portion of the sample was about 0.162 inch.

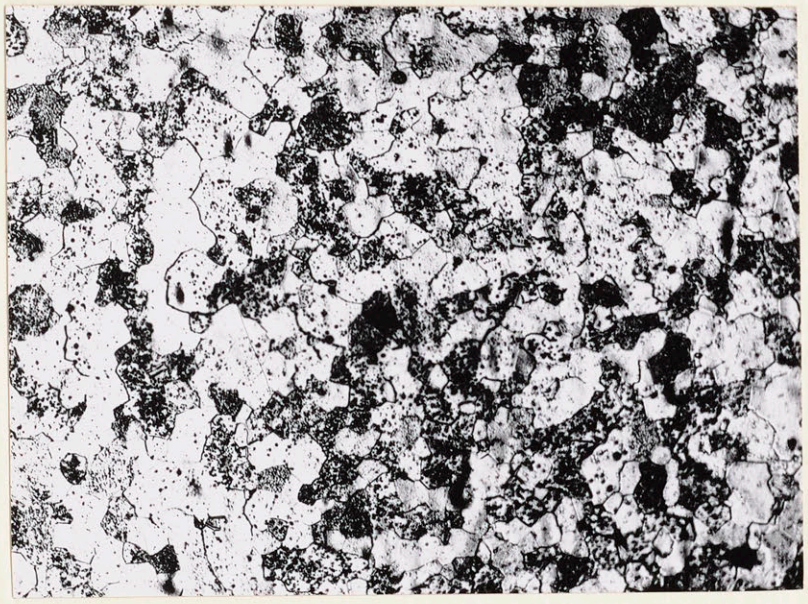

Figure 1. Microstructure of 2S aluminum, after a 3-hour annealing treatment at 1000° F. Cross section. Electrolytic polish and etch. 150 ×.

TABLE II

Data on Aluminum Used in Test Program

Material	"As received"			Heat Treatment		After Heat Treatment	
						Grain Size (mm.)	
	Shape	Temper.	Grain Size	Temp. ° F	Time Hr.	Cross Section	Longitudinal Section
High purity, Coarse grained*	3/8 in. rod	-	1000 grains per cu. mm.	650	0.5	0.05	0.05
High purity, Fine grained*	3/8 in. rod	-	1000 grains per cu. mm.	650 1000	0.5 0.5	1 to 3 (20 to 30 grains per cross section)	1 to 3
2 S	5/16 in. rod	H-18	-	1000	3	0.02 to 0.03	0.02 to 0.03
3 S	3/8 in.	F	-	1000	3	0.05 to 0.1	0.1 to 0.4

* The terms "fine grained" and "coarse grained" refer to the grain size of the sample before testing.

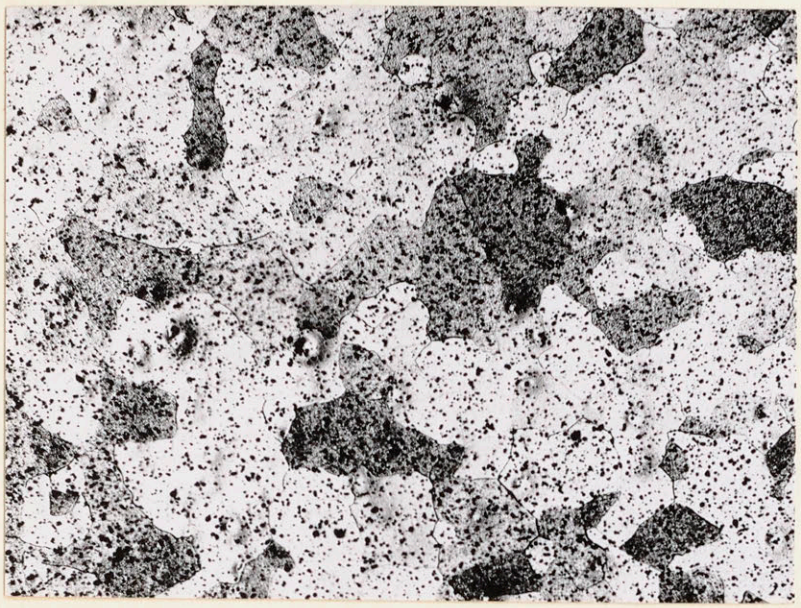

Figure 2. Microstructure of 3 S aluminum after a 3-hour annealing treatment at 1000° F - Cross Section of the bar Electrolytic polish and etch 100 ×

Figure 3. Microstructure of 3 S aluminum after a 3-hour annealing treatment at 1000° F - Longitudinal Section of the bar Electrolytic polish and etch 100 ×

After machining, the straight portion of each sample was polished with 3/0 metallographic paper, coated with paraffin. Final heat treatments were then done in an air furnace. The samples were cooled in air and electropolished in an acetic-perchloric mixture. Details concerning the electropolishing and electroetching techniques are reported in Appendix III.

Figure 4 shows two "coarse grained, high purity" samples. One has been macroetched to reveal the structure. The other is electropolished. All the "standard" tests were conducted using electropolished specimens.

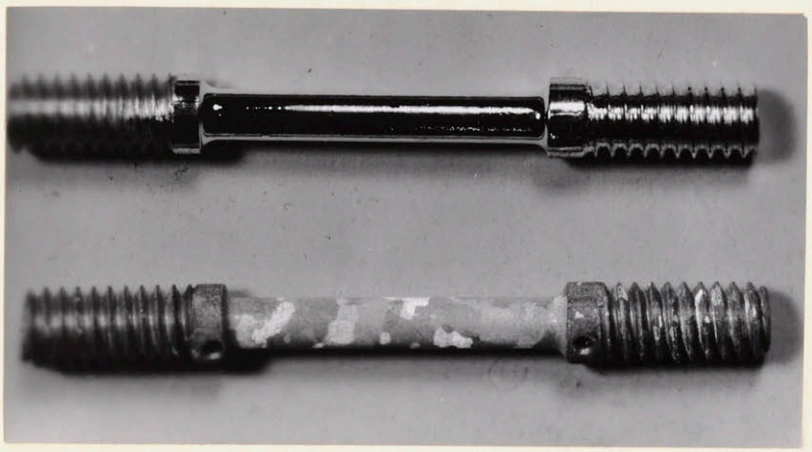

Figure 4. High Purity, Coarse Grained Aluminum Specimens: Above: after electrolytic polishing.
Below: after macroetching in HCl.

6. DETAILED REPORT OF THE EXPERIMENTAL WORK DONE

Part A - Mechanical Testing

6.1 The Rupture and Creep Tests

When the elongation of a tensile specimen under a constant load is plotted versus the time, a typical well-known "creep curve" is obtained. During the earlier part of the test the elongation rate decreases (first stage, or primary creep). Later the elongation rate is practically constant (second stage, or minimum creep rate). Finally there is a period, during which the rate of elongation increases up to the rupture of the sample (third stage creep).

Andrade[5] showed that at constant stress the third stage creep is absent for lead. A similar result was obtained for high purity aluminum. Figure 5 shows a creep curve obtained at constant load; and a creep curve obtained at constant stress, under similar conditions of temperature and initial stress. The "third stage" does not appear in the constant stress curve, since the test was not conducted to completion. The third stage, which is always present for tests reaching failure, is due to a stress intensification. In the case of ductile specimens the stress intensification begins when the sample starts "necking". In the case of brittle specimens the stress intensification is caused by the presence of intercrystalline cracks. In Figure 6, the creep curve obtained for a ductile specimen (test No. 34) is compared to the creep curve obtained for a brittle specimen (test No. 305). The lower curve also shows that the primary stage cannot be detected using the scales of this plot; the apparent absence of the primary stage was often noted at the higher temperatures.

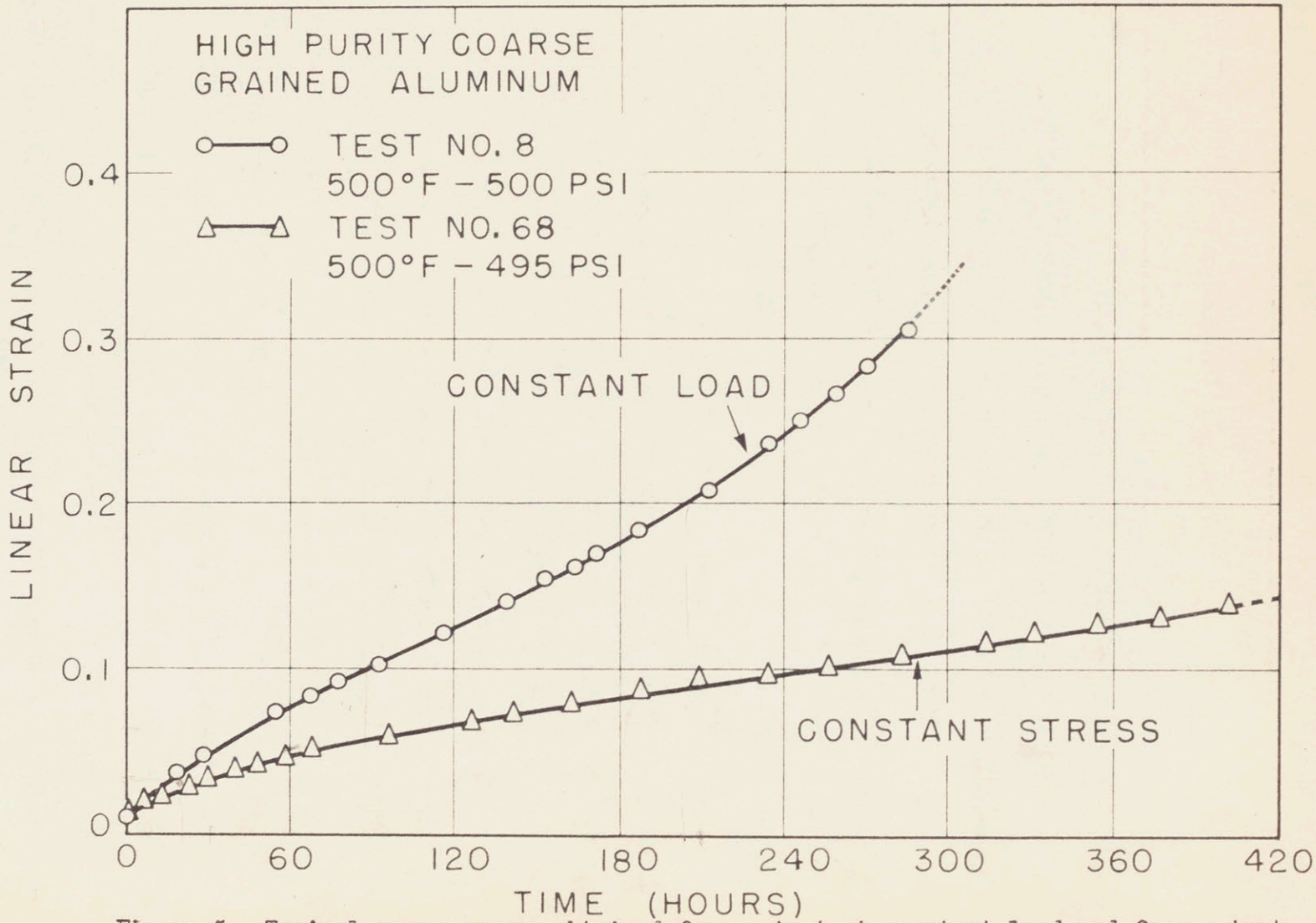

Figure 5. Typical creep curves obtained from a test at constant load and from a test at constant stress.

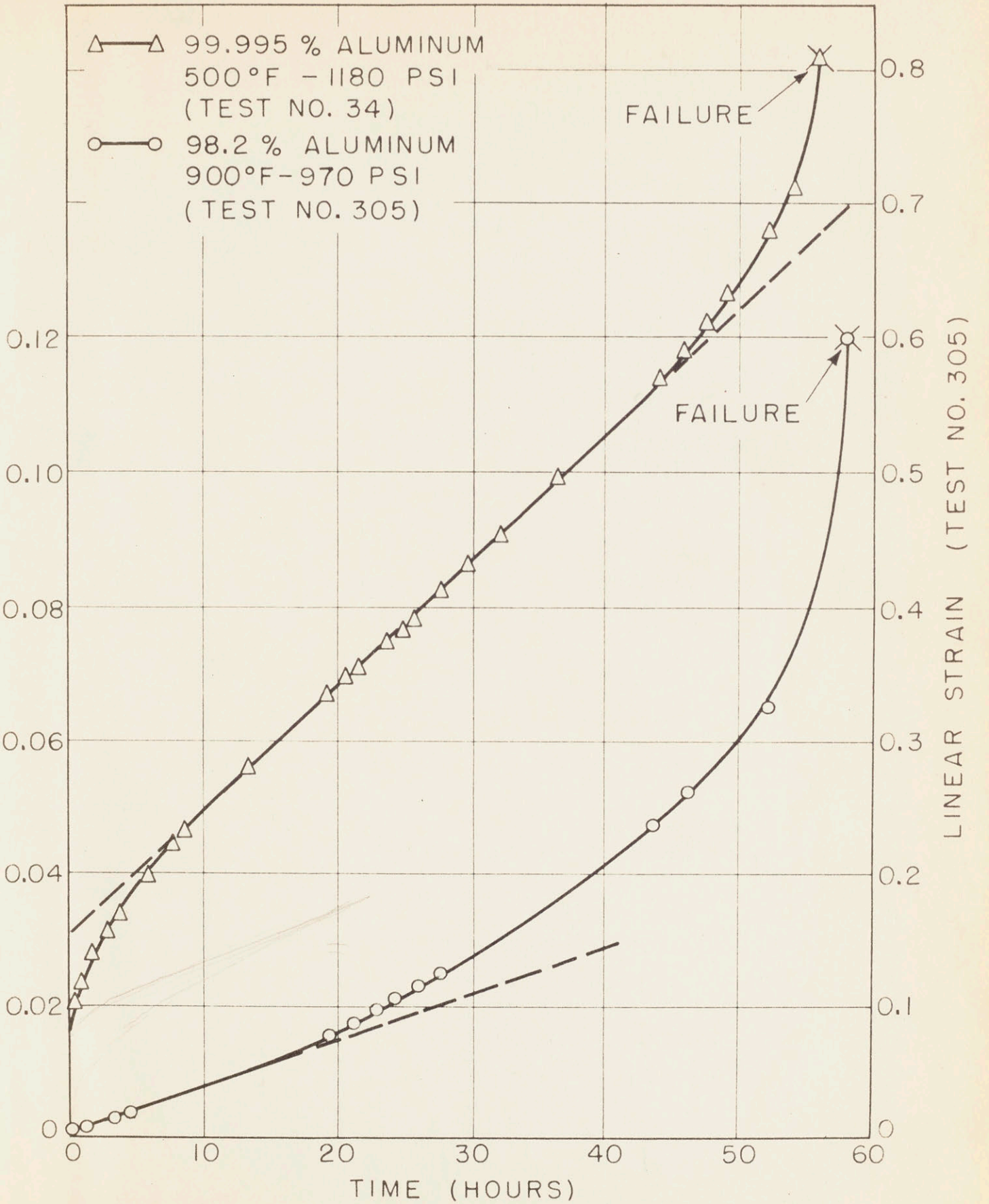

Figure 6. Typical creep curves for a ductile and a brittle specimen.

The creep curves reported above were obtained by plotting the linear strain versus the time, on linear graph paper. The linear strain is defined as $\frac{\Delta \ell}{\ell_o}$

where $\Delta \ell$ is the elongation and ℓ_o is the initial length.

Since the total elongation of aluminum during creep testing is considerable (10 to 110%), there is a marked difference between linear strain and "true" strain. The true strain is defined as

$$\ln \frac{\ell}{\ell_o}$$

and is practically equal to the linear strain when the elongation is small.

In Figure 7 both the linear and the true strains have been plotted versus the time, using the data from the same creep test. Although there is a shift in the position of the curves, the shape of the creep curves is substantially the same. Similar results were obtained in other cases; accordingly, the calculation of the true strain was not extended to all the tests in utilizing the data. Linear strain was plotted versus time in all the cases, and the slope of the "secondary stage" was determined. This was called "Minimum Creep Rate" when referred to a one-inch initial gage length.

Generally the second stage of creep was long enough to permit a very close determination of the minimum creep rate. The largest uncertainity in the determination of the minimum slope of the creep curves was about 2 percent.

It has been said that all the curves can be divided in three stages, and the first stage was more or less pronounced according to the conditions of the experiments. An exception was observed in the behavior of a single crystal of high purity aluminum which gave the typical creep curve presented in Figure 8.

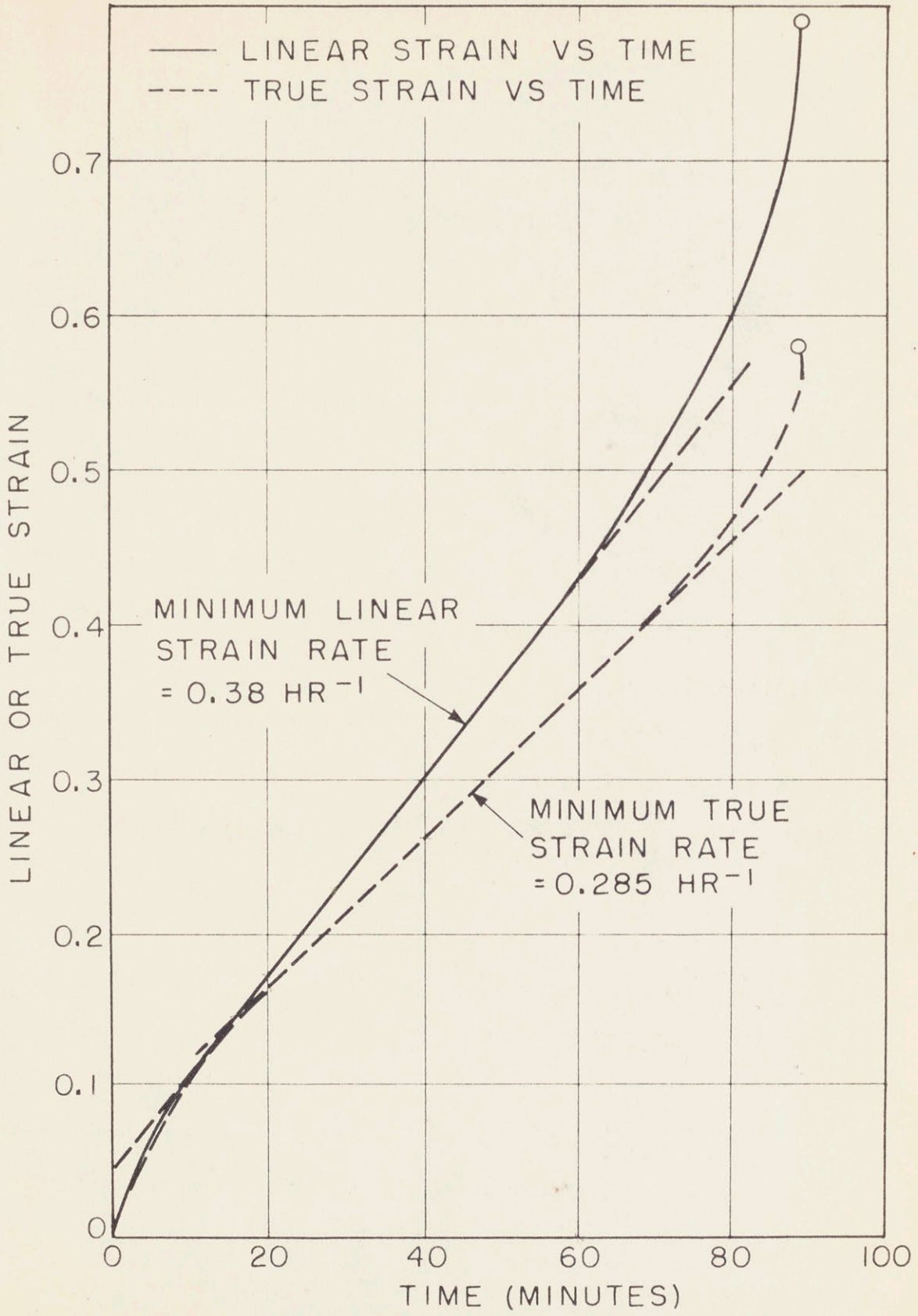

Figure 7. Typical creep curves obtained by plotting linear and true strain versus time.

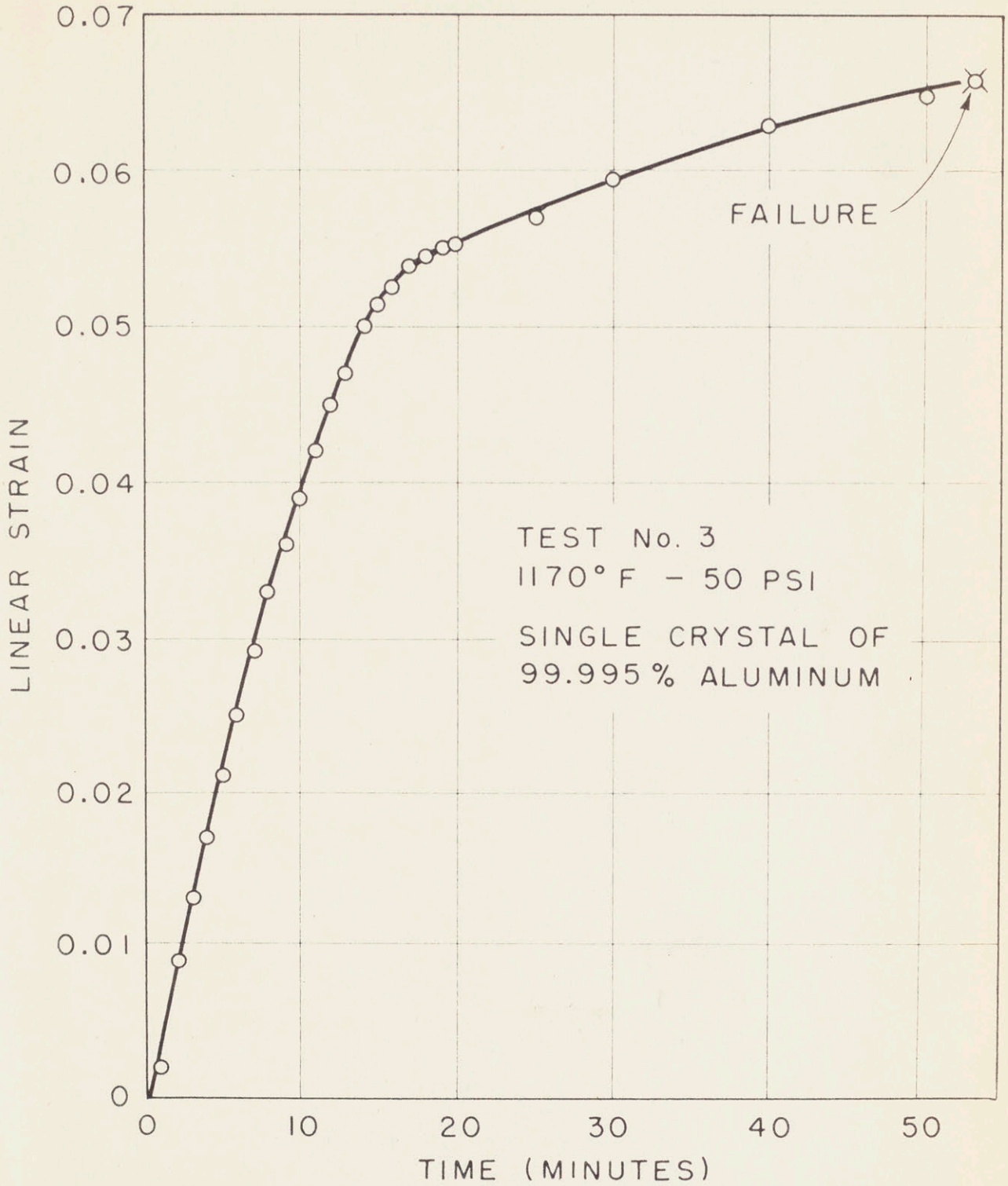

Figure 8. Typical creep curve for a single crystal specimen.

6.2 Study of Primary Creep

The study of primary creep was not planned as one of the primary aims of this thesis. The data are not sufficient to test the validity of the different theories of primary creep; however, enough information was obtained to study the trend of the creep curves during the first stage.

Andrade[5] found that the creep curves of pure metals follow the equation

$$\ell = \ell_0 (1 + \beta t^{1/3}) e^{Kt} \tag{6.21}$$

where ℓ is the length of the specimen at the time t; and ℓ_0 is a constant which is not much different from the initial length. β is the "coefficient" of transient creep" and K is the "coefficient of steady state creep". From formula (6.21) it follows that

$$\ln \frac{\ell}{\ell_0} = \ln (1 + \beta t^{1/3}) + kt \tag{6.22}$$

The true strain at any time can be divided into two parts. The quantity $\ln (1 + \beta t^{1/3})$ is the contribution of the transient creep; the amount kt is the contribution of the steady state creep. When $\beta t^{1/3}$ is small, $\ln (1 + \beta t^{1/3}) \simeq \beta t^{1/3}$. Assuming that the constant ℓ_0 is equal to the initial length of the specimen, for small elongations $\ln \frac{\ell}{\ell_0} \simeq \frac{\Delta \ell}{\ell_0}$ and therefore

$$\Delta \ell = \beta t^{1/3} + Kt \tag{6.23}$$

in the case the initial length is one unit.

At the beginning of the deformation the contribution of the transient creep is much larger than the contribution of the steady state creep. The reverse is true after longer times. Therefore for shorter times

$$\Delta \ell \simeq \beta t^{1/3} \tag{6.24}$$

and for longer times

$$\Delta \ell \simeq Kt \tag{6.25}$$

The second portion (6.25) was found to be true in all the cases; the coefficient k has the same value and meaning of the "minimum creep rate". The first portion (6.24) can be verified by plotting the elongation versus the cubic root of the time. This has been done for several specimens at different stress and temperature conditions. A typical example of the results is presented in Figure 9, where the initial parts of the creep curves of high purity aluminum at 500° F (coarse grained) have been plotted in the form linear strain versus cubic root of the time.

The plot of Figure 9 shows that straight lines are obtained; the slope of these lines increases for longer times. This was expected, since the contribution of the steady state creep becomes appreciable at longer times. The curves obtained at the lower stress levels show an anomalous "transient", which is in disagreement with Andrade's formula. This transient was indeed observed, to a minor extent, by examining the linear creep curves: an example is given in Figure 10. It was not possible to ascertain whether this anamolous transient stage is a property of the material or an effect due to the inertia of the testing machine.

The crossing of several curves of Figure 9 is due to the uncertainity in the determination of the initial elongation after loading, as mentioned before. The intercepts of the curves at zero time are not exact, since the loading time was not sufficiently constant.

The slopes of the straight lines of Figure 9 was determined and called the "β coefficient". The logarithm of the stress was plotted versus the logarithm of the "β coefficient" in Figure 11 and a straight line was obtained.

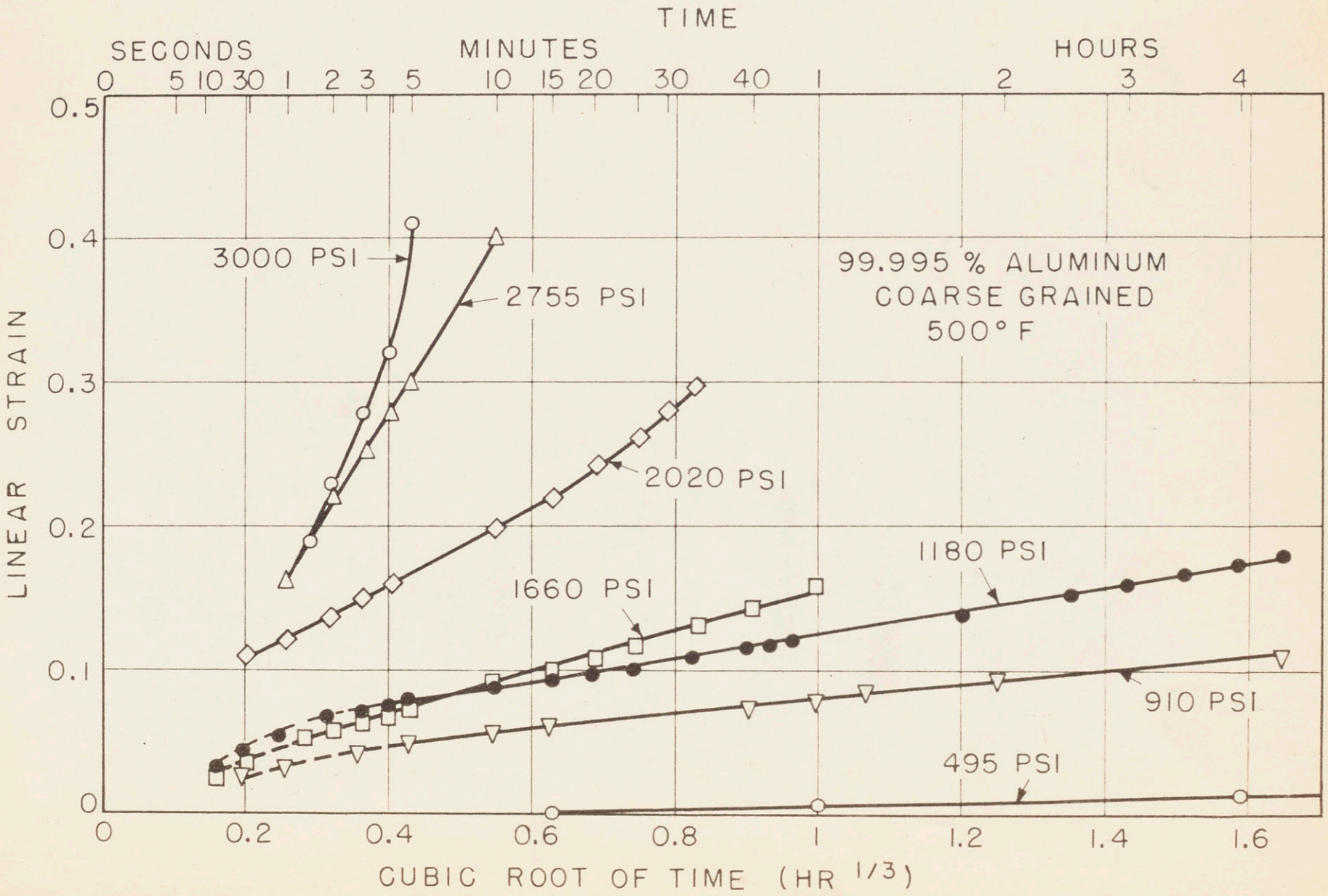

Figure 9. Plot of linear strain rate versus cubic root of time. High purity coarse grained aluminum tested at 500° F.

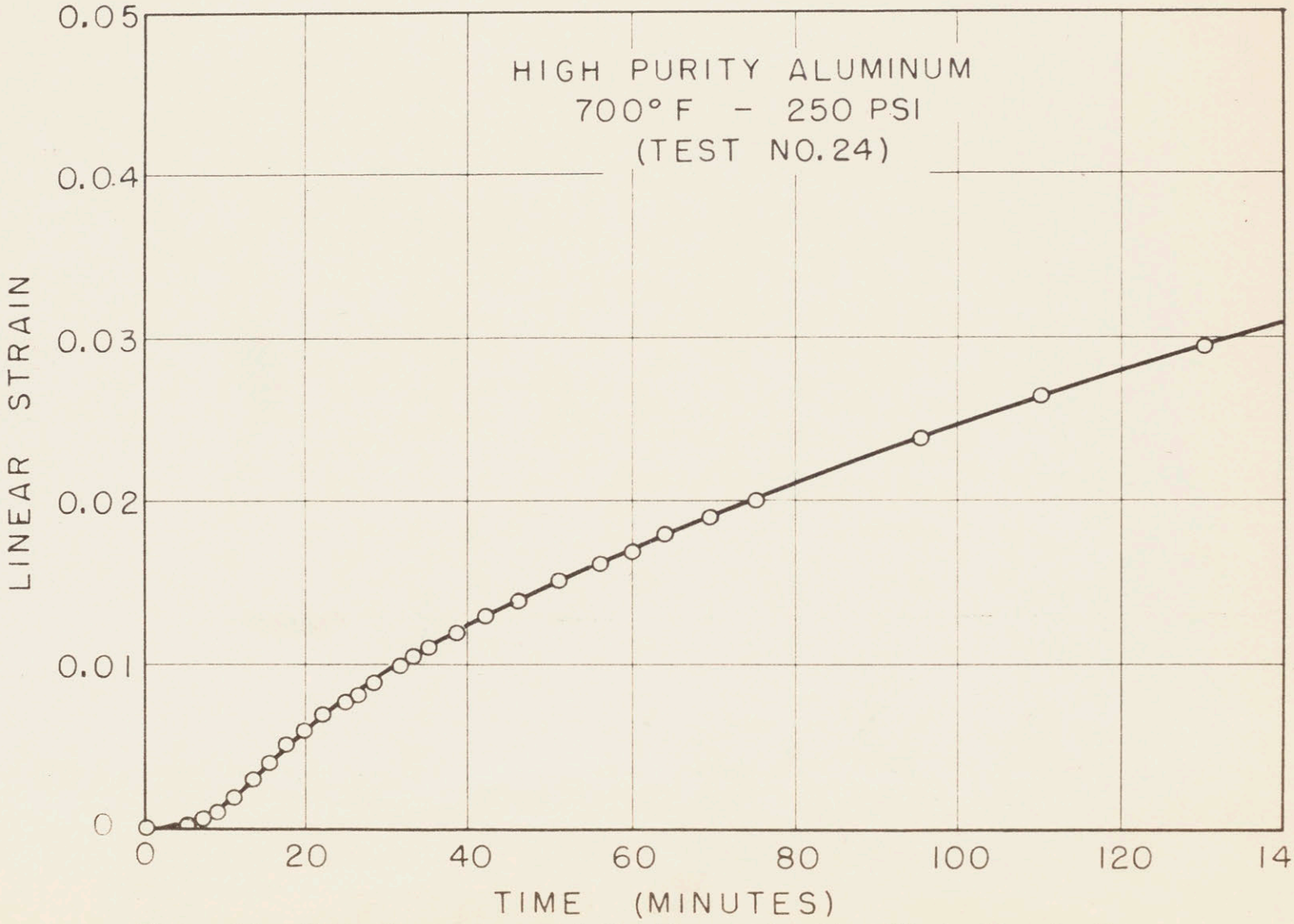

Figure 10. Typical creep curve indicating an inertia effect after loading.

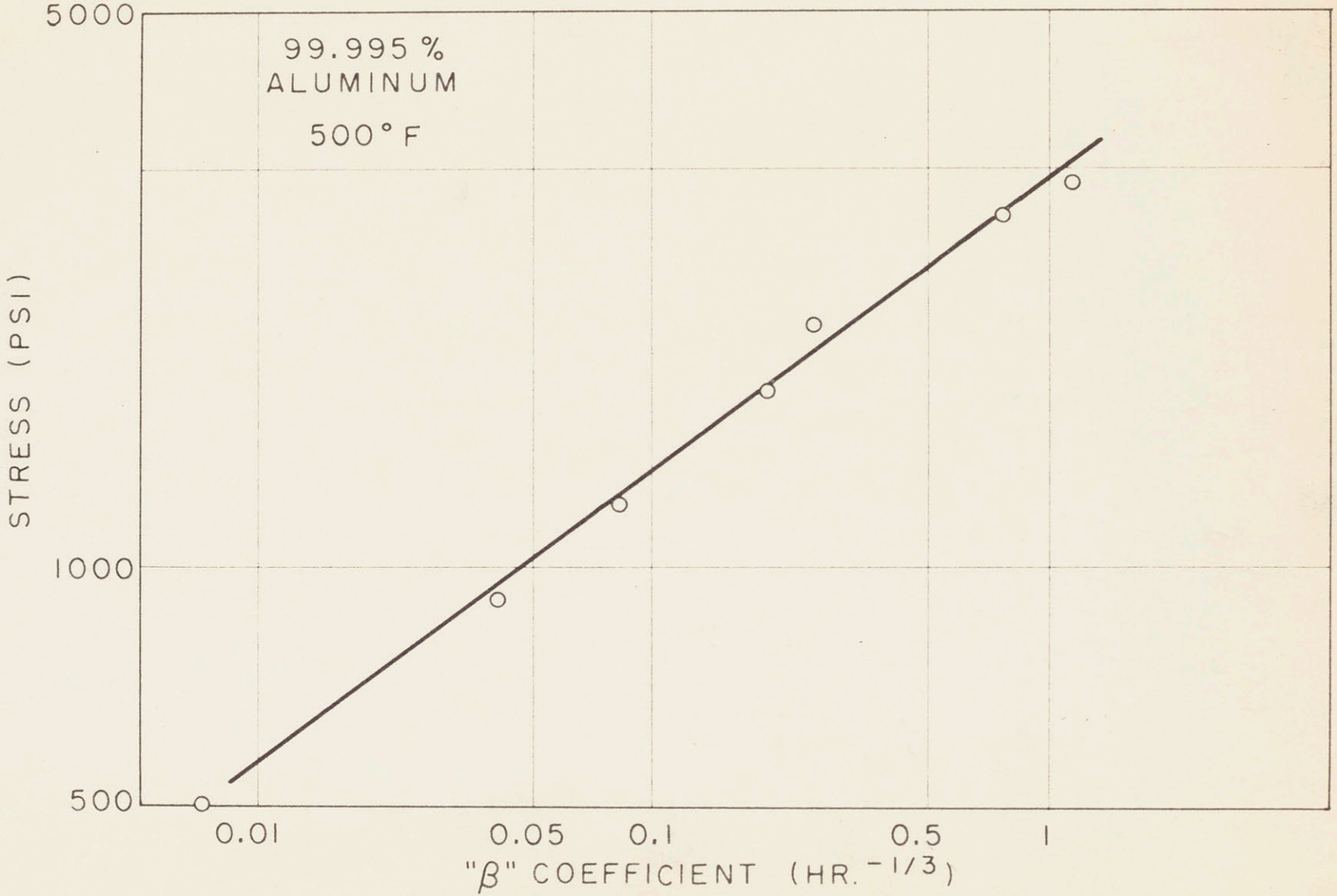

Figure 11. Log-log plot of stress versus β coefficient of primary creep. High purity coarse grained aluminum tested at 500° F.

It should be understood that the graphical determination of the "β coefficient" involves many assumptions and therefore is not as accurate as the determinations of the minimum creep rate. Further speculation on this topic is not likely to be constructive, lacking more accurate data on primary creep.

Similar results were obtained when the true strain was substituted for the linear strain in the analysis mentioned above.

A few creep curves were plotted in other non-conventional ways. When the logarithm of the strain was plotted versus the logarithm of the time, a curve of increasing slope was always obtained. This result suggests that the relation

$$\text{strain} = A\, t^{B} \tag{6.26}$$

does not apply to high purity aluminum at constant stress. Equation (6.26) was found to be valid for pure nickel by Carreker and Hollomon[27].

In another attempt at studying primary creep, the strain was plotted versus the logarithm of the time for a series of tests: the slopes of the curves increase as the time increases. This result suggests that the law

$$\text{strain} = A + B \ln t \tag{6.27}$$

does not apply to the primary creep of the materials investigated. Equation (6.27) is similar to the equation given by Mott[28] for the "exhaustion" primary creep.

6.3 Stress Dependence of Minimum Creep Rate at Constant Temperature

6.31 Semi-log Dependence

Since the earliest times, in the study of creep, investigators have sought a simple relationship describing the stress dependence of the minimum creep rate at constant temperature. Ludwick[29] proposed an empirical formula of the type

$$r = A\, e^{Bs} \tag{6.31}$$

where r is the minimum creep rate, s is the applied stress and A, B are constants. According to this formula a straight line should be obtained when the applied stress is plotted versus the logarithm of the minimum creep rate. Bailey[30] suggested a formula of the type:

$$r = A\, s^{B} \tag{6.32}$$

according to which a stright line should be obtained when the logarithm of the applied stress is plotted versus the logarithm of the minimum creep rate. Bailey's formula is not supported by theoretical considerations. On the other hand, Ludwick's formula is in agreement with Eyring's theory of activated complex[31], as demonstrated by Kauzmann[32] and by Dushman et al[7].

According to this theory, the rate of shear is proportional to the rate at which an hypothetical "unit of flow" crosses a free energy barrier. Assuming that the free energy barrier is a function of the applied stress, and introducing several simplifying assumptions, the following equation is obtained:

$$r = M\, e^{-\Delta F/RT} \sinh (Ns) \tag{6.33}$$

where r = minimum creep rate

s = applied stress

T = absolute temperature

ΔF = Free energy of activation

R = gas constant per mole

M, N = constants, at constant temperature.

When (Ns) is large, $\sinh Ns \simeq \frac{e^{(Ns)}}{2}$ and

$$\text{Log. } r = \text{Log } r_o + P\, s; \qquad (6.34)$$

where r_o and P are constants at constant temperature.

Equation (6.34) is of the same form as Ludwick's equation. Creep rate data by Grant and Bucklin[26], obtained by testing cobalt base alloys, have been analyzed[33] to test the above theory for validity. It was shown that, when the stress is plotted versus the logarithm of the minimum creep rate at constant temperature a straight line is not observed if sufficient data are available over a wide range of creep rates. If the data are restricted to a very narrow range of strain rates, the theory of activated complex can be applied, at least as a first approximation.

The analysis mentioned above[33] also showed that straight lines are obtained when the logarithm of the stress is plotted versus the logarithm of the minimum creep rate, in the case that the same mechanism of deformation and fracture prevails. The approximate relationship:

$$\text{Log. } r = a + (b/T - c)\ (\text{Log. } s - d) \qquad (6.35)$$

was suggested to express the temperature and stress dependence of the minimum creep rate, with the understanding that this empirical equation is not to be regarded as a true "mechanical equation of state".

In order to verify whether Eyring's theory can be applied to an extensive amount of data obtained for a pure material, the stress was plotted versus the logarithm of the minimum creep rate for high purity, coarse grained aluminum (solid lines of Figure 12). The "straight lines" obtained

by Dushman et al.[7] for a similar material were also included on the same plot (dotted lines of Figure 12). Figure 12 shows that straight lines are not obtained over a wide range of creep rates although they may, erroneously, be assumed to exist in such a limited range of minimum creep rates as the range investigated by Dushman et al[7]. The trend of the semi-log curves is quite similar to the trend observed for complex cobalt-base alloys[26].

The solid curves plotted in Figure 12, even on careful inspection, do not indicate any discontinuous change in the stress dependence of the minimum creep rates as structural instabilities occur in the material. For instance, the marked grain growth which has been found to take place at 900° F and 1100° F is not revealed by any change in shape or slope of the semi-log curves. On the other hand, the log-log plot of the same data points out this instability very clearly as shown below.

6.32 Log-Log Dependence

6.321 High Purity Aluminum:

The Log-Log dependence of the minimum creep rate on the applied stress was verified by plotting the logarithm of the stress versus the logarithm of the minimum creep rate. Figure 13 presents the results for high purity aluminum. The solid lines represent the behavior of the coarse grained samples; straight lines are observed at all the temperatures. However, a sharp change in the slope of the lines is observed very clearly at 500° F, and less clearly at 400° F and 700° F. These "breaks" determine three "transition points" A, B, and C. Metallographic studies showed that appreciable grain growth occurs at 700° F, and very extensive grain growth at 900° F and 1100° F. At the two higher temperatures the grain growth is such that the results can be hardly compared

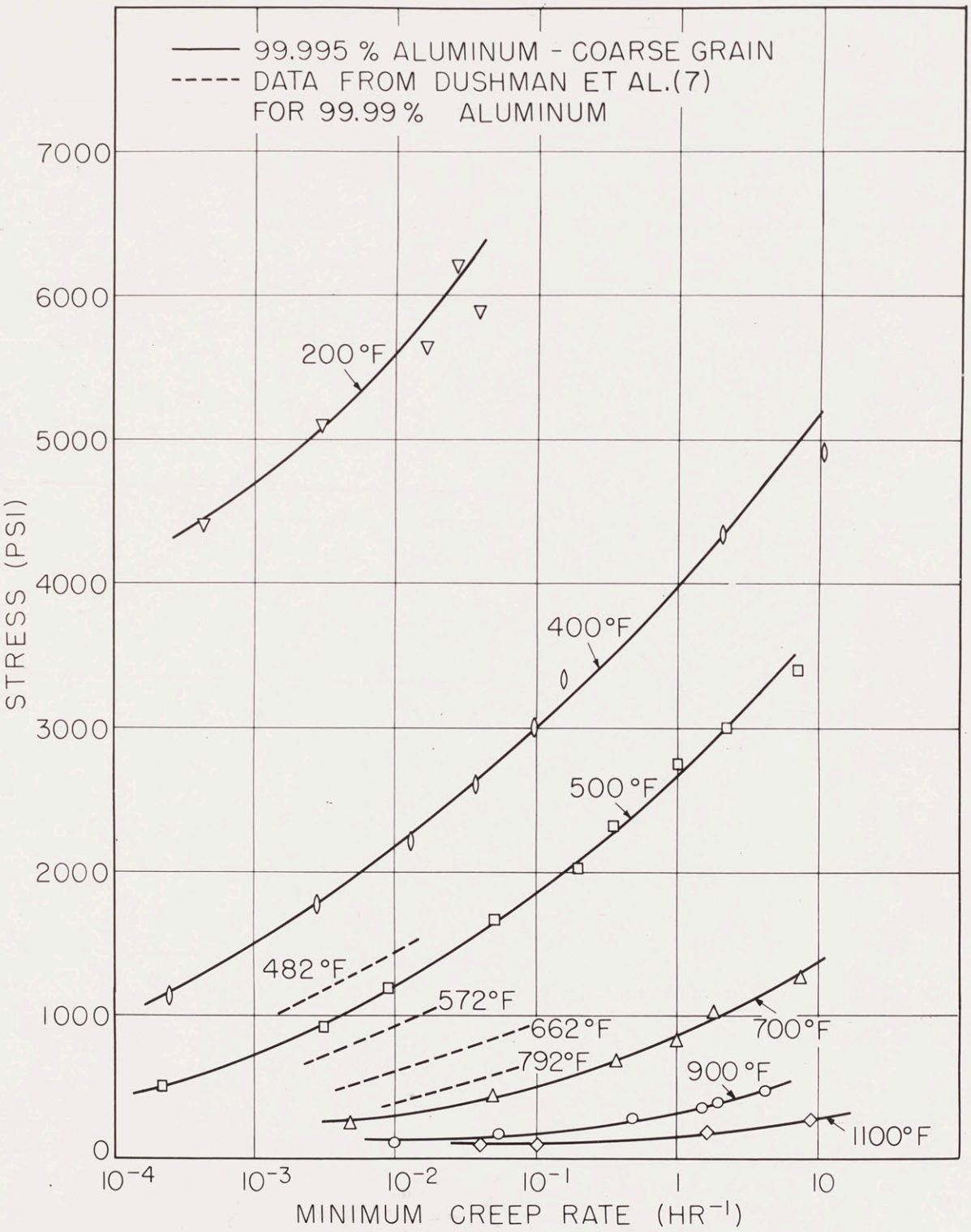

Figure 12. Semi-log plot of stress versus minimum creep rate. High purity coarse grained aluminum.

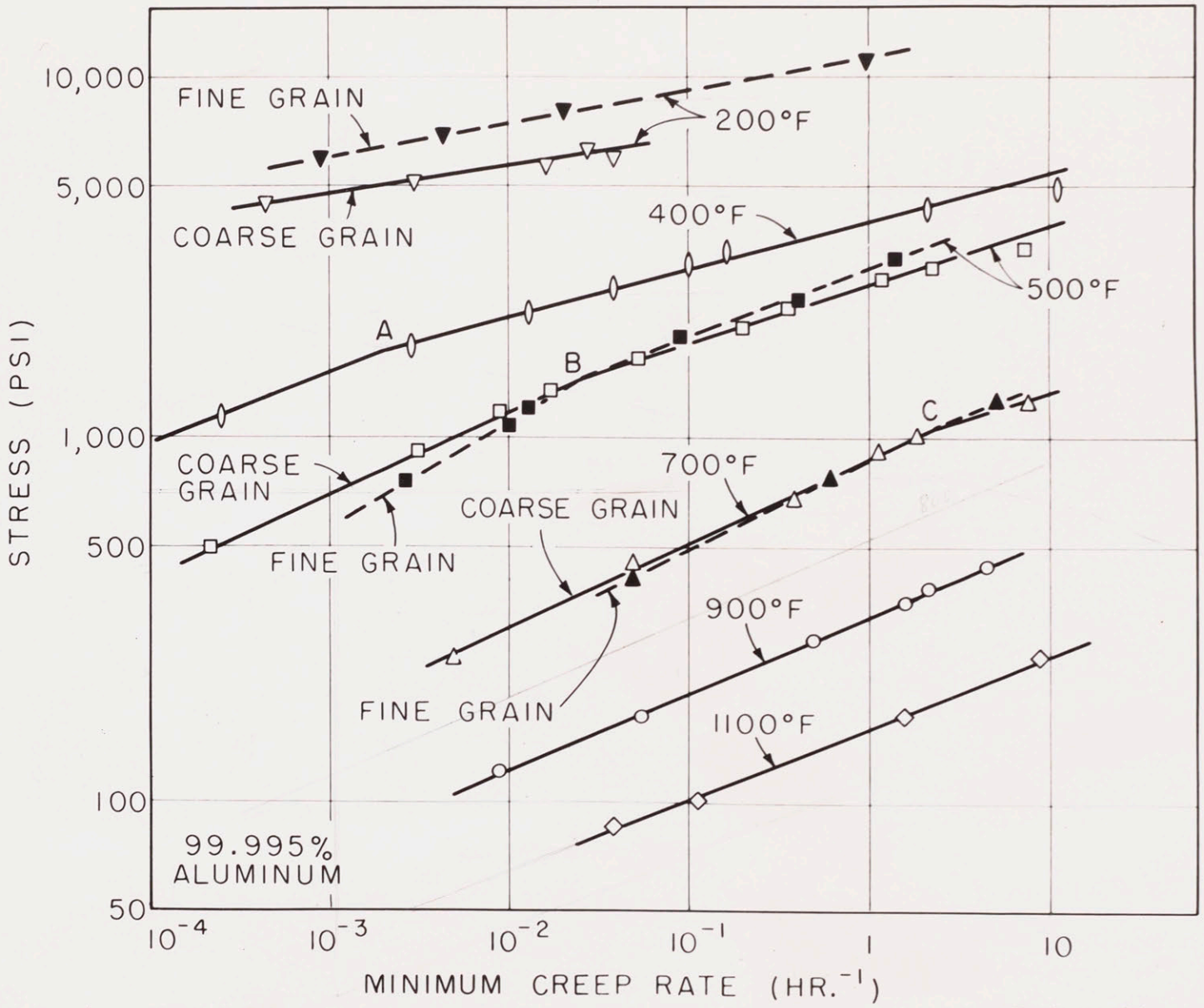

Figure 13. Log-log plot of stress versus minimum creep rate. High purity coarse and fine grained aluminum.

with the results obtained at the lower temperatures. Figure 14 shows the structures of three samples after testing at 900° F and 1100° F. It is noticed that some grains now occupy the whole cross section of the specimen.

The fracture of all the samples was typically ductile; although the shape of the rupture zone changed with the conditions of testing. A detailed discussion of the change in slope of the curves of Figure 13 will be made later when the photomicrographs of several samples will be presented. It is assumed for the present that the metallographic research showed that the transition A-B-C of Figure 13 corresponds to a transition in the mode of deformation of the samples. In the region above the line A-B-C the grain boundaries appear to be stronger than the grains; they do not give any contribution to the deformation of the sample and hinder the deformation of the grains.

Figure 14. Left to Right: Specimens No. 45, No. 74 and No. 76 after testing (respectively, 900° F and 0.11 hrs. rupture time; 900° F and 6.7 hrs; 1100° F and 0.31 hrs.) "Galvanic" etch in HCl.

Below the line A-B-C the grain boundaries are weaker than the grains; they contribute to the initial deformation of the specimen and do not hinder the deformation of the grains.

The region above the line A-B-C is associated with the "Low Temperature Behavior" of the material while the region below that line is associated with the "High Temperature Behavior" of the material.

Figure 15 shows the appearance of three specimens tested at 500° F. Specimen No. 63 (Rupture Time = 0.05 hours) shows "Low Temperature" behavior; the grain boundaries resist deformation more than the grains and form grain boundary "crests" from which the deformed grains slope down. Specimen No. 68 (interrupted after 500 hours) shows "High Temperature" behavior; the grain boundary flow which occurs during the test causes step formation on the polished surface, therefore the grain boundaries appear "thicker" under the microscope and appear shining to the unaided eye. Specimen No. 34 (Rupture Time = 56.25 hours) belongs to the "Transition" region, and has an intermediate behavior.

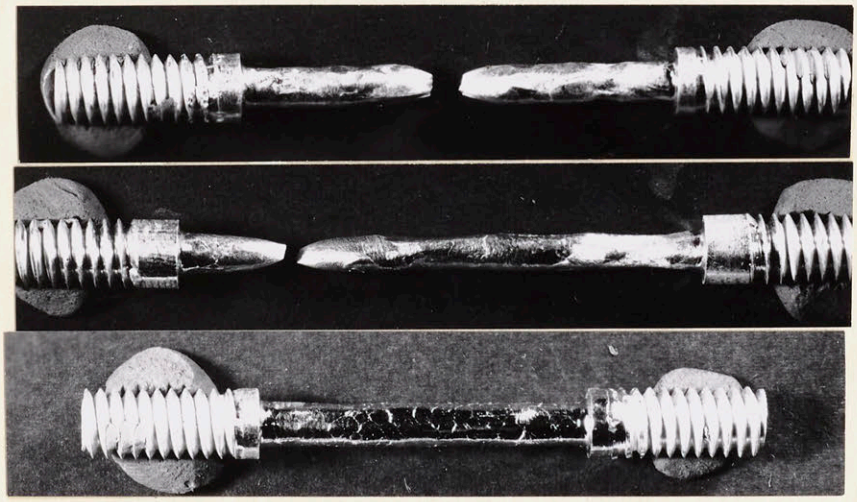

Figure 15. Top to bottom: Specimen No. 63 (Rupture time = 0.05 hours); No. 34 (56.25 hours); No. 68 (interrupted after 500 hours); tested at 500° F. Unetched.

The dotted lines of Figure 13 represent the behavior of the fine grained, high purity aluminum. The fine grained material is stronger than the coarse grained material in the "Low Temperature" region, while the reverse is true in the "High Temperature Region". This behavior is unmistakably noticed at 200° F and at 500° F. Not much difference in the creep rates is noticed at 700° F, since the fine grained samples are not stable at this temperature. A considerable amount of grain growth occurs in the sample before and during testing; therefore the difference in final grain size between "coarse grained" and "fine grained" specimens is not as large as after testing at 500° F.

In order to demonstrate that the use of linear strains instead of true strains does not affect the final results on this analysis, a series of creep rate data have been replotted in Figure 16; the logarithm of the stress has been plotted versus the logarithm of the minimum linear strain rate (minimum creep rate) and versus the logarithm of the minimum true strain rate. A straight line relationship was obtained in both cases, resulting only in a small shift in the curve.

6.322 Commercial 2S and 3S Aluminum:

The logarithm of the stress was plotted versus the logarithm of the minimum creep rate for 2S and 3S aluminum in Figure 17. A change in slope of the straight lines occurs at the points D, E, F, and G for the 2S aluminum; and at the point M for the 3S aluminum. It may be observed that a continuous straight line could be drawn at 700° F. Although this behavior has not been investigated thoroughly, it is believed that the anomalous behavior is due to some aging effect. In fact the creep

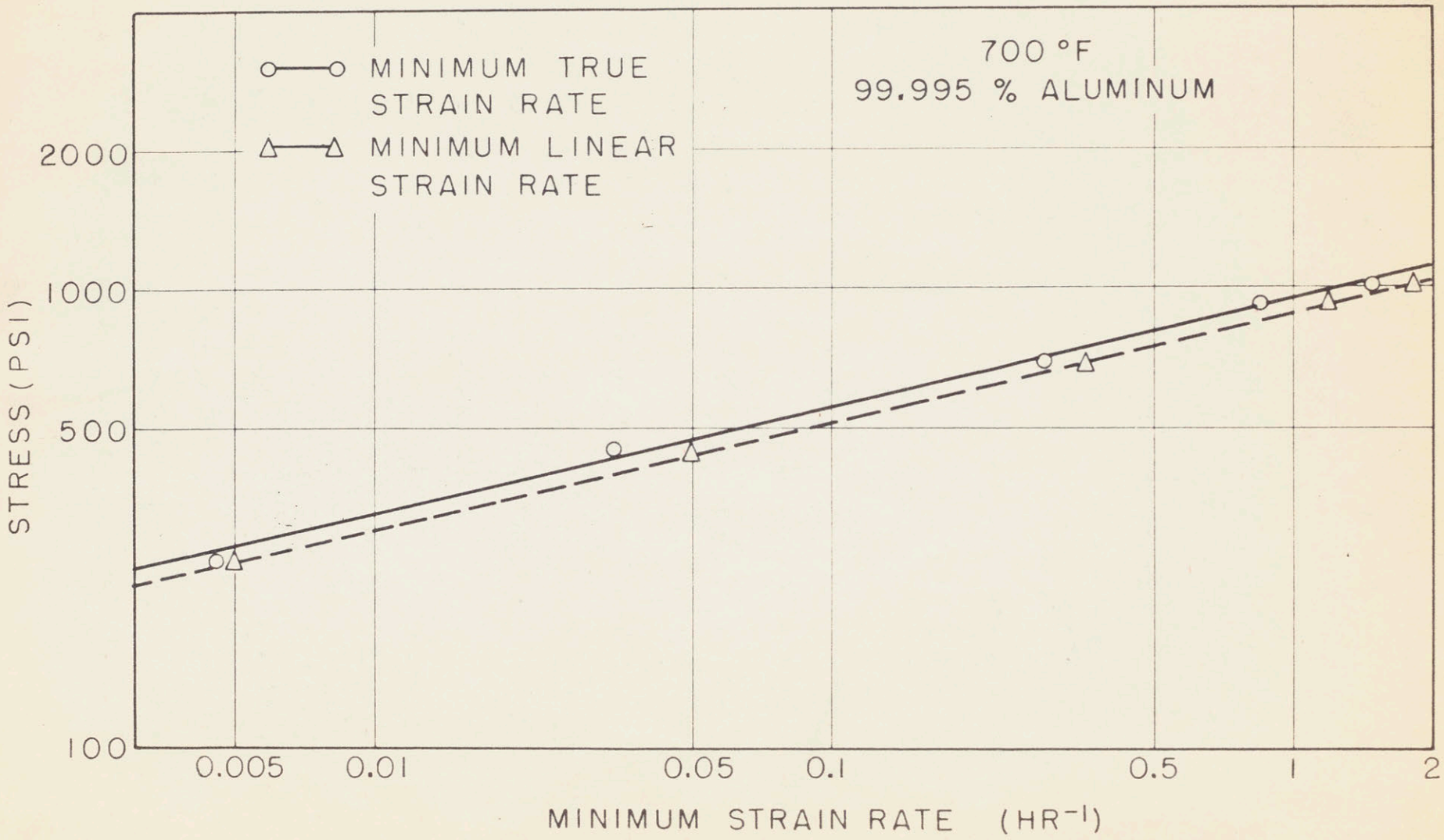

Figure 16. Log-log plot of stress versus minimum linear strain rate and versus minimum true strain rate. High purity coarse grained aluminum tested at 700° F.

curves show that very little primary creep occurs at 700° F up to a rupture time of about 20 hours. If the duration of the test is longer than 20 hours, the creep rate decreases markedly with time. Obviously in this case the primary stage of creep is not due to a strain hardening effect otherwise it would be more pronounced in faster tests than in slower tests.

The hypothesis that some aging occurs in those conditions was also supported by Brinnell hardness measurements of 2S aluminum which was tested at 700° F by Gervais. According to Gervais[34] the hardness of the specimens which had a rupture life longer than 20 hours is a few points higher than in the case of rupture life shorter than 20 hours. This was true in spite of the fact that the amount of strain was smaller for the specimen which had a longer rupture life.

The region above the "transition zone" D-E-F-G of Figure 17 may be called the "Low Temperature Region" and it is characterized by a ductile type of fracture. The region below the zone D-E-F-G is the "High Temperature Region" and it is characterized by the intercrystalline (brittle) type of fracture. The same change in the mode of failure is observed for the 3S aluminum at the transition point M.

The change in type of failure is gradual: in the "Low Temperature" region, necking occurs and the specimen fails by drawing down to a point. In the "High Temperature" region the diameter remains practically uniform and many intercrystalline cracks are present. In the "Transition" region there is a combination of necking and intercrystalline fracture. A demonstration of the transition from "ductile" to "brittle" type of fracture is shown in Figure 18 and Figure 19 for 2S aluminum; and in

Figure 20 for 3S aluminum. It is noticed that the change in type of fracture is sharper for the more impure 3S aluminum, than for the 2S aluminum. No brittle fracture was observed in high purity aluminum specimens.

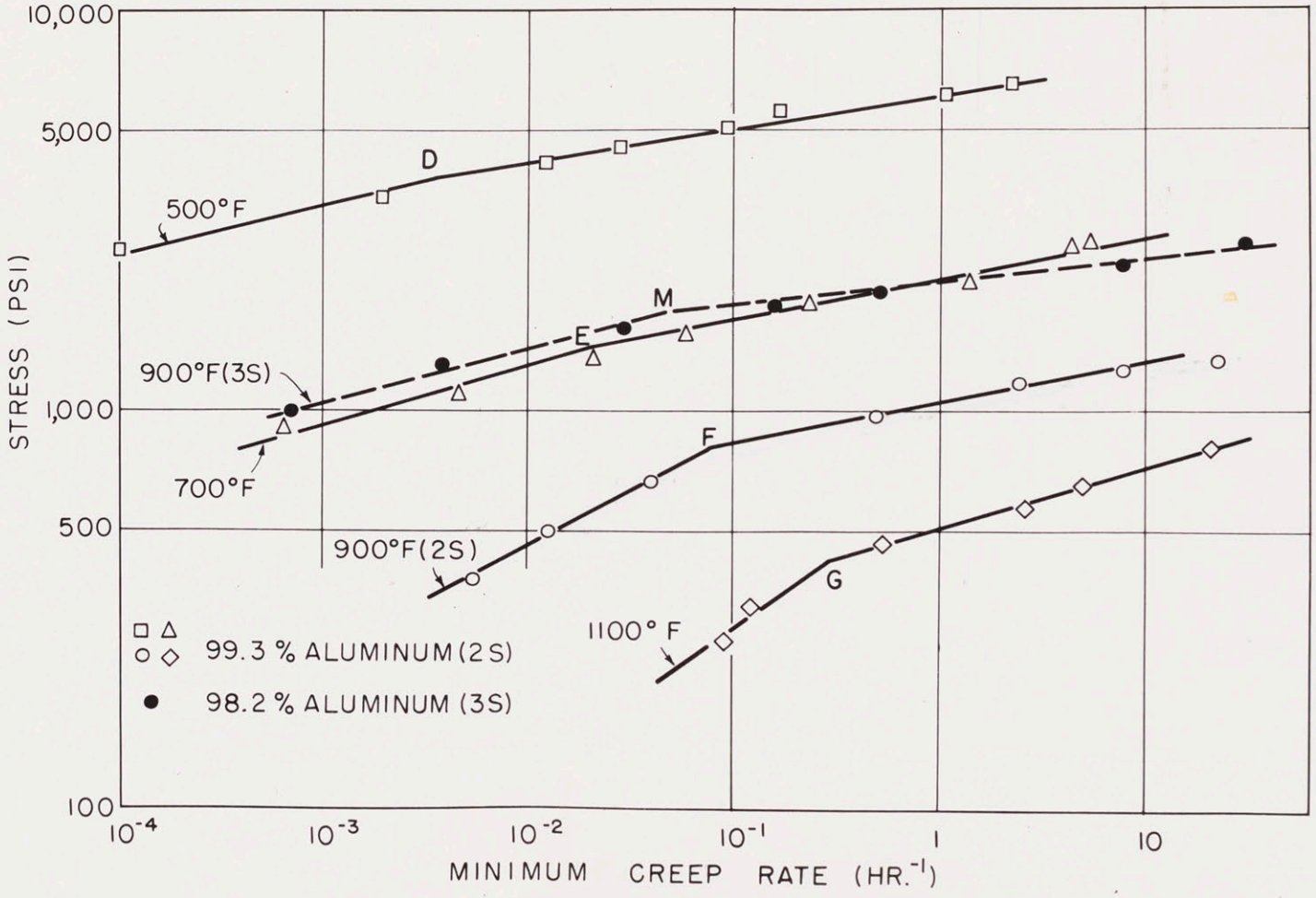

Figure 17. Log-log plot of stress versus minimum creep rate, 2S and 3S aluminum.

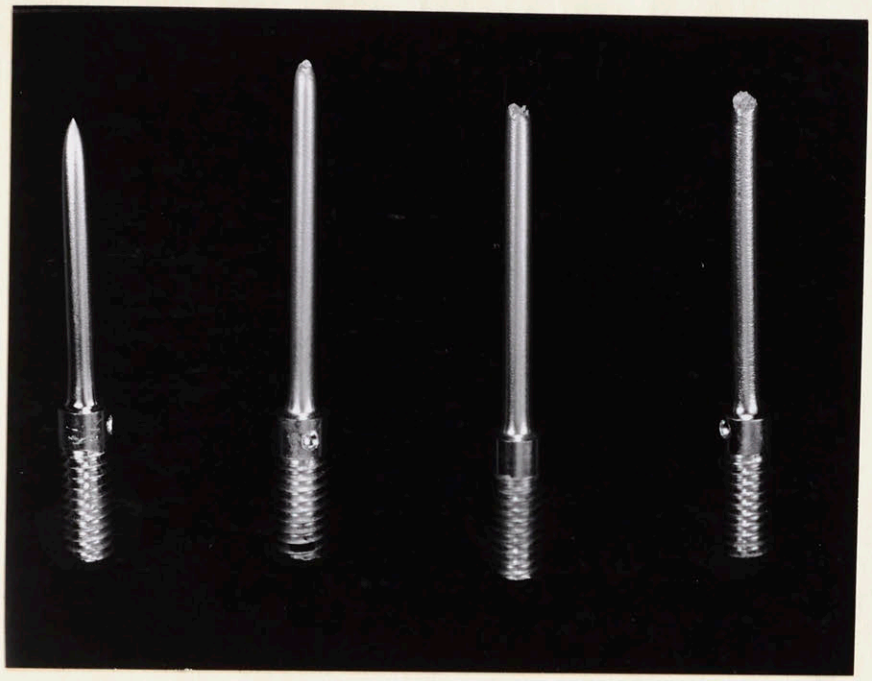

Figure 18. Transition from ductile to brittle fracture as the rupture time increases. 2S aluminum tested at 900° F; left to right: specimen No. 212 (rupture time = 0.02 hrs.); No. 207 (18.4 hrs.); No. 221 (41.5 hrs.); No. 213 (81.5 hrs.).

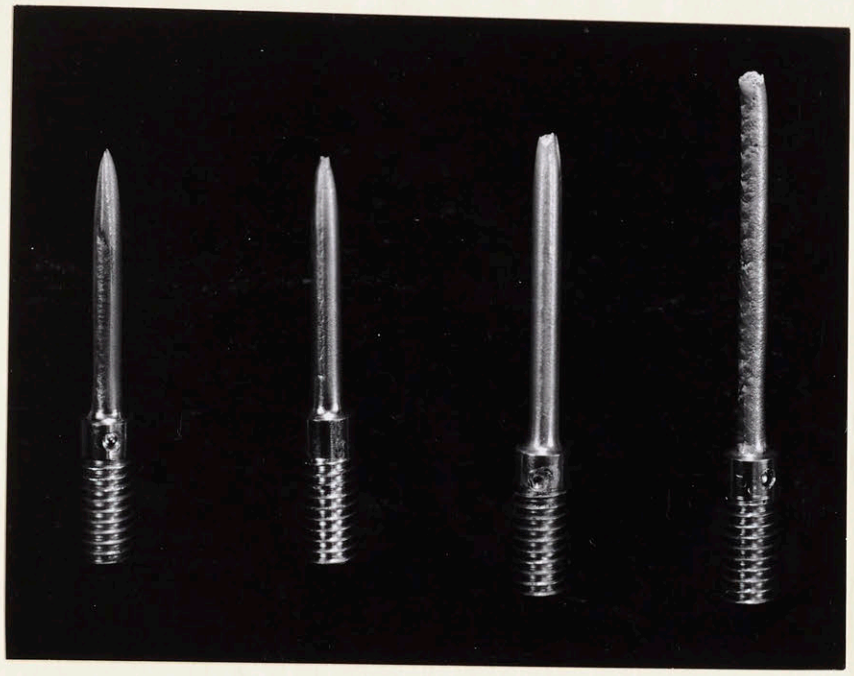

Figure 19. Transition from ductile to brittle fracture as the rupture time increases. 2S aluminum tested at 1100° F. Left to right: specimen No. 224 (rupture time = 0.023 hrs.) No. 232 (0.14 hrs.); No. 225 (0.93 hrs.); No. 226 (13 hrs.)

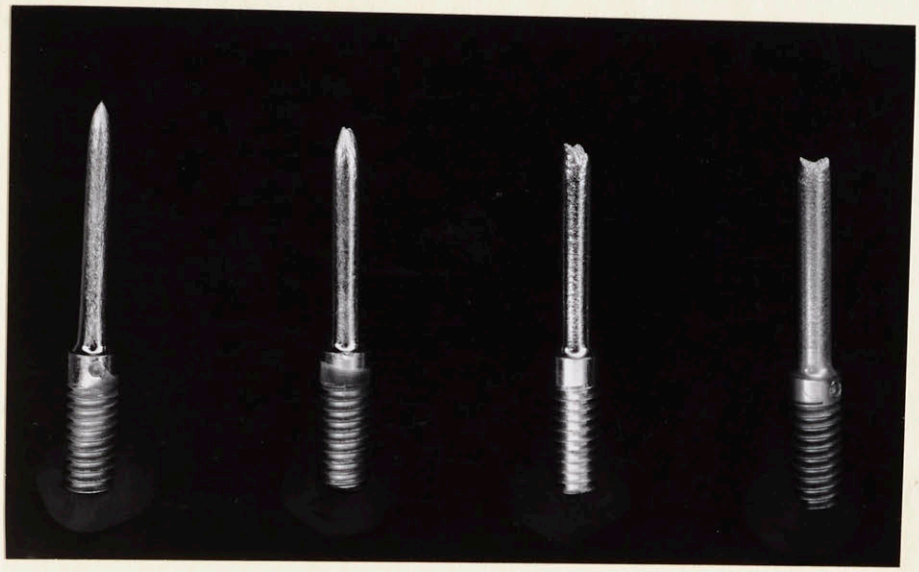

Figure 20. Transition from ductile to brittle fracture as the rupture time increases. 3S aluminum, tested at 900° F:
Left to right: specimen No. 301 (rupture time = 0.01 hrs.); No. 307 (0.93 hrs.); No. 302 (4.1 hrs.); No. 305 (58 hrs.).

The change in slope at 900° F (Figure 17) appears to be sharper for the 2S than for the 3S aluminum. This is true only when log-log co-ordinates are used, since the curve for 2S aluminum is placed at a much lower stress level than the curve for 3S aluminum. Portions of the two curves mentioned above were plotted in Figure 21 on a magnified scale (solid lines) and were then replotted on linear co-ordinates in the same Figure 21 (dotted lines). The dotted lines show that the more impure 3S aluminum has a sharper change in slope than the 2S aluminum, when the behaviors are expressed in linear co-ordinates.

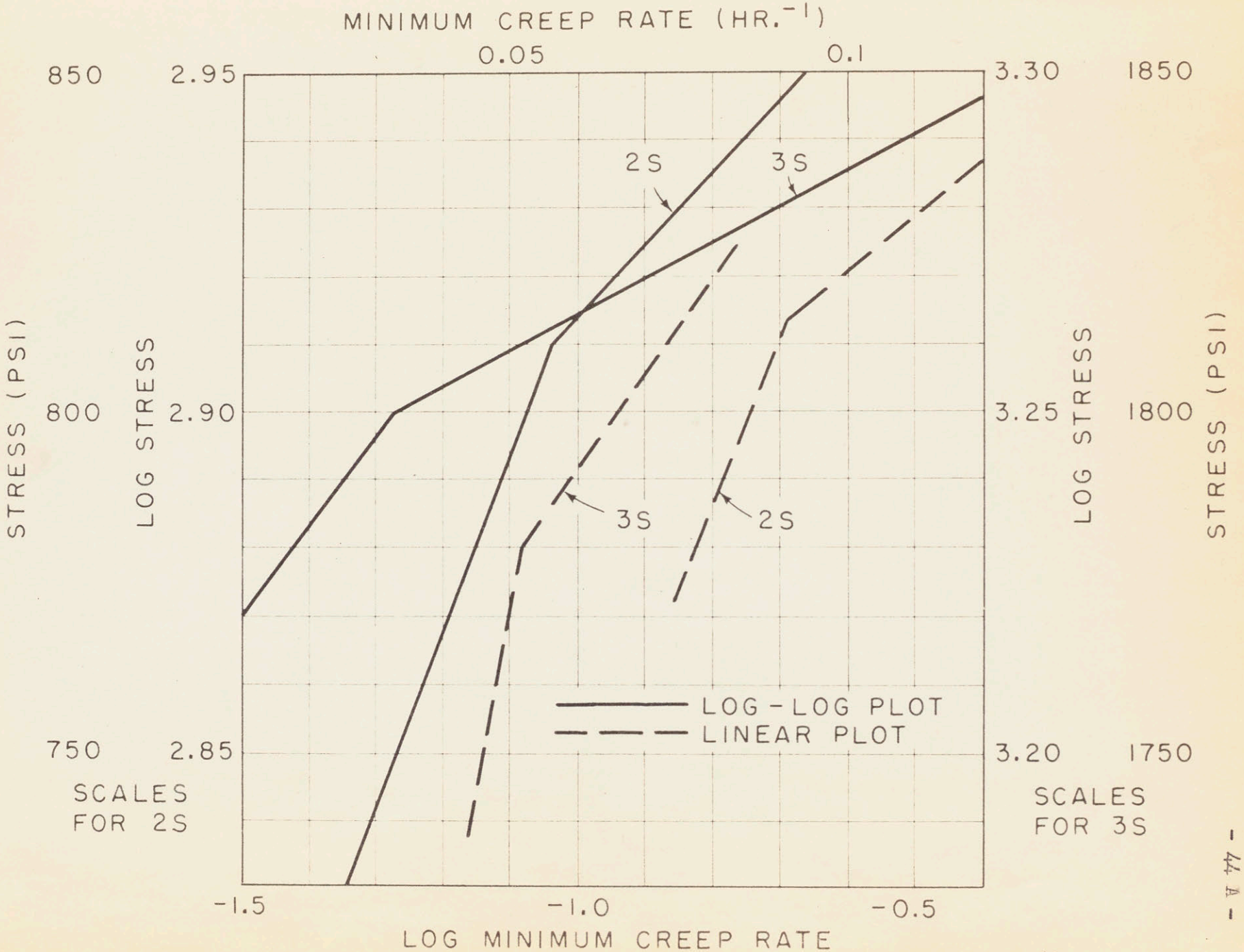

Figure 21. Log-log and linear plot of stress versus minimum creep rate near the transition from low temperature to high temperature behavior. Replotted from Figure 17.

6.4 Stress Dependence of Rupture Times at Constant Temperature

The logarithm of the stress was plotted versus the logarithm of the rupture time in Figure 22 for the high purity aluminum and in Figure 23 for the 2S and 3S aluminum. A few values of the rupture times were estimated, since the tests were not conducted to completion. The uncertainties introduced by estimating a few rupture times were not appreciable, since in all cases the third stage of creep had begun at the time the test was interrupted.

The stress dependence of the rupture time is quite similar to the stress dependence of the minimum creep rate. A series of "breaks" is found for each material investigated. Since the rupture times are not as reproducible as the minimum creep rates, a larger scatter is expected. For the same reason stated above the difference in behavior of the fine grained and of the coarse grained high purity aluminum at 700° F cannot be detected from rupture time data. On the other hand, that difference is clearly demonstrated at 500° F.

In Figure 23 a single straight line could be drawn at 1100° F. The curve drawn in Figure 23 for this testing temperature is based on the uncertainty of the last point, (test No. 226) which was affected by a great amount of grain growth.

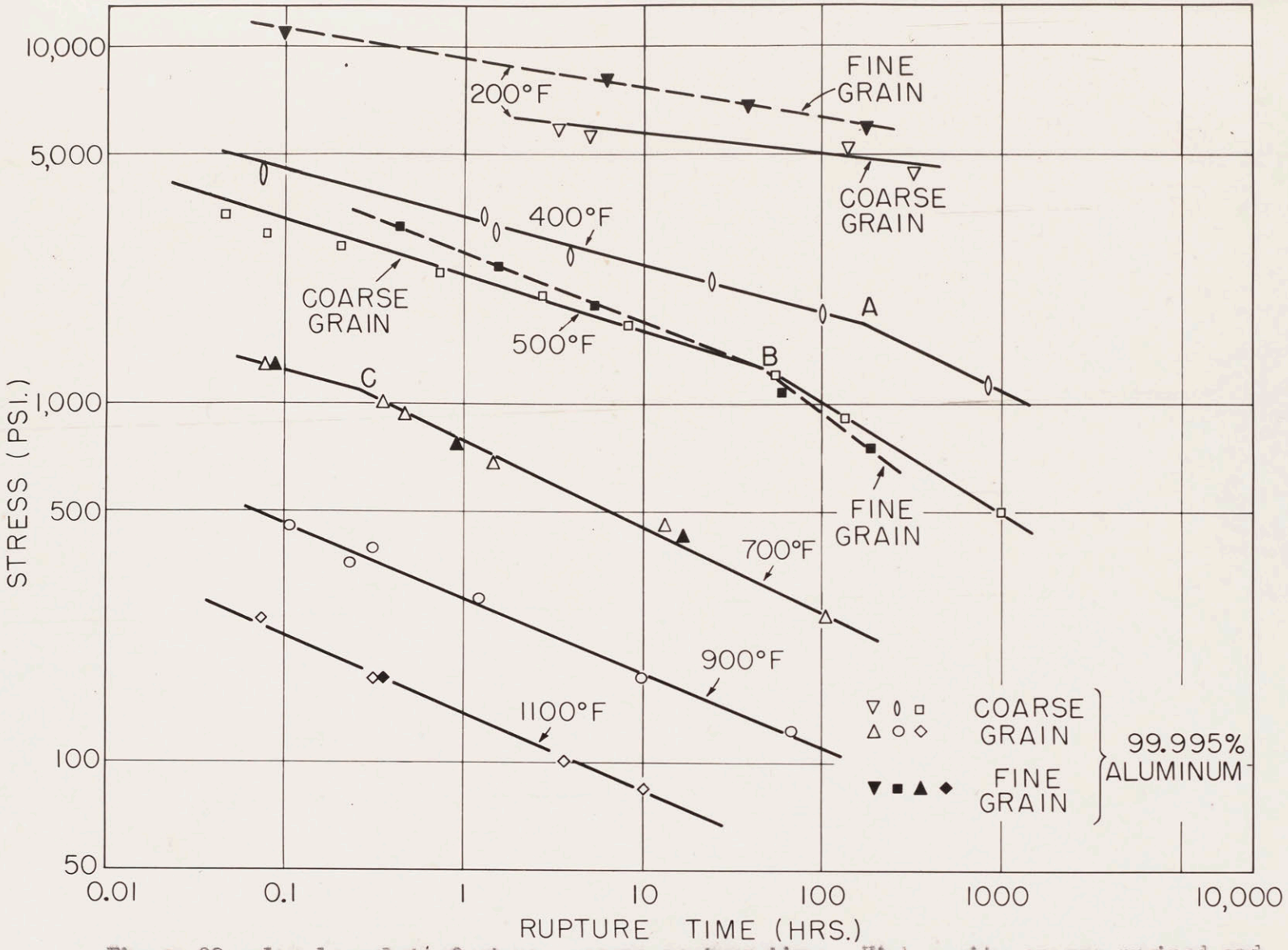

Figure 22. Log-log plot of stress versus rupture time. High purity coarse grained and fine grained aluminum.

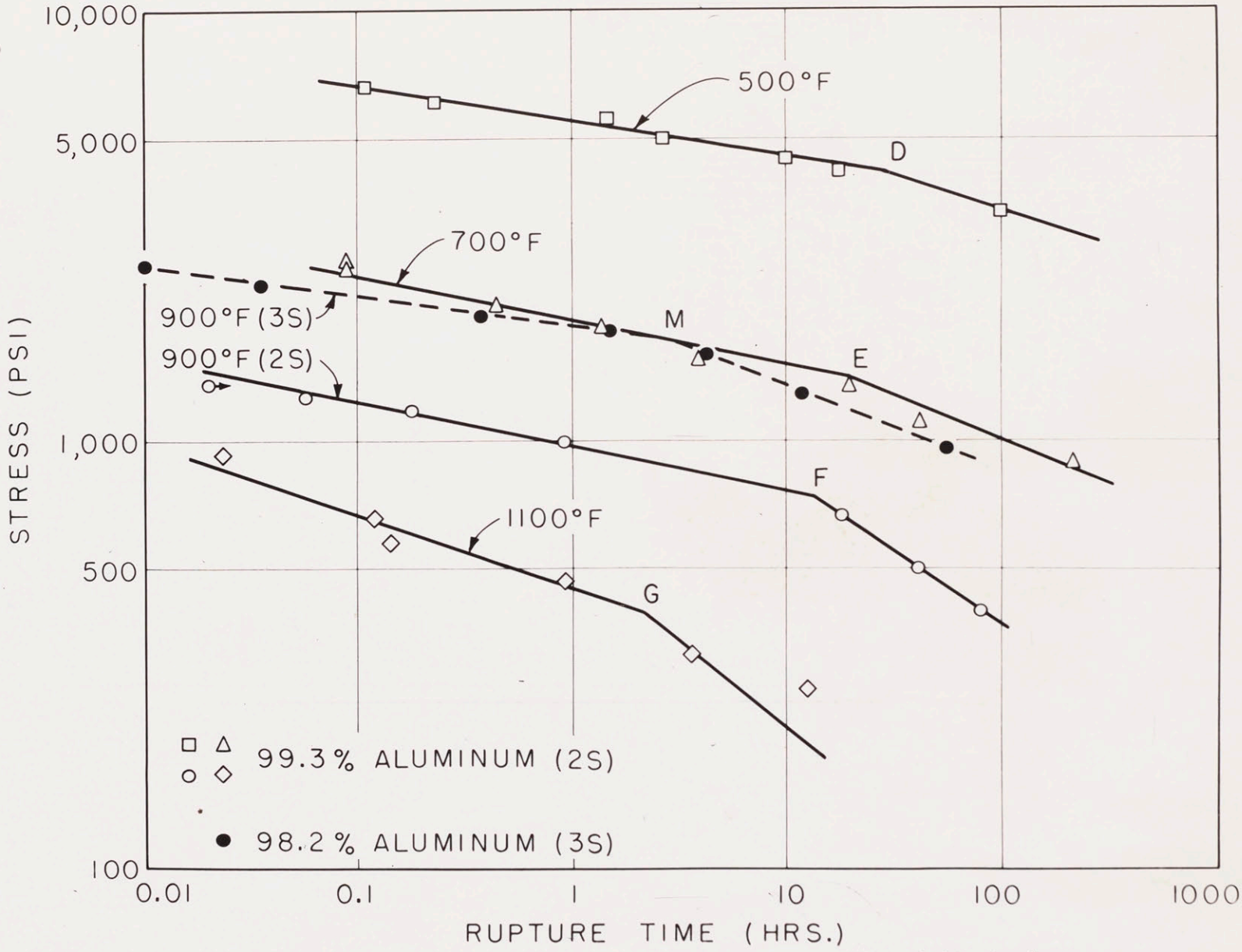

Figure 23. Log-log plot of stress versus rupture time. 2S and 3S aluminum.

6.5 Relation Between the Minimum Creep Rate and the Rupture Time

The log-log plots "stress versus minimum creep rate" and "stress versus rupture time" appear to be almost mirror images. This fact has been observed for many other materials. It was thought that this similarity might be caused by the existence of a very simple relationship between the minimum creep rate and the rupture time.

In order to determine such a relationship, the logarithm of the minimum creep rate was plotted versus the logarithm of the rupture time in Figure 24, for high purity aluminum. The points obtained from tests conducted at different temperatures fall within a band of slope -1. This suggests the relationship

$$\log. \text{M.C.R.} = \text{Log } E_o - \text{Log R.T.} \qquad (6.51)$$

or

$$\text{M.C. R.} = E_o \,/\, \text{R.T.} \qquad (6.52)$$

where E_o is a constant.

The average line drawn through the experimental points of Figure 24 (solid line) indicates that the constant E_o has an average value of 0.316. The constant E_o must be related to the total elongation of the specimen, in the sense that the larger to total elongation, the larger the constant E_o.

In Figure 25 a similar plot was obtained for 2S and 3S aluminum. The behavior of the 2S aluminum suggests the same relationship expressed by formula (6.52), with a constant $E_o = 0.350$.

The solid lines of Figure 24 and Figure 25 could be used to predict the approximate life of a specimen, as soon as the minimum creep rate has been established. The experimental values of the rupture time are

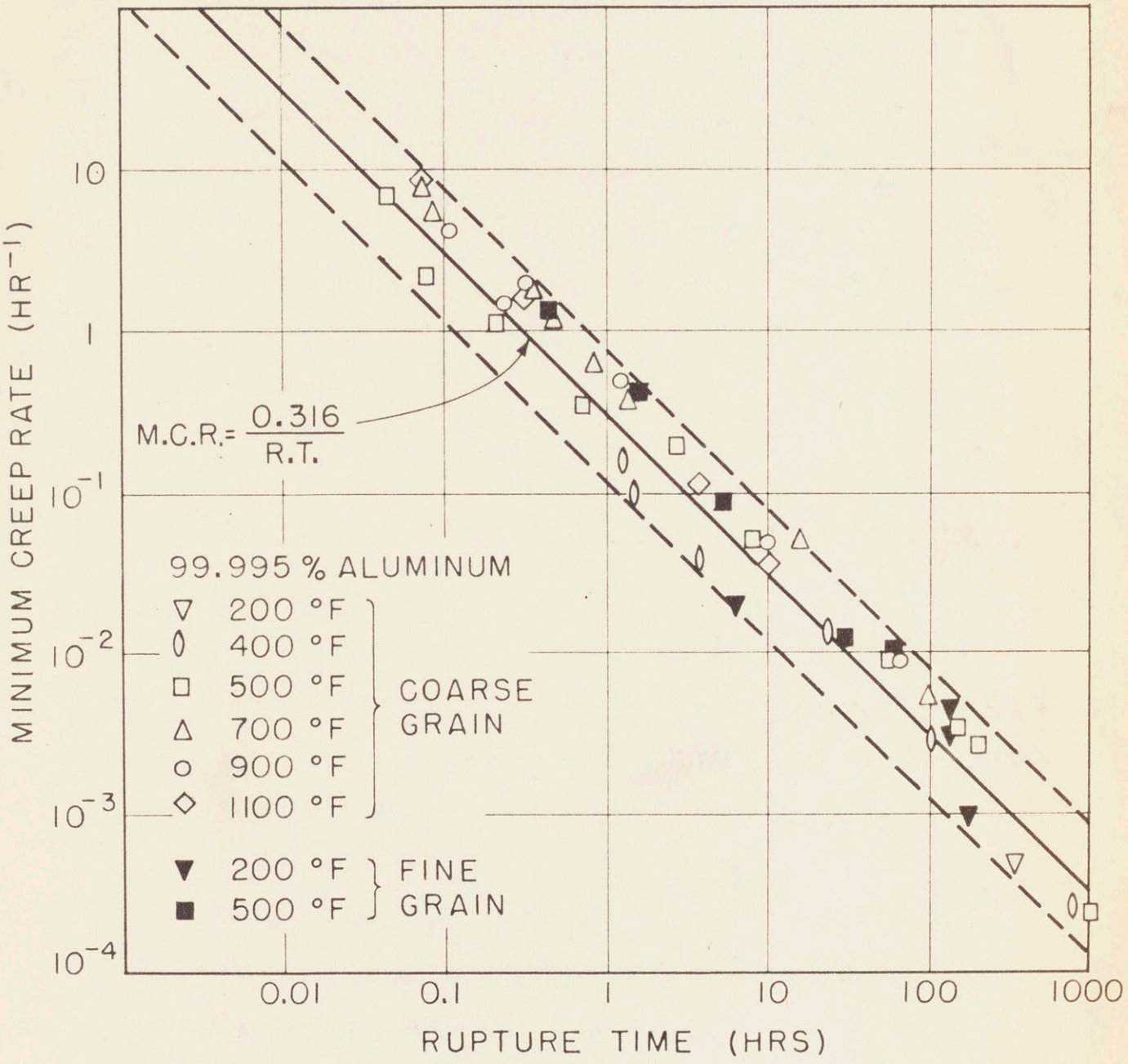

Figure 24. Log-log plot of minimum creep rate versus rupture time. High purity coarse and fine grained aluminum.

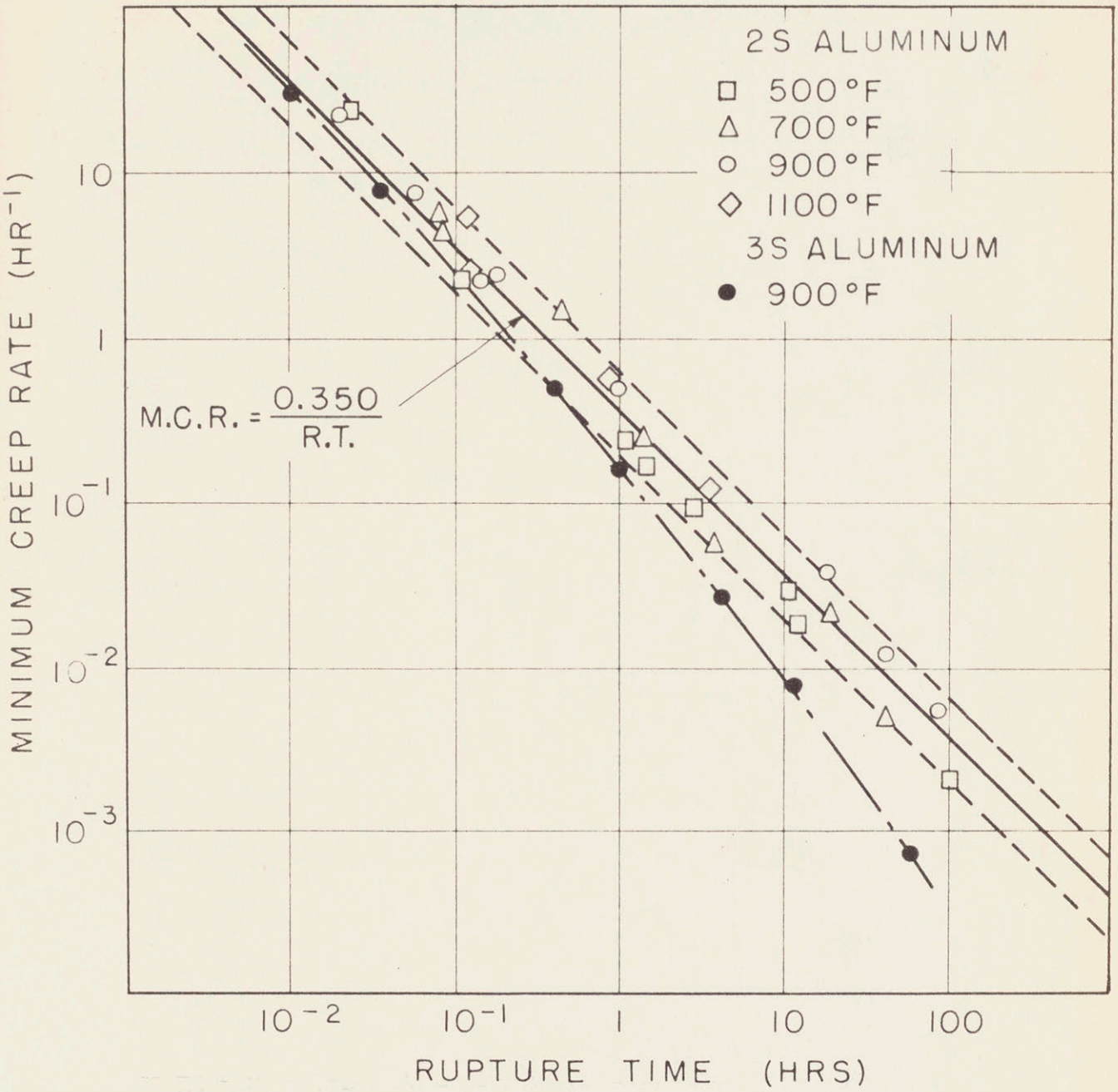

Figure 25. Log-log plot of minimum creep rate versus rupture time. 2S and 3S aluminum.

not more than 2.5 times larger or smaller than the predicted values.

The "Low Temperature" points obtained for 3S aluminum fall within the band established by the 2S points.

The high temperature points plotted in Figure 25 for 3S aluminum do not agree with the results obtained for 2S aluminum. The divergence is larger at longer rupture times; this fact may be explained by observing that the elongation of the 3S samples decreases very markedly as the rupture time increases. Therefore E_o cannot be regarded as a constant, but as a function of the rupture time.

6.6 Temperature Dependence of the Transition Points

The transition from low temperature to high temperature behavior probably occurs over a range of stresses and of strain rates. In order to study the temperature dependence of the transition points, it is convenient to assume that the transition occurs at a definite stress and at a definite strain rate, as indicated by the sharp change in slope of the curves of Figure 13 and Figure 17. The average values of the transition stress and of the transition strain rates at different testing temperatures have been determined from the "breaks" of Figure 13 and Figure 17 and from the results of metallographic examinations.

The logarithm of the transition stress and the logarithm of the transition strain rate have been plotted versus the temperature in Figure 26 and Figure 27 respectively. The results indicate that:

(a) Impurities raise the transition stress

(b) Impurities lower the transition strain rate

(c) The transition stress has a finite value at temperature close to the melting point.

(d) Below a certain critical temperature, no transition will be observed within a reasonable testing time.

The results of Figure 27 agree with the results obtained by Grant and Bucklin[26] for cobalt-base alloys. In fact, Grant and Bucklin found that the higher the temperature, the shorter the rupture time at which the transition occurs.

An attempt has been made to compare the experimental results reported above with the Mott theory of "grain boundary slip". According to Mott[35] slip along the grain boundaries cannot occur below a critical temperature T_c. This critical temperature can be calculated from the equation:

$$T_c = \frac{Q}{R \ln \left(\frac{b\sigma}{x\dot{\varepsilon}} \right)} \qquad (6.61)$$

where:

Q, b = constants associated with the viscous flow at the grain boundaries

σ = applied stress

x = linear grain size

$\dot{\varepsilon}$ = creep rate

Based on Ke's work[14] Mott calculated the theoretical critical temperature for aluminum, and obtained a value of 410° K, for "normal" creep testing conditions. Moreover he predicted that grain boundary slip should not be very structure sensitive, "unless a dense film of impurity is formed at the grain boundary".

For high purity, coarse grained aluminum, equation (6.61) can be re-written as follows (utilizing Mott's values of Q and b):

$$\text{Log} \frac{\sigma}{\dot{\varepsilon}} = -10.4 + \frac{7680}{Tc} \qquad (6.62)$$

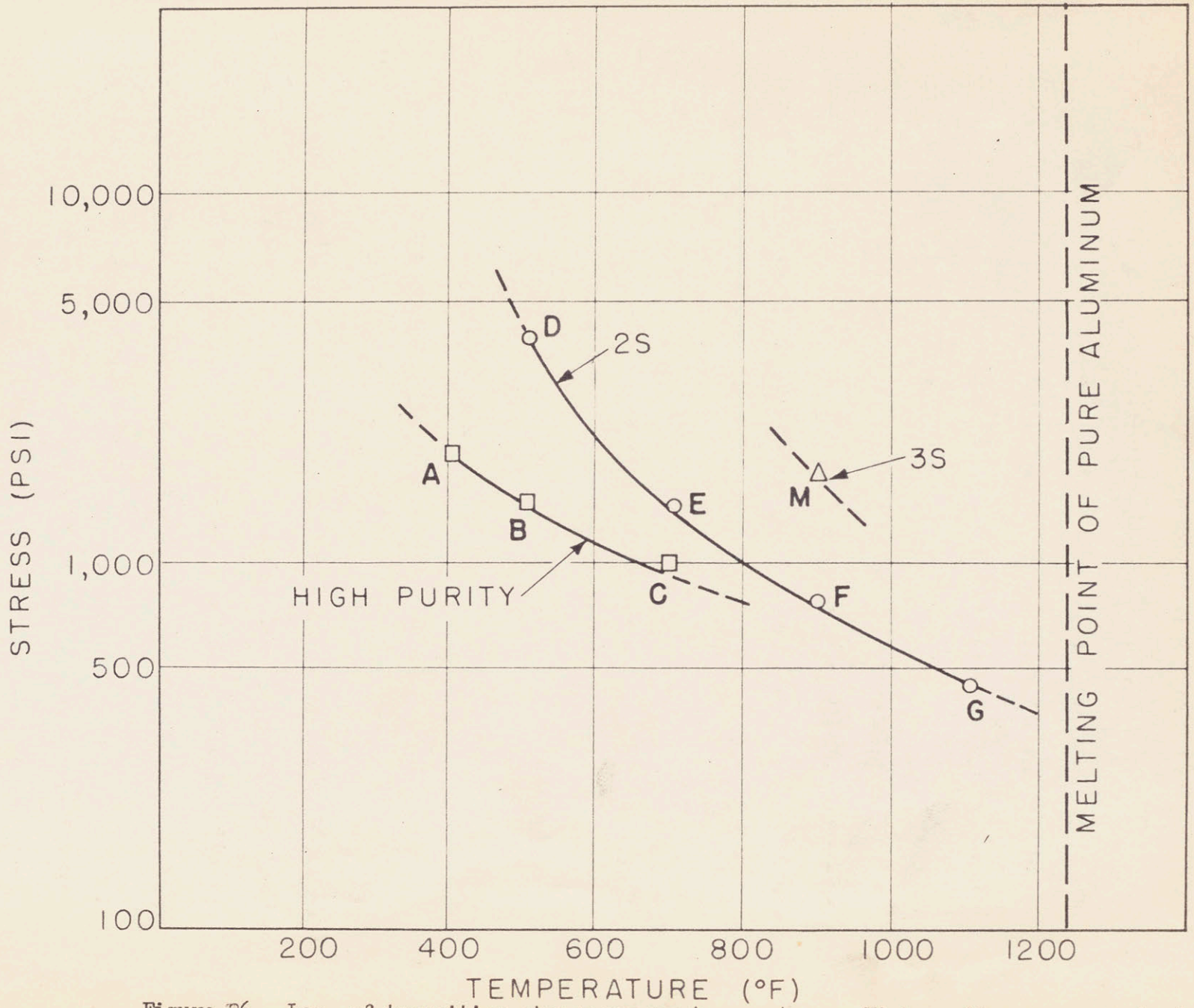

Figure 26. Log. of transition stress versus temperature. High purity coarse grained, 2S and 3S aluminum.

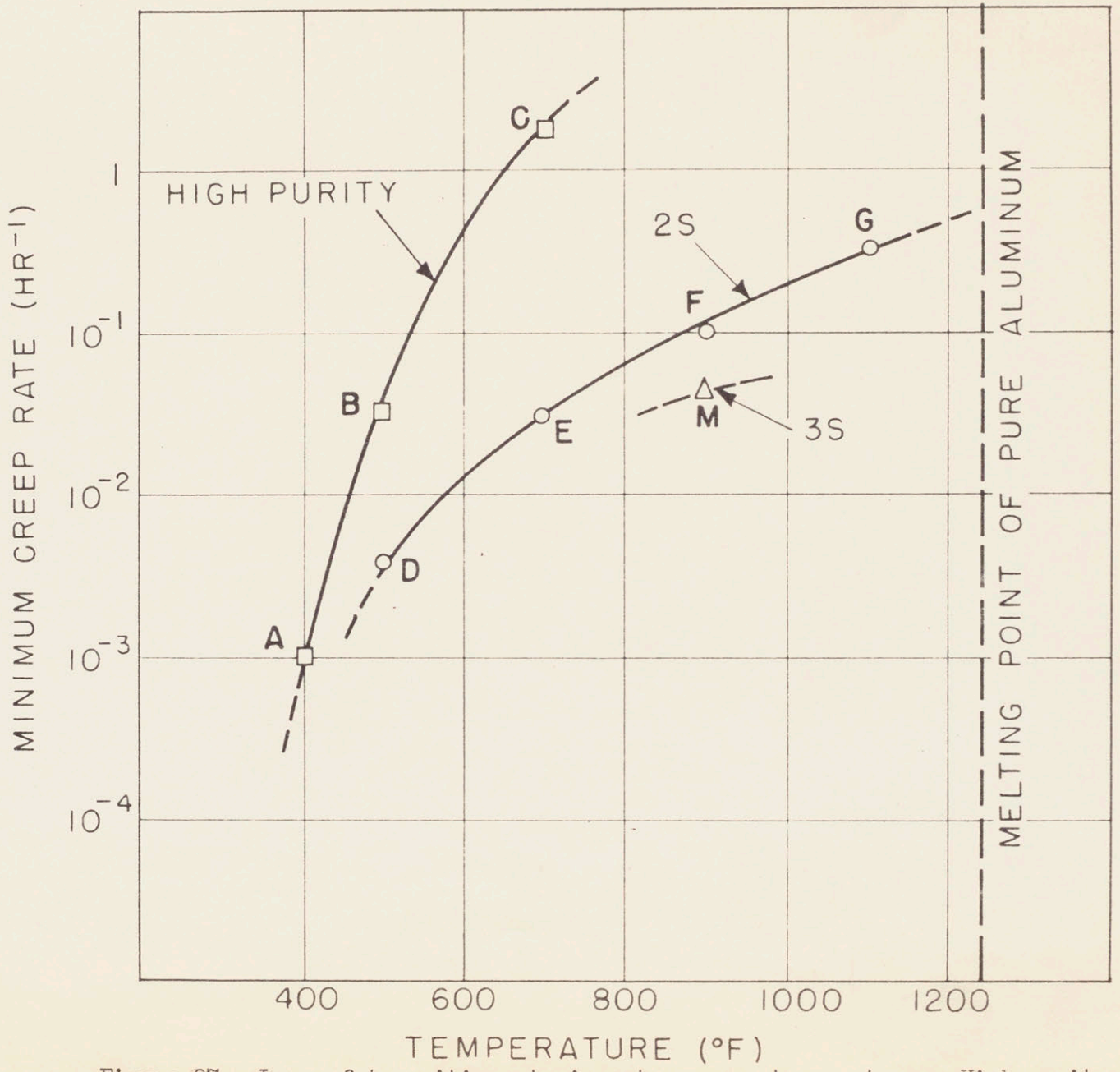

Figure 27. Log. of transition strain rate versus temperature. High purity coarse grained, 2S and 3S aluminum.

if the stress σ is expressed in psi

and the creep rate $\dot{\varepsilon}$ is expressed in $hr.^{-1}$.

The values of the transition stress and of the transition strain rates from Figure 26 and Figure 27 have been used to calculate the theoretical transition temperature T_c according to equation (6.62). The results are tabulated in Table III.

Table III indicates that the order of magnitude of calculated transition temperatures is correct: this fact supports the hypothesis that the transition from low temperature to high temperature behavior is associated to the beginning of grain boundary flow.

TABLE III

Calculated and Experimental Transition Temperatures for High Purity, Coarse Grained Aluminum

Testing Temperature	Transition Stress	Transition creep rate	Transition Temperature (T_c)	
			Calculated	Experimental
°F	psi	$hr.^{-1}$	°K	°K
400	1950	0.001	460	477
500	1400	0.03	510	533
700	1000	1.7	585	644

A similar analysis of the data for 2S aluminum did not lead to a reasonable agreement between the calculated and the experimental values of the critical temperature. This fact was expected, since the Mott theory (35) does not apply to other than high purity metals.

In order to find an explanation for the behavior of 2S aluminum, values of Log. $\frac{\sigma}{\dot{\varepsilon}}$ have been plotted versus the reciprocal of the absolute

temperature in Figure 28. This was done for high purity, 2S and 3S aluminum. The theoretical curve which follows equation (6.62) has also been plotted in Figure 28.

Figure 28 shows a linear relationship for both high purity and 2S aluminum. The curve drawn for 2S aluminum follows the equation

$$\text{Log}\,\frac{\sigma}{\varepsilon} = -0.75 + \frac{3500}{Tc} \qquad (6.63)$$

Equation (6.63) suggests that the Mott theory[35] of grain boundary slip may probably be extended to less pure materials if it is assumed that the constants Q and b of equation (6.61) are smaller for impure than for high purity aluminum. The values of the constants Q and b of equation (6.61) were calculated from the curves of Figure 28. The following results were obtained:

(a) high purity aluminum: $Q = 29{,}000$ calories per gram atom

$b = 10^{-2}$ cgs units

(b) 2S aluminum: $Q = 16{,}000$ calories per gram atom

$b = 10^{-11}$ cgs units

The values of the constants used by Mott[35] to calculate the theoretical critical temperatures are:

$Q = 35{,}000$ calories per gram atom

$b = 20$ cgs units.

The curves of Figure 28 and the calculated constants indicate that the critical temperature T_c is a structure sensitive property. The critical temperature T_c is markedly affected by the impurity content.

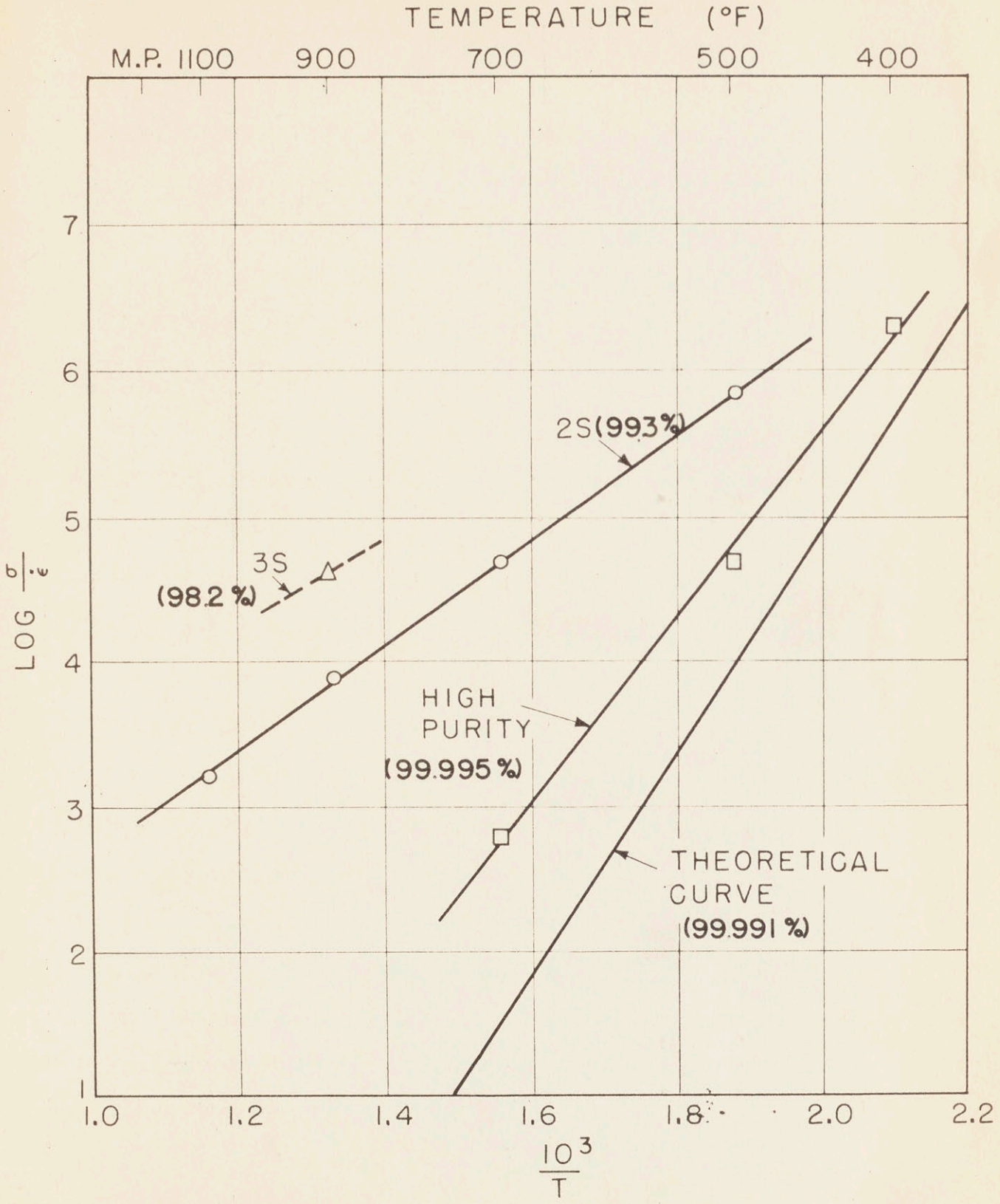

Figure 28. Log. of the ratio transition stress to transition strain rate versus the reciprocal of the absolute temperature. Experimental and theoretical curves.

6.7 Study of Ductility

The total elongation of a specimen after fracture is not only a property of the material tested, but also of the test apparatus used. For instance, if temperature gradients are present along the samples, more than one necked region may be formed before rupture occurs. In this case the total elongation is larger than in the case of single-necked specimens.

Grant and Bucklin[26] observed that the elongation of the sample at the beginning of the third stage of creep ("true elongation") is a more reproducible and significant property of the material than the total elongation. Studying cobalt-base alloys, they found that the "true elongation" drops markedly to smaller values as the testing conditions change from "Low Temperature" to "High Temperature".

It was not possible to determine the "true elongation" of aluminum with a better accuracy than $\pm$ 0.02 inches. However, this accuracy was sufficient to determine the trend of the"true elongation" as the rupture time is increased.

Figure 29 shows that for high purity aluminum at 200° F, 400° F, 500° F and 700° F there is no definite trend of the true elongation as a function of the rupture time for the test times used; all the data are scattered around an average value. This average value increases as the testing temperature increases. Figure 30 shows that at 900° F and 1100° F there is a decrease in true elongation as the rupture time increases. This trend may possibly be partly ascribed to grain growth. It is worth noting that no truly brittle failures were observed in high purity aluminum samples in spite of this decreased elongation.

The same type of plot was repeated in Figure 31 for the 2S and 3S aluminum. This plot shows that the "true elongation" decreased as the transition points "D-E-F-G" and "M" of Figure 17 are reached.

The decrease in true elongation is much sharper for 3S than for the 2S aluminum: for both these materials the decrease of the "true elongation" corresponds to the incidence of intercrystalline cracking.

The results reported above demonstrate that impurities promote the formation of intercrystalline cracking when a sample is strained at "high temperature". The results also support the interpretation given to the "breaks" in the curves of Figure 17.

6.8 Temperature Dependence of Creep Rates

The data obtained for high purity and 2S aluminum are not extensive enough to permit an accurate analysis of the temperature dependence of steady state creep. The data reported in Figure 13 for the high purity material show that the slopes of the straight lines increase as the temperature increases up to 700° F. At 900° F and 1100° F there is a decrease in slope, which may be ascribed to the grain growth occurring in the specimens. Therefore the data obtained at the highest temperatures cannot be compared directly to the other data.

The data reported in Figure 17 for 2S aluminum are also unsuitable for studying the temperature dependence of the creep rates, since the "transitions" divide each curve into two branches. The position of each branch is fairly approximate.

Therefore the method used to analyze data for cobalt-base alloys[33], which lead to the final formula (6.35), is not applicable to the present data. Since the transition from "Low Temperature" to "High Temperature"

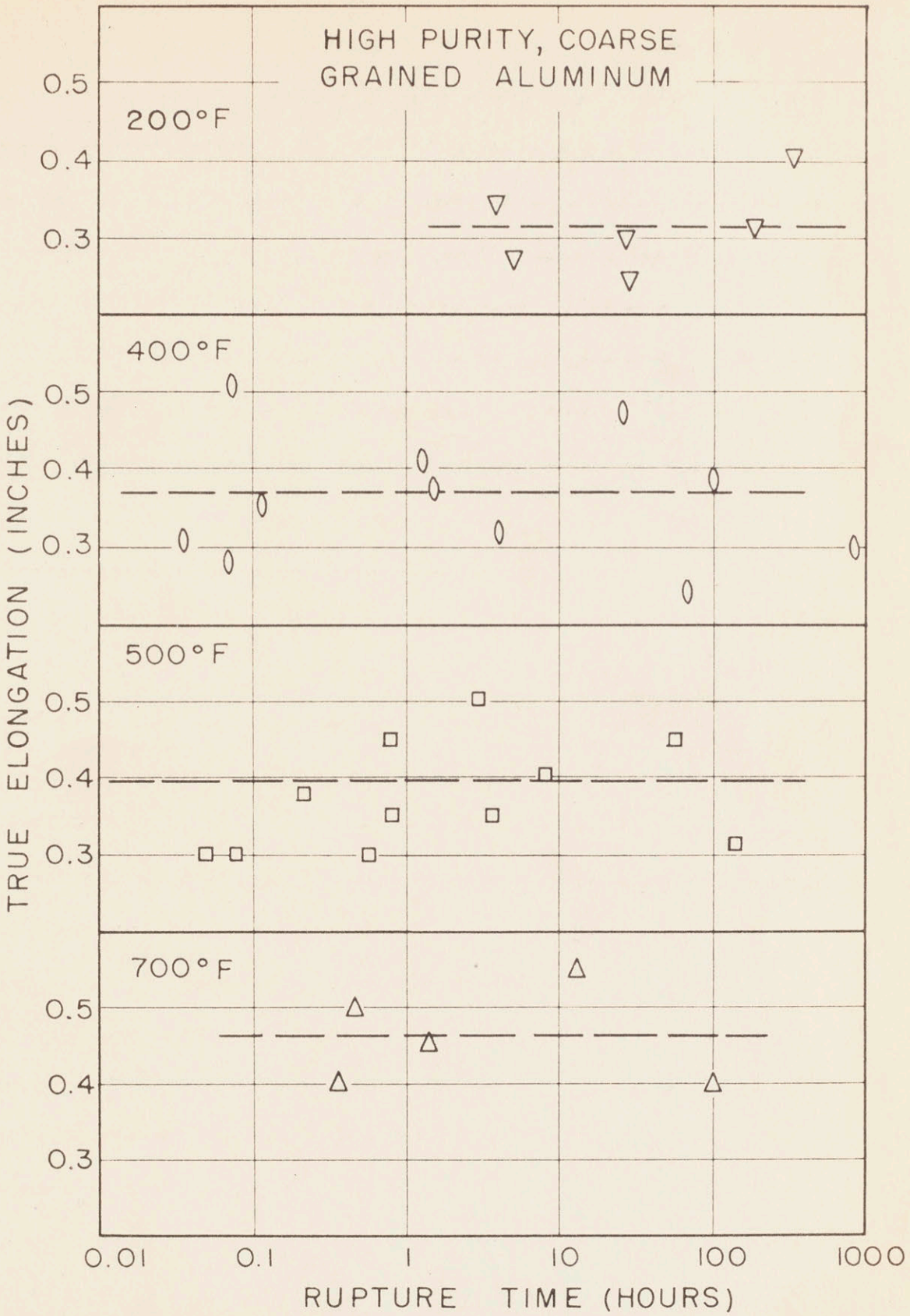

Figure 29. True elongation versus logarithm of rupture time. High purity coarse grained aluminum.

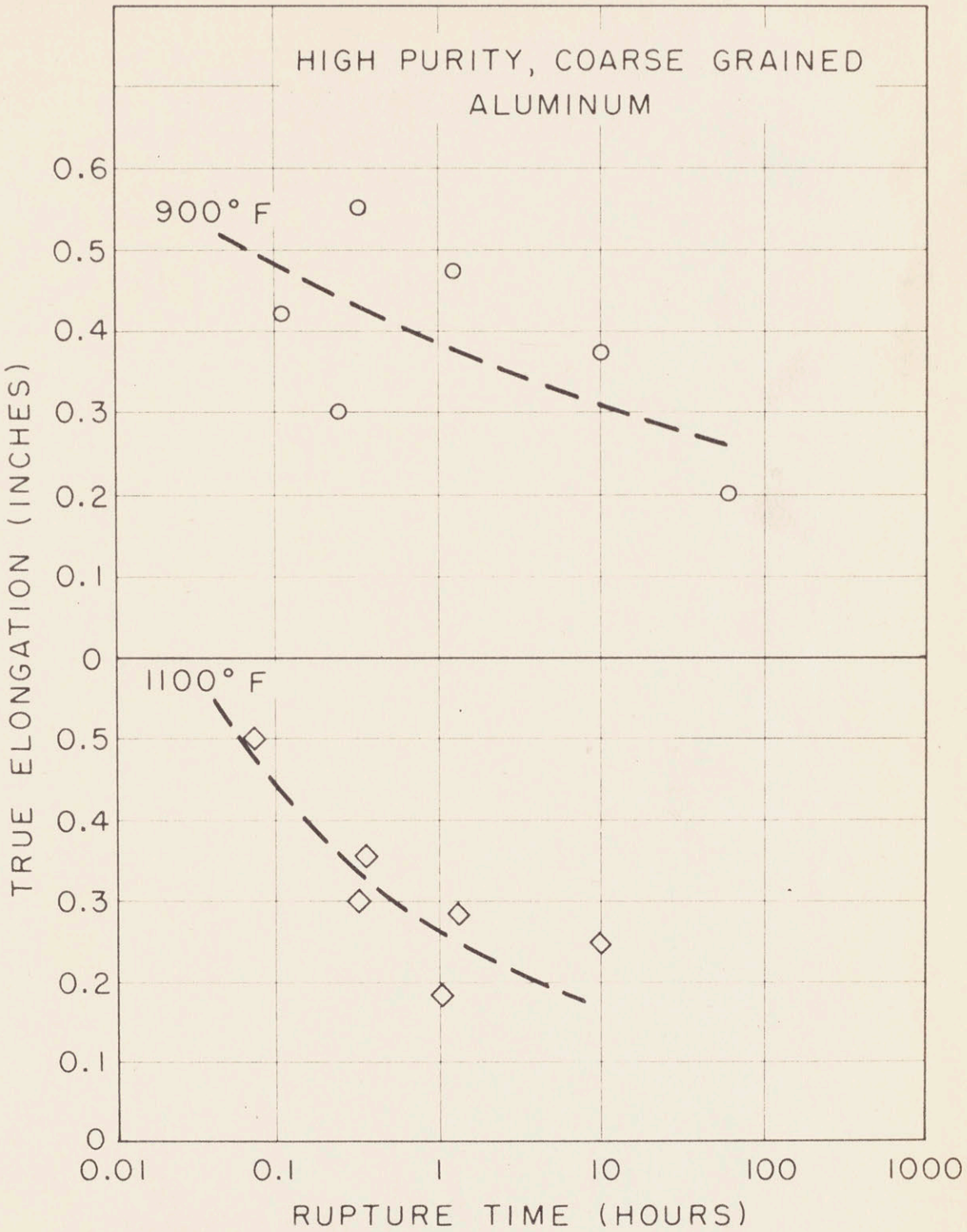

Figure 30. True elongation versus log. of rupture time. High purity coarse grained aluminum.

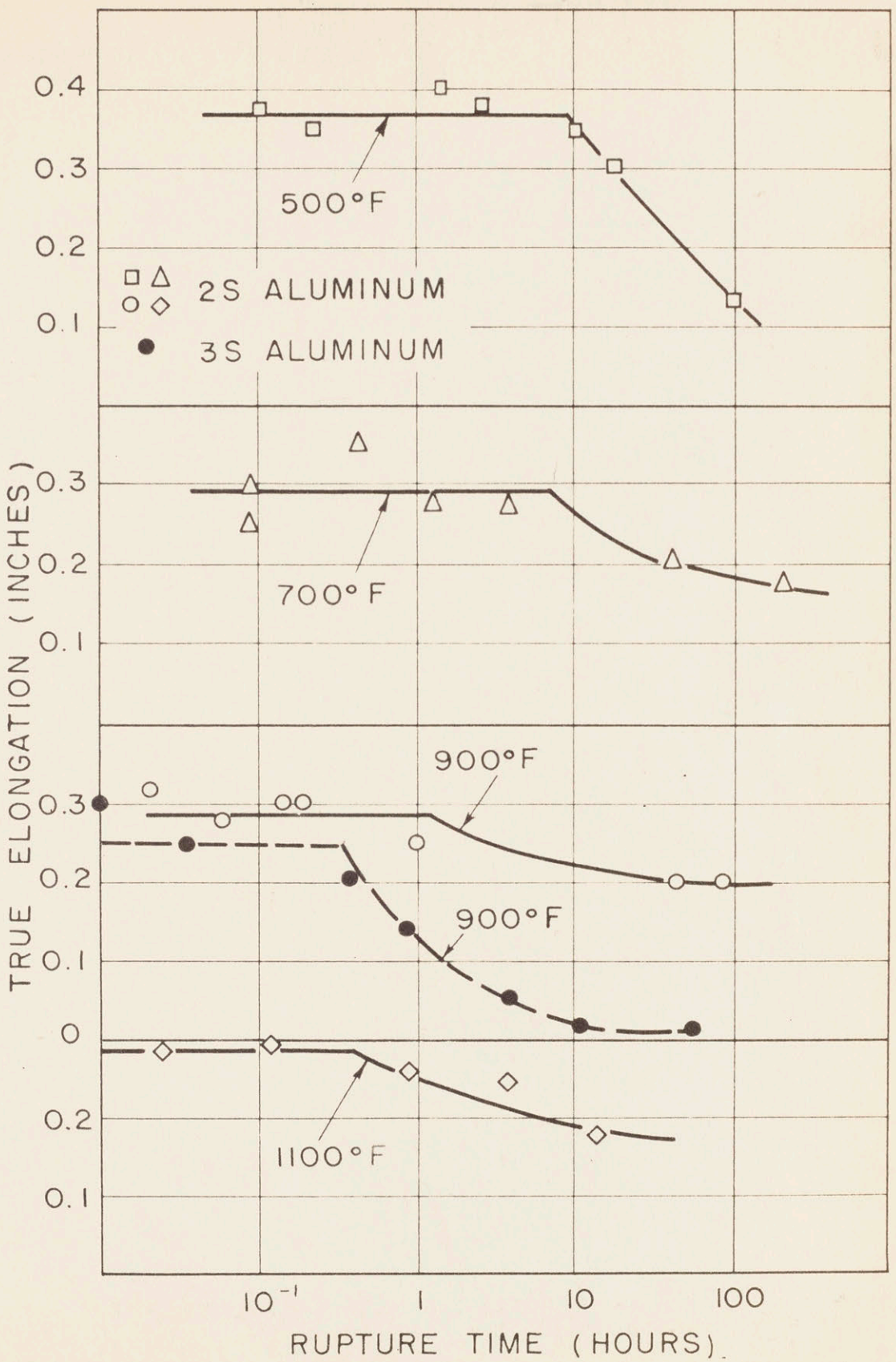

Figure 31. True elongation versus log. of rupture time. 2S and 3S aluminum.

for purity aluminum does not produce a very sharp change in the slope of the curves of Figure 13, the whole set of data from 200° F to 700° F was used to determine the temperature coefficient of secondary creep. From the curves of Figure 13, the minimum creep rates at constant stress was calculated as a function of testing temperature. The logarithm of the minimum creep rates at constant stress was plotted versus the reciprocal of the absolute temperature in Figure 32.

Only two or three points were obtained at each stress level: therefore the straight lines of Figure 32 do not constitute proof for a linear relationship. However, it was possible to determine the approximate slope of these lines and to calculate the "temperature coefficient" Q of the Boltzmann's formula:

$$r = A\, e^{-Q/RT} \tag{6.81}$$

where r is the rate of a process

R is the gas constant per mole

T is the absolute temperature

A is a constant.

The logarithm of the stress was plotted versus the temperature coefficient Q in Figure 33; an approximate linear relationship was obtained.

The results indicate that the Boltzmann formula can be applied to the steady state creep and that the temperature coefficient Q is related to the stress by the equation

$$Q = A + B \log. s \tag{6.82}$$

where A, B = constants

s = applied stress.

The equation (6.82) is in agreement with the equation (6.35) mentioned before.

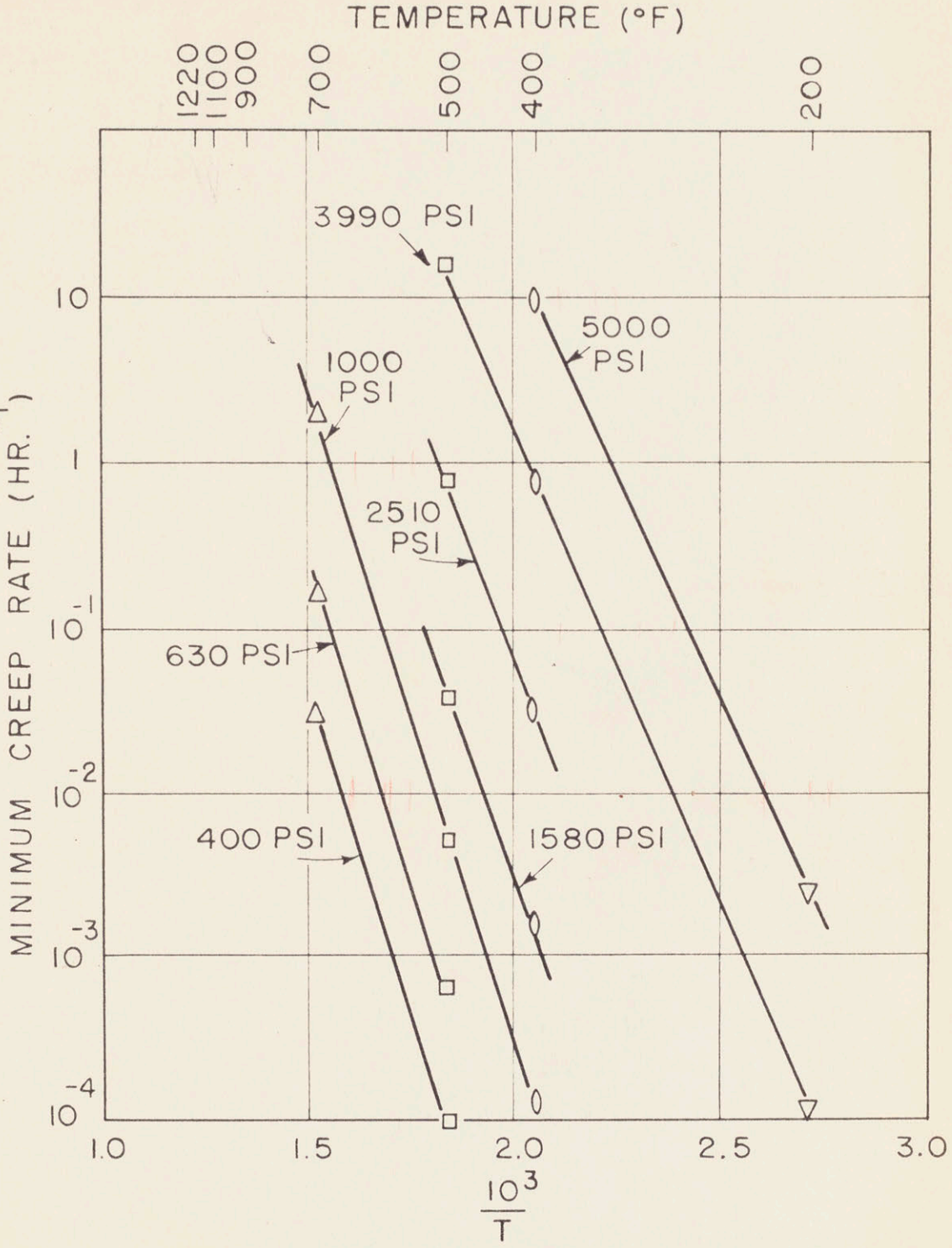

Figure 32. Log. minimum creep rate at constant stress versus the reciprocal of the absolute temperature. High purity coarse grained aluminum.

Figure 33 does not indicate any sharp change of the temperature coefficient Q at the transition from "Low Temperature" to "High Temperature" behavior. Such a negative conclusion is not absolute, since the determination of the temperature coefficient Q was only approximate.

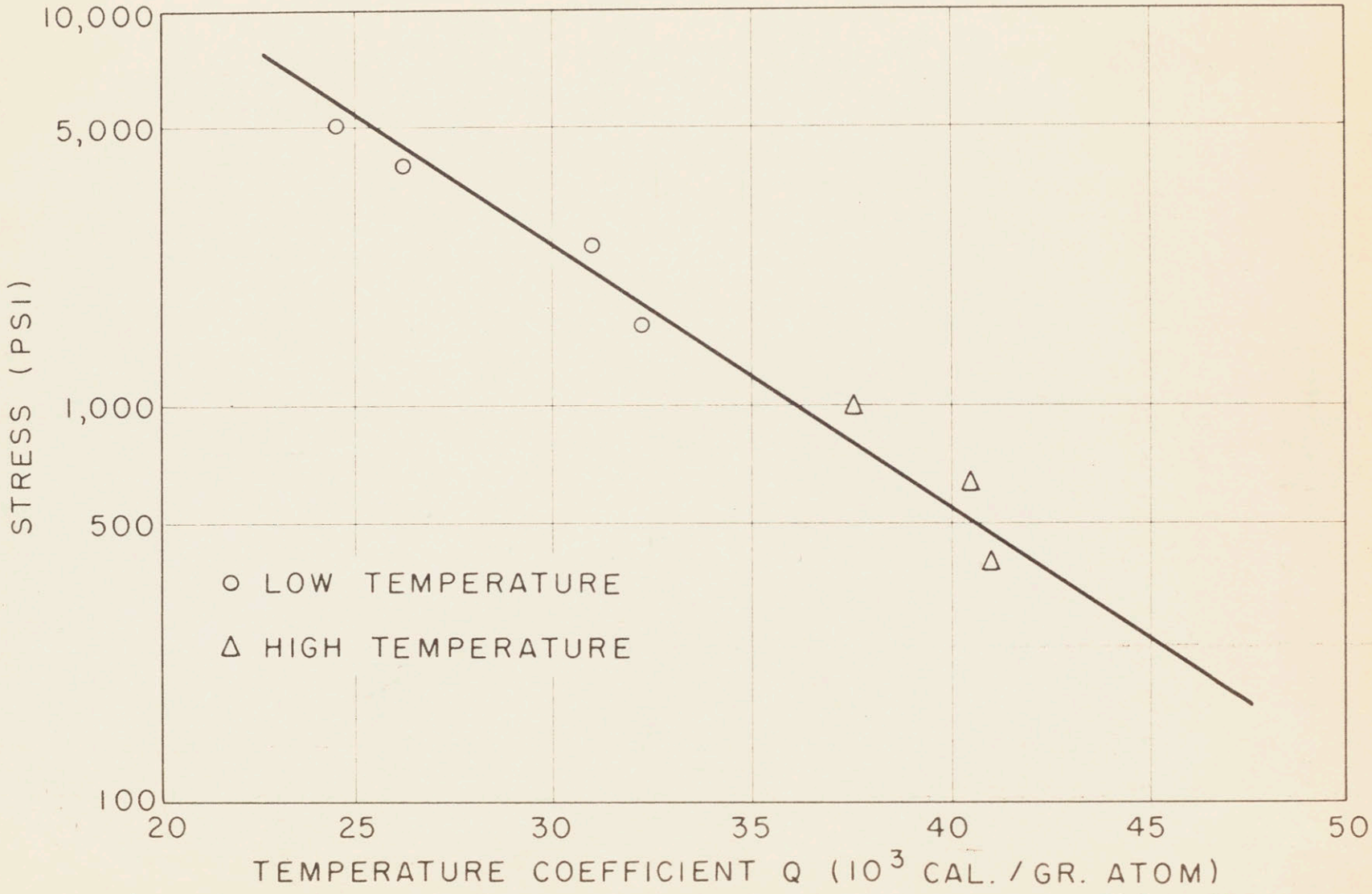

Figure 33. Log. stress versus temperature coefficient of strain rate. High purity coarse grained aluminum.

PART B

STRUCTURE OBSERVATIONS DURING CREEP

6.9 Introduction

In Part A creep rate and rupture time data for three grades of aluminum have been presented. It was found that the stress coefficients of the creep rates and of the rupture times change under certain conditions of testing. This change was identified with the transition from "Low Temperature" behavior to "High Temperature" behavior of the material. It was also found that the "transition" corresponds to the conditions at which grain boundary flow begins; therefore the "transition" corresponds to the "equi-cohesion" of the grains and of the grain boundaries.

In order to support the conclusions of Part A, and to obtain further information on the subject of high temperature deformation, the deformed specimens were observed metallographically and a few special tests were conducted. The results of these qualitative observations are presented below.

Before presenting such results the work previously done shall be summarized briefly because of its current rapid development. Observations of deformed aluminum have been made by many investigators for different conditions of testing. Several experimental results suggested a change of the mechanism of deformation as the temperature is increased, or as the strain rate is decreased.

Wilms and Wood[11] proposed the "cell mechanism" of deformation at elevated temperatures, basing their conclusions on metallographic and X-ray back reflection evidence. According to Wilms and Wood, for

proper conditions of temperature and strain rate, each grain breaks down into sub-grains (called cells) which rotate by sliding along their "sub-grain boundaries". For these test conditions the common "slip" mechanism of deformation is not operative. These results seemed to offer an explanation to the "slipless flow" observed by Hanson and Wheeler[10].

The "cell mechanism" theory has been supported by other results, which have been obtained by Wood and Rachinger[12], Wood and Scrutton[13], Calnan and Burns[36], and Greenough and Smith[48].

Breakdown of grains into fragments is observed in two other cases:

(a) During cold working. According to the "Crystallite theory" which was proposed by Bragg[37] during cold working the grains are fragmented into "crystallites". Bragg's crystallites are not stress free and have a much smaller size than the "cells" which are formed during working at elevated temperatures.

(b) During annealing after cold working. According to Lacombe and Beaujard[38] annealed high purity aluminum may be in the "polygonized" state. The "sub-grains" which are formed during heat treatment are stress free and have dimensions similar to the size of the "cells" mentioned above. Cahn[39] discussed the phenomenon of polygonization in relation to the dislocation theory.

The question can be raised, whether "cell mechanism", "crystallite formation" and "polygonization" are essentially the same process.

A great deal has been written on this subject[40] but no definite

conclusion has been reached regarding the mechanism of creep. The latest contribution to this subject was given by Crussard and Wyon[41], who found no relation between the "cells" and the sub-grains of a polygonized material. They found that the metallographic observations of an unetched sample reveals the "cells", while X-ray diffraction, or the observation of an etched sample reveals the polygonized state, which is quite independent of the deformation process.

Observations of aluminum that was deformed at room temperature were made long ago by Yamaguchi[42], who found a linear relation between the number of slip bands per unit length and the shear stress. This relation is of the same form as Orowan's formula[43]:

$$d = \frac{G\,a}{2\,\tau} \tag{6.91}$$

where

d = minimum spacing between slip bands

G = Modulus of elasticity in shear

a = interatomic spacing

τ = shear stress

Assuming that

$$\frac{G}{\tau} \simeq \frac{E}{\sigma} \tag{6.92}$$

where E is the modulus of elasticity in tension and

σ is the applied tensile stress,

for aluminum:

$$d \simeq 1/\sigma \tag{6.93}$$

when d is expressed in millimeters and σ is expressed in pounds per square inch.

According to formula (6.91) the spacing d should be practically independent of the temperature, the strain, and the strain rate. However, any spacing larger than d can be observed in a deformed specimen if the amount of deformation is not sufficient to give "saturation" of the slip bands, or if some slip bands escape visual observation.

The term "slip bands" has been used instead of the more common term "slip lines", since themarkings visible under the microscope are actually clusters of slip lines, as it was found by Heidenreich and Schokley[15].

For proper testing conditions the grain boundaries contribute to the deformation of polycrystalline specimens. This fact was observed in aluminum by Hanson and Wheeler[10] and by other investigators. However, no systematic research has been conducted on the behavior of the grain boundaries of aluminum. King, Cahn and Chalmers[44] tested a two-crystal sample of tin at a few degrees below the melting point. The sample had a macroscopically straight boundary. A displacement of the two crystals was observed along the grain boundary: the rate of displacement diminished with time, until it reached a very small value. The results of this simple experiment suggest that in a polycrystalline material at elevated temperatures the grain boundaries should make a large contribution to the initial deformation, while a larger amount of strain can be introduced only if the grain deforms too.

6.10 Special Tests

6.101 Single Crystal Tested at 1170° F (Test No. 3)

A high purity aluminum specimen was heat treated for thirty minutes at 1000° F and electro-polished. An uncontrolled amount of deformation was applied to the specimen by bending and twisting. The

sample was then placed in the creep testing apparatus and heated to 1000° F in two hours. It was kept at this temperature for 18 hours, then heated up to 1170° F and kept at this temperature for two hours before loading. From the start of the heating schedule the lower specimen holder was hanging from the sample; this corresponds to an applied stress of about 20 psi. The test loading was accomplished by increasing the applied stress from 20 to 50 psi. The creep curve has been reported in Part A (Figure 8). The total elongation was 0.45 inch, of which 0.066 inch was recorded after loading.

After the additional load was applied the specimen was seen to slip along one plane which was at approximately 45 degrees to the axis of tension. The specimen failed by gliding along this plane.

After testing, the specimen was macro-etched; Figure 34 shows that the specimen consisted of a single crystal, except for a few very small crystals near the failure zone. It is assumed, based on other observations, that the single crystal was formed before the application of the additional load.

6.102 Coarse Grained Sample Tested at 1000° F (Test No. 5)

A high purity aluminum sample was heat treated for 30 minutes at 1000° F. The two end portions of the sample were deformed by bending, while the central portion was left in the annealed state. The sample was then re-annealed at 1100° F overnight. During the second heat treatment a few very coarse grains grew at the two ends of the specimen while the middle portion did not recrystallize, leaving the middle portion with a finer grain size than the end portions. This special specimen was tested at constant load at 1000° F, under an initial applied stress of 50 psi.

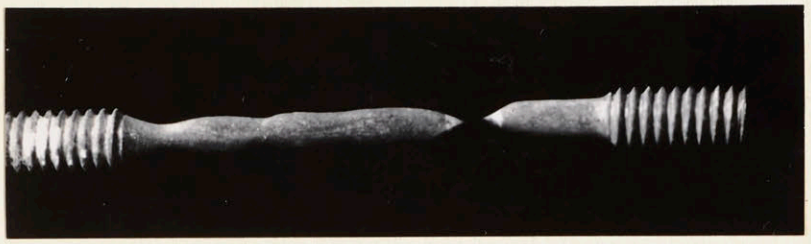

Figure 34. Special Test No. 3 - High Purity Aluminum Single Crystal After Testing at 1170° F - Etched in HCl.

Figure 35. Special Test No. 5 - High Purity Aluminum Specimen After Testing at 1000° F - Etched in HCl.

Since no appreciable elongation was observed after 24 hours the stress was raised to 100 psi. A comparison of these test conditions with the results plotted in Figure 13 shows that the specimen was tested at "high temperature" conditions. The specimen deformed by slipping along parallel planes in the coarse grained portion and by necking in the fine grained portion. It failed after 48 hours in the middle fine grained portion. The appearance of the macro-etched sample after testing is shown in Figure 35.

6.103 Coarse Grained Sample Tested at 1100° F (Test No. 90)

A similar test was performed at 1100° F. The preparation of the sample was similar to the preparation of sample No. 5: in this case the specimen was bent only at one end before reannealing. Therefore a large crystal grew at one end, while a polycrystalline zone remained at the other end. The specimen was electro-polished and electro-etched before testing (Figure 36). The viewing window of the furnace was placed in front of the junction between the polycrystalline and the single crystal part of the specimen.

A stress of about 50 psi. was applied to the cold specimen and the temperature was raised to 1100° F in about 3 hours. The temperature was kept at 1100° F for 3 plus hours and was then lowered to room temperature in 2 hours.

The first visible deformation was observed on the single crystal one hour after the sample reached 1100° F. Ten minutes later some markings were observed in the polycrystalline zone. Later on, several parallel slip bands appeared on the single crystal until one band became much more operative than the others. The appearance of the sample after test is shown in Figure 37.

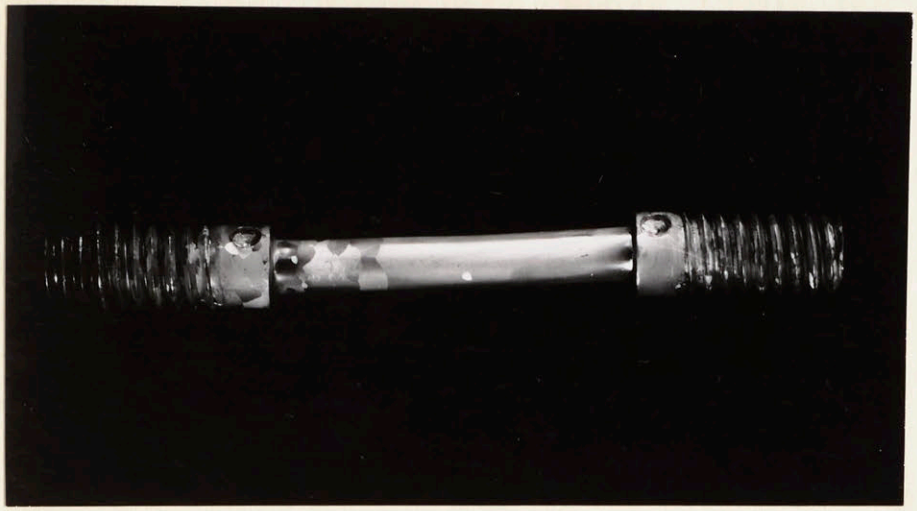

Figure 36. Special Test No. 90 - High Purity Aluminum Specimen Before Testing - Electrolytic Etch

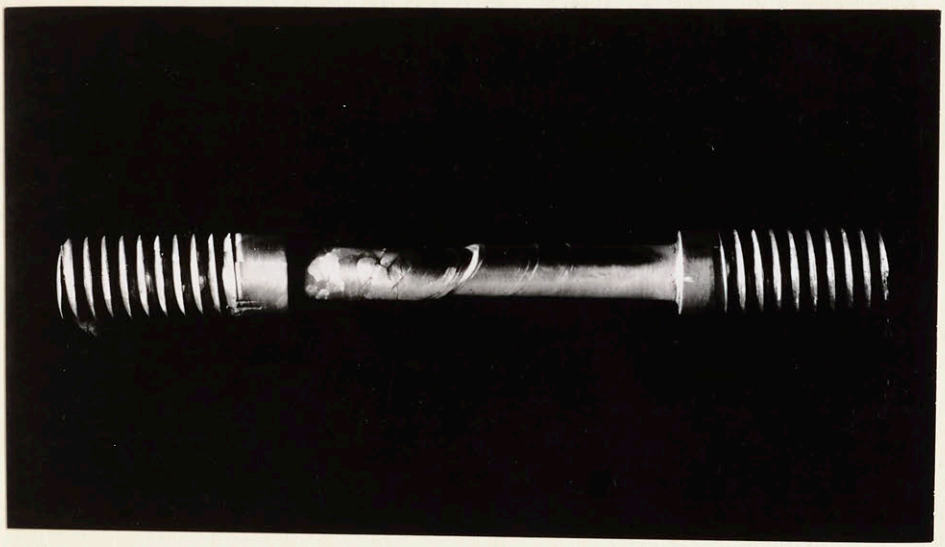

Figure 37. Special Test No. 90 - High Purity Aluminum Specimen of Figure 36 After Testing at 1100° F

It is observed that the single crystal deformed by slipping along parallel planes, which are at 45 degrees to the axis of tension. The polycrystalline zone resisted to the applied stress better than the single crystal. However, there is indication of flow at the grain boundaries. Moreover, considerable grain growth took place.

Figure 38 shows that the grain boundary flow did not occur along the original grain boundaries. In fact the "thickened" grain boundaries are displaced with respect to the grain boundaries of the original structure which is revealed by the etch.

6.104 Evidence of Grain Boundary Migration Under Strain (Test No. 33)

Sample No. 33 was a "standard" high purity, coarse grained specimen (heat treatment: 30 minutes at 1000° F), having a very large crystal in the middle portion of the sample after heat treatment. This crystal extended through the whole cross section of the specimen.

This specimen was first electro-etched to reveal the structure (Figure 39), then re-polished and tested at 700° F under a constant stress of 175 psi. The test was interrupted after 30 hours.

The specimen was then photographed in the same position shown in Figure 39 (see Figure 40). A comparison of Figure 39 with Figure 40 reveals that there was grain boundary flow along the original boundaries whereas the large central crystal slipped along parallel planes.

The microscopical observation confirmed the occurrence of grain boundary flow during testing. It also revealed the evidence of grain boundary migration under strain.

Figure 41 shows a micrograph of the sample after test in a part where scratches (horizontal lines) crossed a grain boundary (vertical line). The micrograph can be interpreted as follows: a boundary was

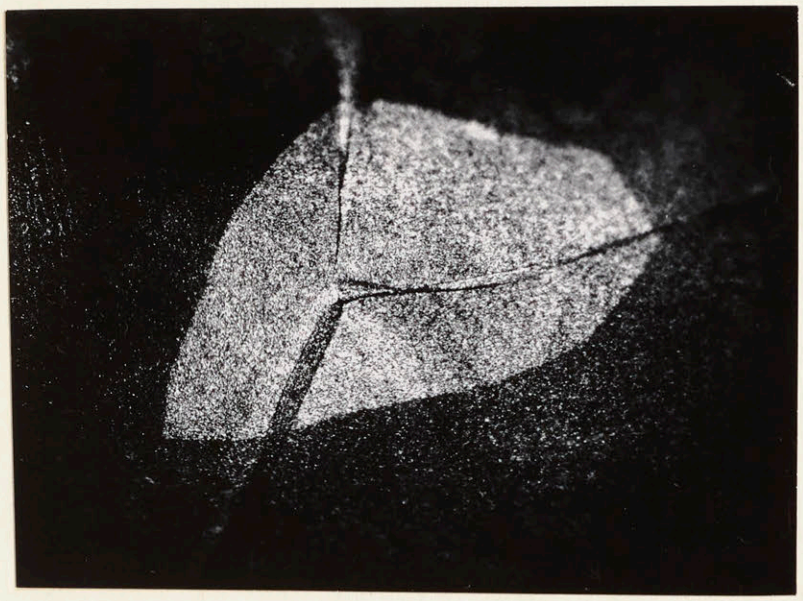

Figure 38. Specimen No. 90 After Testing at 1100° F. Electrolytically Etched to Reveal Grain Size Before Testing. Polarized Light. 50 x.

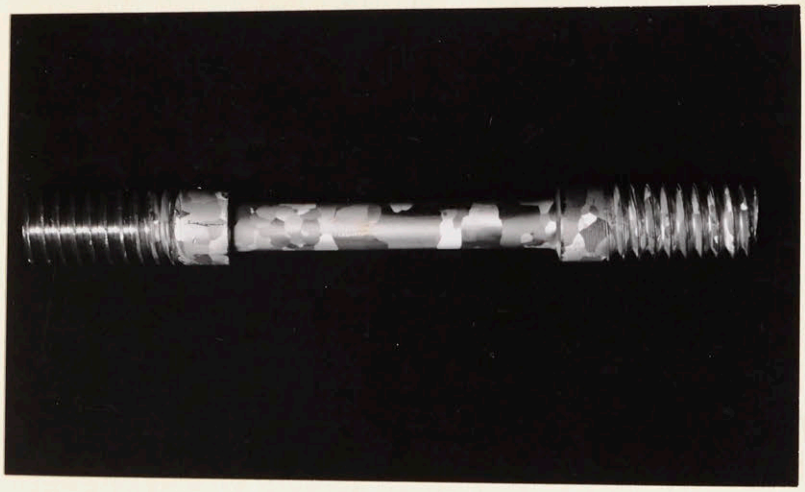

Figure 39. Special Test No. 33 - High Purity Aluminum Specimen Before Test - Electrolytic Etch

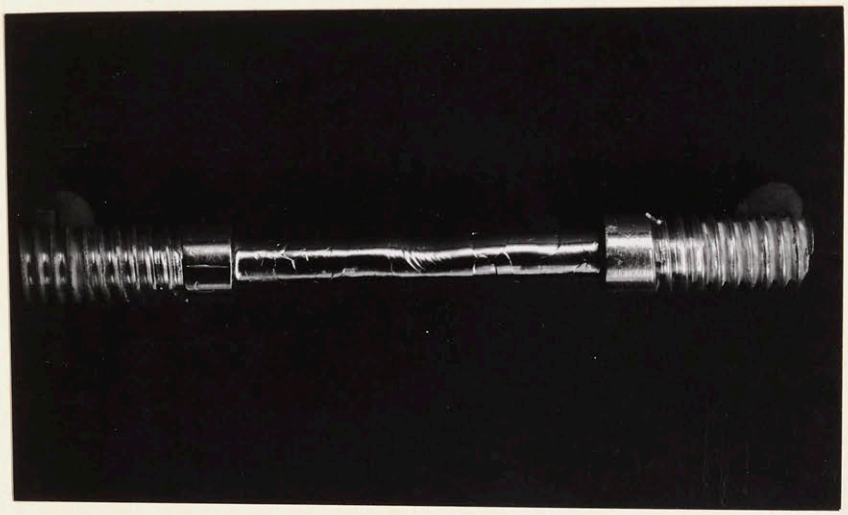

Figure 40. Special Test No. 33 - Specimen of Figure 39 after Testing at 700° F (total elongation = 8 percent). Repolished before testing. Unetched.

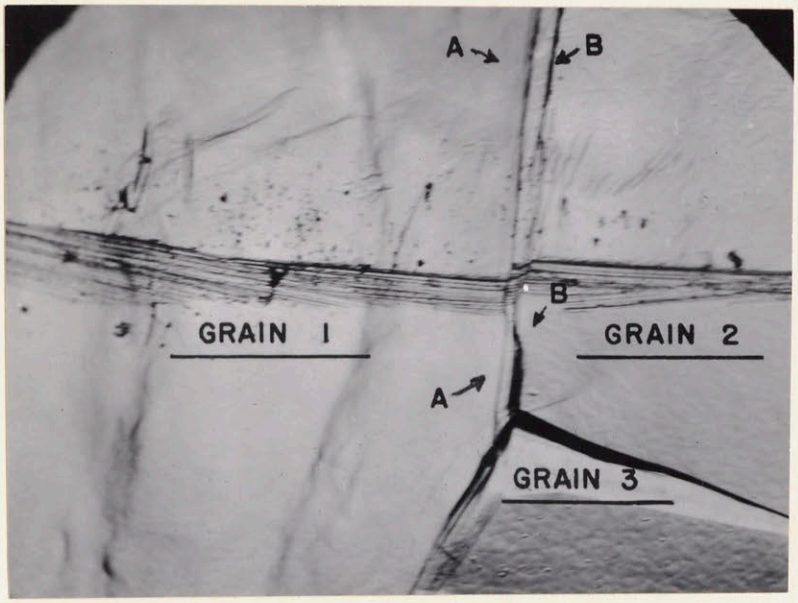

Figure 41. Special Test No. 33 - Micrograph showing grain boundary flow and grain boundary migration under strain. 150X (oblique illumination).

originally in the position A. Grain 1 and Grain 2 moved by gliding along the boundary A (see displacement of scratches). After a certain amount of displacement, strain was introduced in the system, due to the interlocking action of Grain 3. Under this driving force (strain energy) the boundary migrated from A to B, where it was able to flow again (see new displacement of the scratches).

As the boundary flows, a step is formed on the polished surface of the specimen; therefore the boundary is revealed under the microscope as a black line. The apparent "thickness" of the grain boundary depends on the amount of displacement, and on the relative orientation of the boundary with respect to the polished surface (see "very thick" boundaries at the 3-grain junction in Figure 41).

This interpretation of Figure 41 was supported by many other observations. Evidence of the same phenomenon is reported in Figure 42. After the pictures of Figure 42 were taken, the sample was partially etched and the position of the grain boundaries after testing was revealed by using the techniques described in Appendix III. ("Galvanic" etching and observation in polarized light). A sketch of the micrographs reported before was done in Figure 43. The position of the grain boundaries after creep testing was superimposed.

Figure 43 suggests that the combined mechanism of grain boundary flow and grain boundary migration was operative in this case. The initial structure A changed into the final structure F by grain boundary migration under strain. A few intermediate steps B, C, D, E were revealed by the grain boundary flow.

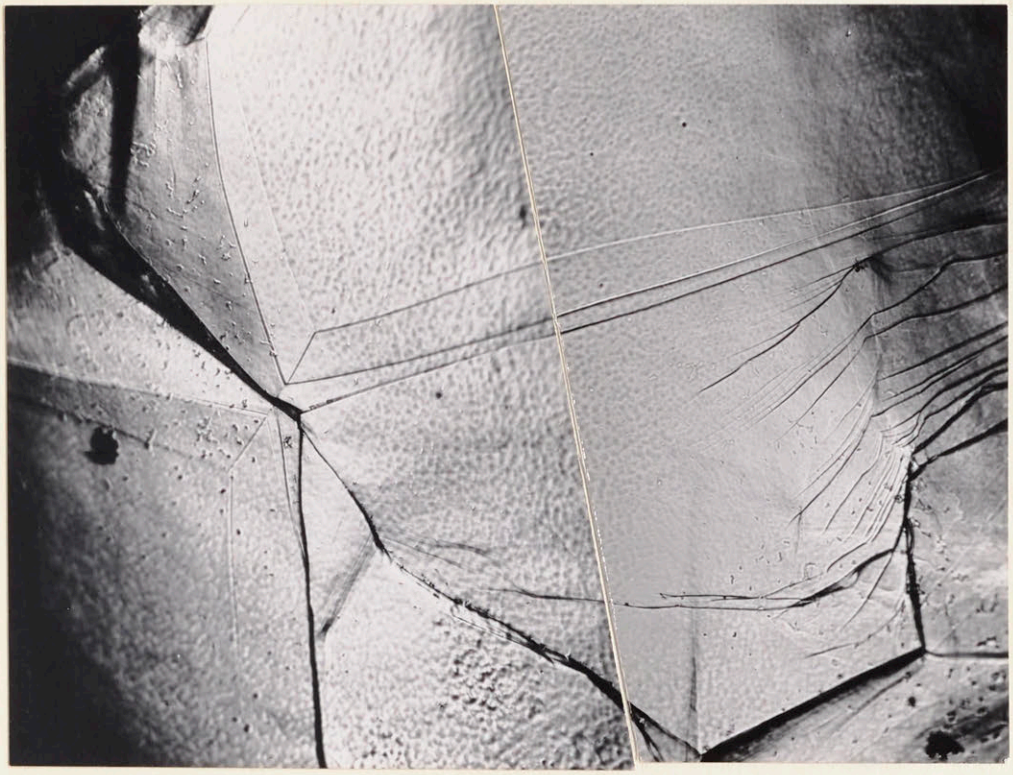

Figure 42. Special Test No. 33 - Micrograph showing grain boundary flow and grain boundary migration under strain - 150 × oblique illumination.

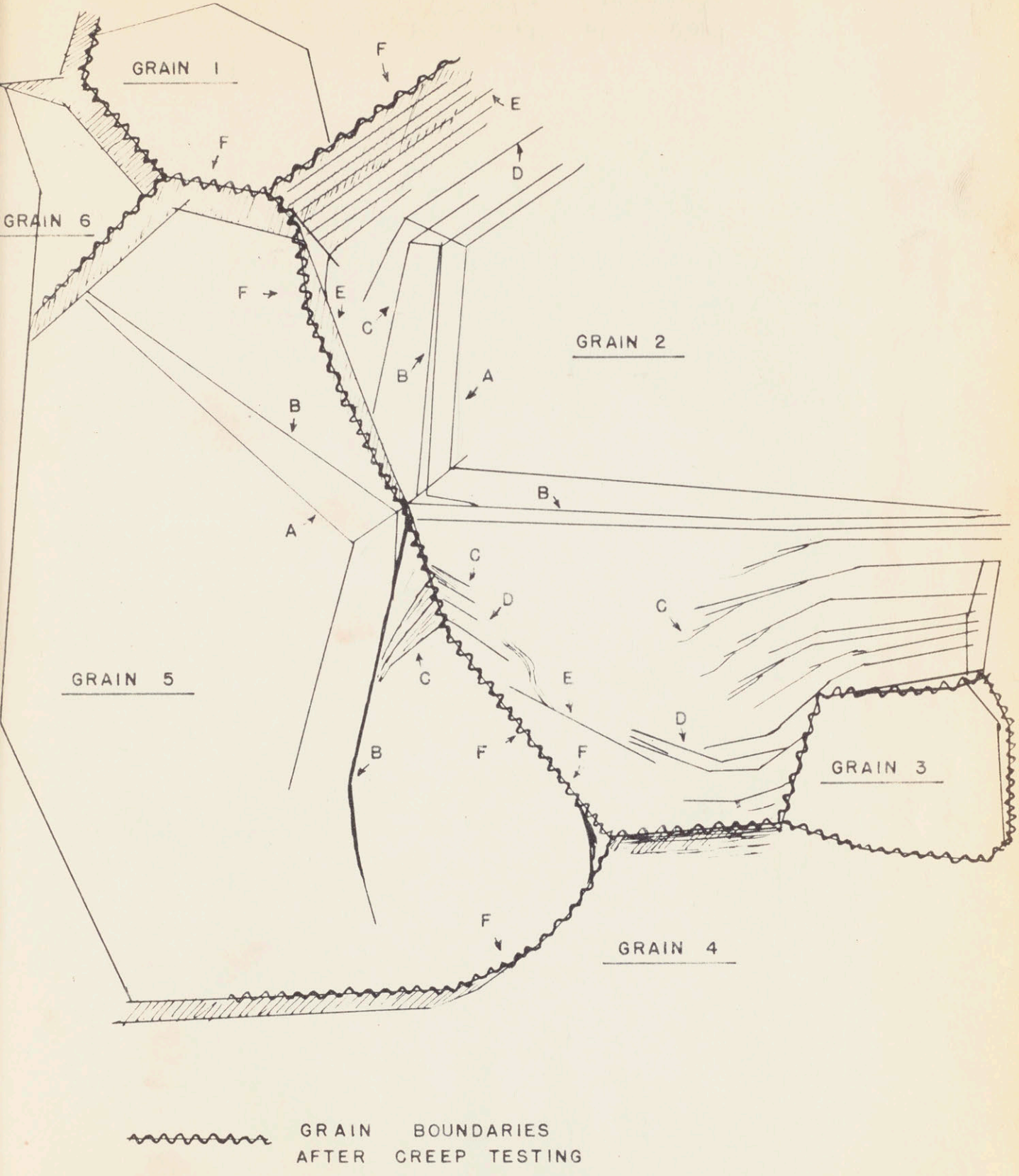

Figure 43. Sketch of the microstructure presented in Figure 42. The direction of grain boundary migration is indicated by the steps A-B-C-D-E-F.

The grain boundary migration under strain in aluminum was observed before by Sperry [45] and by Beck and Sperry [46] [47], who used different techniques. Their investigation lead to the conclusion that the grain boundaries move away from their center of curvature, when the driving force is strain energy, while the grain boundaries move toward their center of curvature when the driving force is surface energy. The results of Test No. 33 agree with the conclusions reached by Beck and Sperry; although the experimental conditions were quite different.

The combination of grain boundary flow and grain boundary migration gives very peculiar effects in certain cases. Figure 44 and Figure 45 are two examples. The "stair-stepped" appearance of these micrographs can be interpreted as follows: one grain boundary was located in such a position as to undergo a considerable amount of flow without straining the neighboring grains. This grain boundary which appears very "thick" in the micrograph did not migrate. The position of other grain boundaries was such as to induce strains after a small amount of flow. Therefore these grain boundaries had to migrate. The combination of these processes gave origin to the"stair-stepped" appearance.

The combination of grain boundary migration and grain boundary flow was observed in many other specimens, but only for those testing conditions in which "High Temperature" behavior prevails.

Figure 44. High Purity Aluminum - Coarse Grained - Specimen No. 82. 1100° F - Rupture time = 3.66 hours - 0.25 inch part of the sample 150× (oblique illumination).

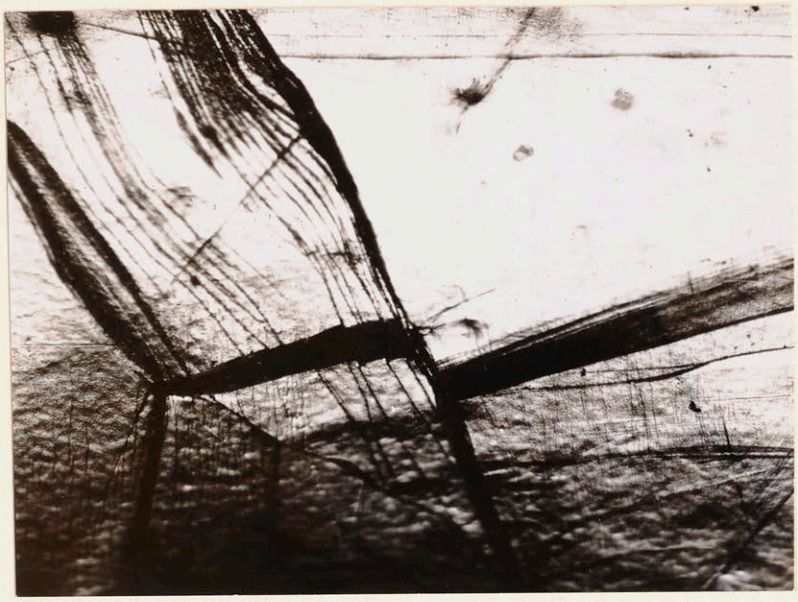

Figure 45. High Purity, Coarse Grained - Specimen No. 49. 900 ° F, after 197 hours - total elongation = 12.5 percent. 150×

6.11 Standard Tests

6.111 High Purity Aluminum

Coarse Grained Specimens

A change in the appearance of the deformed samples occurs as the testing conditions change. The effect of the strain rate at constant temperature on the mode of deformation has been demonstrated in Part A by comparing the photographs of three specimens tested at 500° F (see Figure 15). In this section, further evidence of this fact will be given.

For this purpose the curves "Log. Stress versus Log. Minimum Creep Rate" of Figure 13 have been replotted in Figure 46. The reference numbers which appear in Figure 46 help relate the photographs to the conditions of testing. It has been said before that a "Transition" occurs along the line A-B-C, of Figure 46. If lines are drawn parallel to the line A-B-C, the isothermal curves are approximately cut in the points 1, 2, 3 - 4, 5, 6 - 7, 8, 9- and 10, 11, 12. The testing conditions corresponding to these reference points are:

(a) Points 1, 2, 3,: "Low Temperature"

(b) Points 4, 5, 6,: "Transition"

(c) Points 7, 8, 9: "High Temperature"

(d) Points 10, 11, 12,: "Higher Temperature than (c)"

The specimens corresponding to the conditions (a), (b), (c) and (d) are presented in Figure 47 through Figure 50.

Figure 47 shows that the "Low Temperature" specimens are characterized by very strong grain boundaries, which hinder the deformation of the grains. The grains deform by slip; the slip spacing is very small. The fracture occurs along a more or less irregular edge.

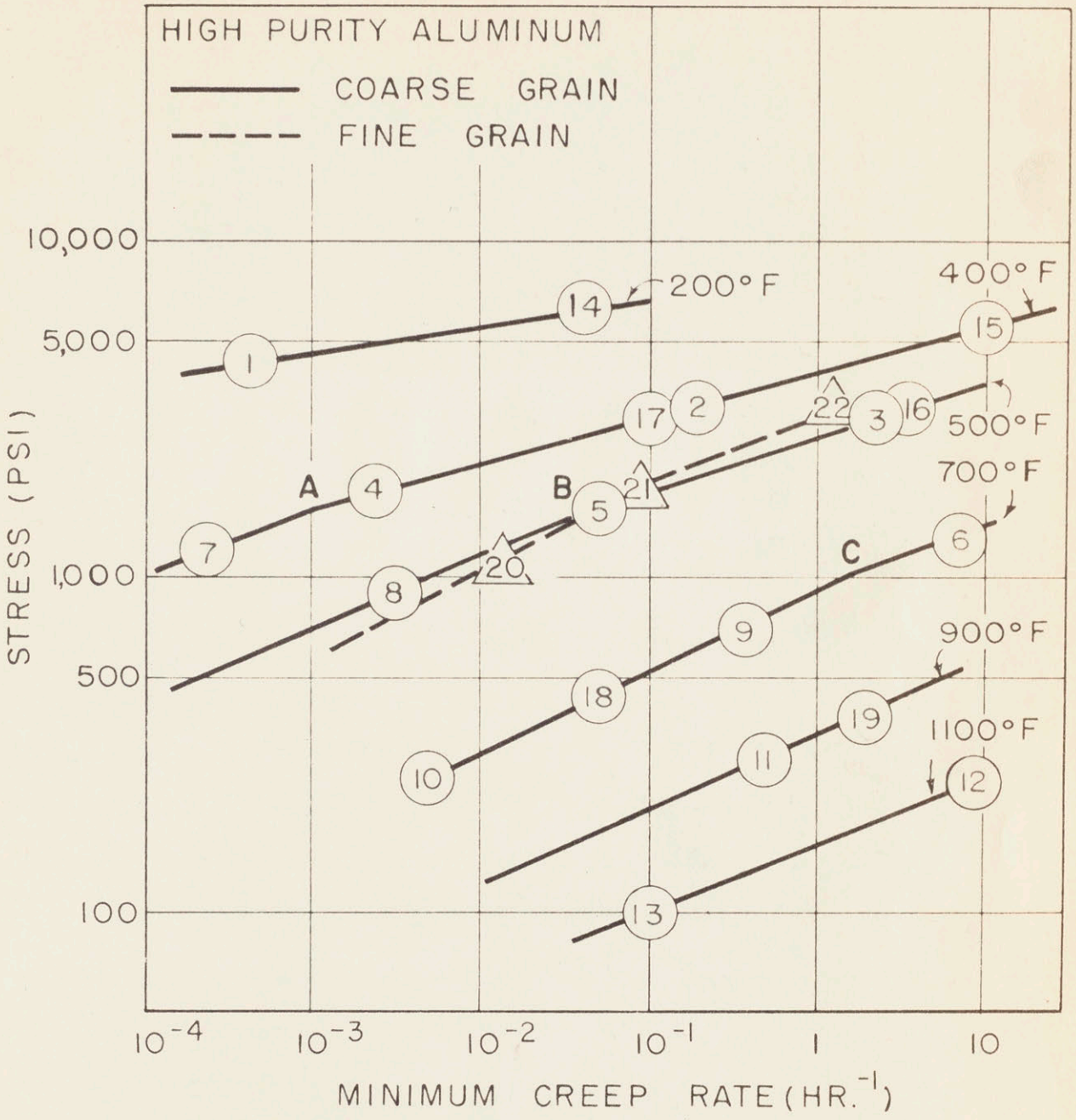

Figure 46. Log-log plot of stress versus minimum creep rate for high purity aluminum, replotted from Figure 13. The reference numbers refer to the photographs and micrographs of Figure 47 to Figure 49.

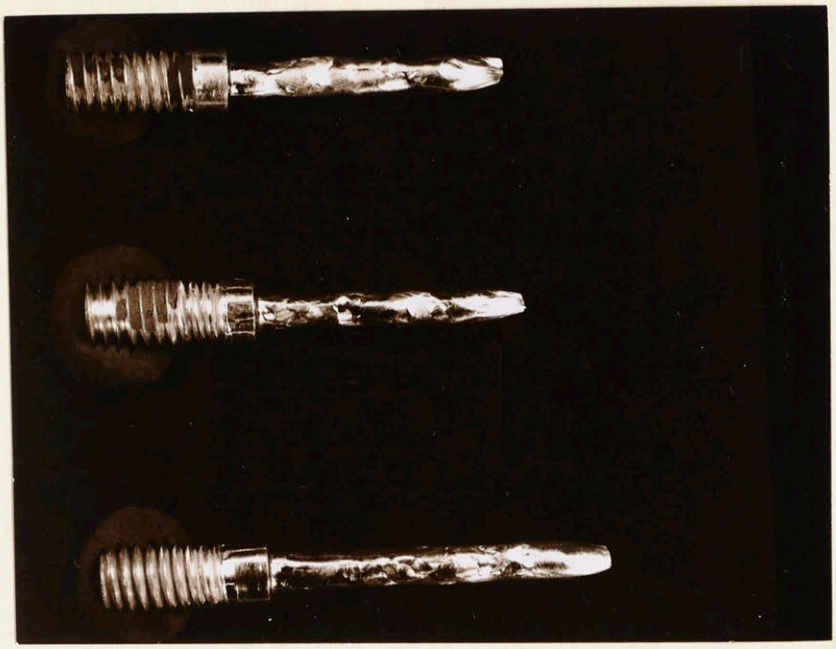

Figure 47. Top to Bottom: Specimens No. 70, 37, and 88 (Points No. 1, 2, and 3 of Figure 46.) High purity coarse grained aluminum tested at low temperature conditions.

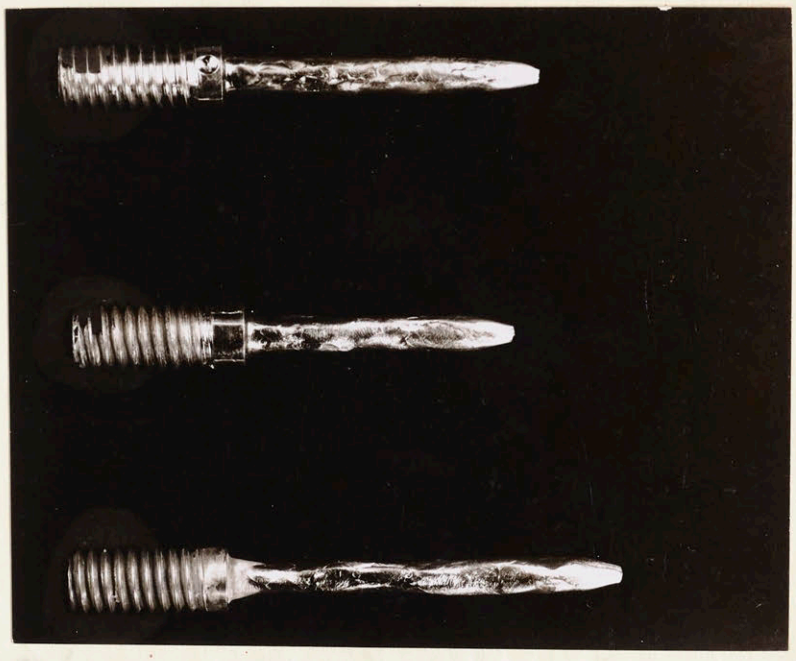

Figure 48. Top to Bottom: Specimens No. 48, 32 and 89 (Points No. 4, 5, and 6 of Figure 46). High purity coarse grained aluminum tested near the transition from low temperature to high temperature behavior.

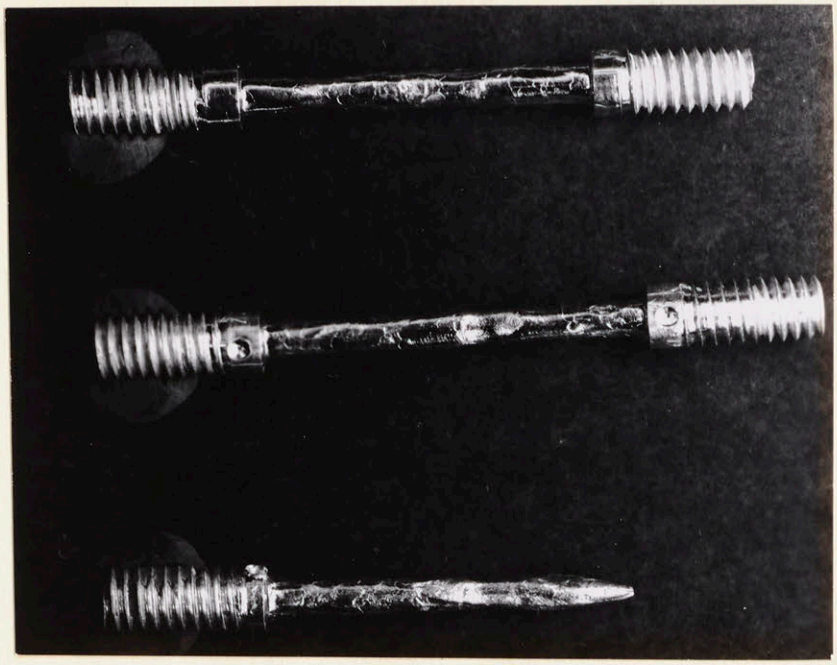

Figure 49. Top to Bottom: Specimens No. 66, 71, and 22 (Points No. 7, 8, and 9 of Figure 46). High purity coarse grained aluminum tested at high temperature conditions.

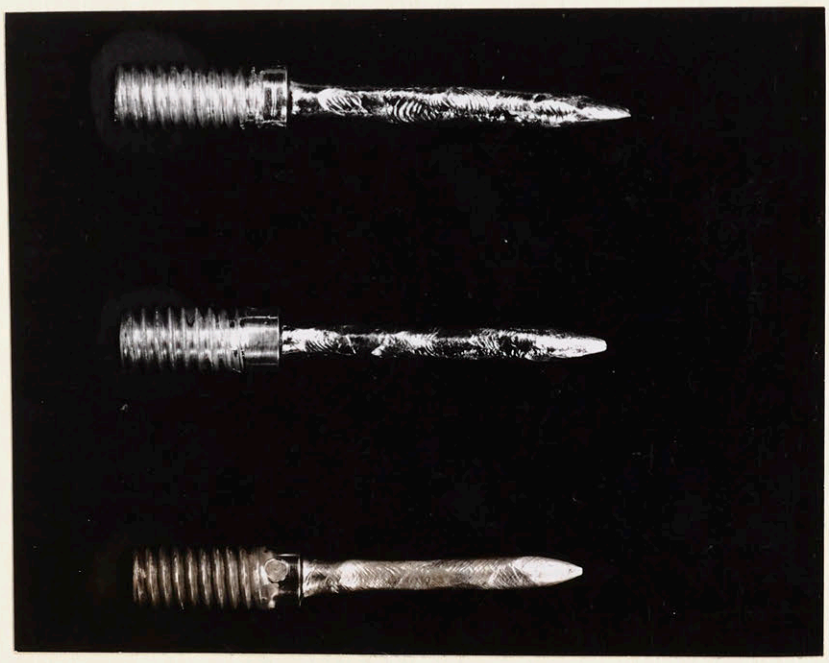

Figure 50. Top to Bottom: Specimens No. 24, 44 and 80 (Points No. 10, 11 and 12 of Figure 46). High purity coarse grained aluminum tested at higher temperature than the specimens of Figure 49.

Figure 48 shows that, as the "Transition" is approached, the specimens deform in a more uniform way, since the grain boundaries do not hinder the deformation of the grains. The fracture edges are smaller than in the case of "Low Temperature" conditions. The slip spacing is larger.

When the "High Temperature" conditions are reached (Figure 49) the grain boundaries contribute to the deformation of the specimen by flowing; therefore, the grain boundaries appear "thicker". The slip spacing is larger, and the fracture edges are smaller.

At still higher test temperatures (Figure 50) the grain growth becomes appreciable and the slip spacing becomes larger: consequently the deformation of the specimen is more irregular. The dull appearance of the specimen No. 80 is due to oxidation.

If the testing conditions are changed to much higher temperature or slower strain rates, big crystals are formed and the deformation is not uniform at all, as shown by Figure 51. This picture shows that a big crystal was formed at one end of the specimen and deformed by gliding along two parallel planes.

Other information on the mode of deformation of high purity aluminum was obtained by observing the samples under a magnification of 150×. A few micrographs are presented in Figures 52 through 64. In these pictures an horizontal line is parallel to the axis of tension. Only one or two micrographs of each sample appear (these micrographs have been chosen as the most representative ones). However, it should be emphasized that a great variation in the appearance of the sample occurs from one point to another, and therefore no micrograph can be called completely representative.

The micrographs presented above show that, as the conditions of testing change from "Low Temperature" to "High Temperature", :

(a) the spacing of the slip bands increases

(b) the grain boundaries become more active ("thicker")

(c) the deformation becomes less localized along definite planes.

Figure 51. Specimen No. 82 (Point No. 13 of Figure 46). High Purity coarse grained aluminum tested at very high temperature.

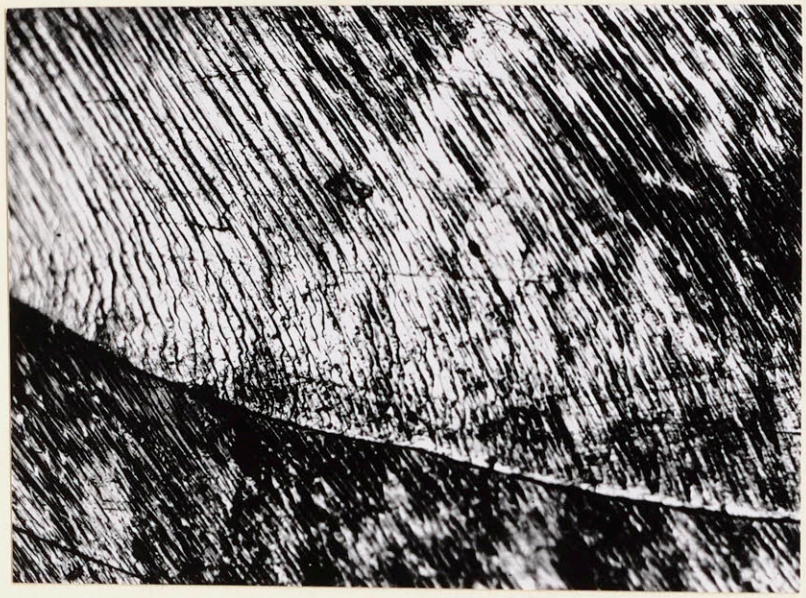

Fig. 52 Specimen No. 84. (Point No. 14 of Figure 46). High Purity coarse grained aluminum. R. A. = 18 percent. 200° F, 3.4 hours rupture time. 150 ×.

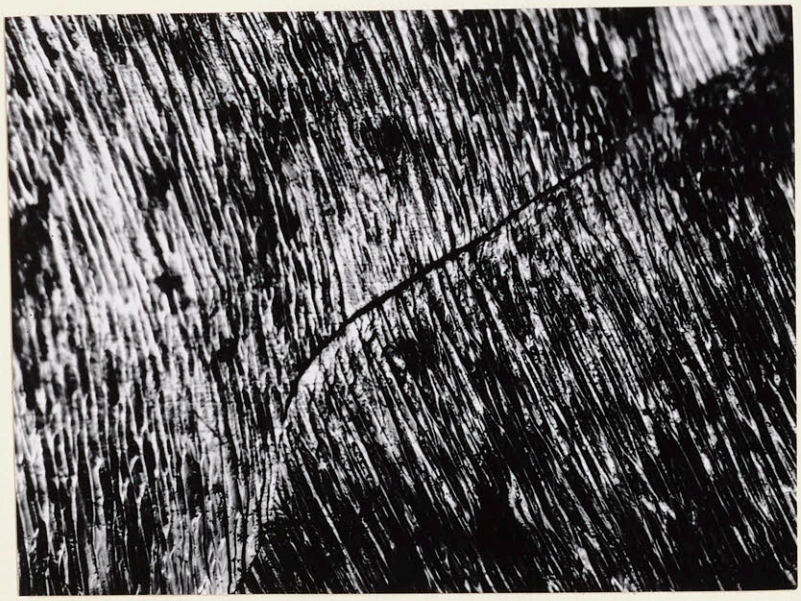

Figure 53. Specimen No. 93 (Point No. 15 of Figure 46). High Purity coarse grained aluminum. R. A. = 12 percent 400° F, less than 0.01 hour rupture time. 150 ×.

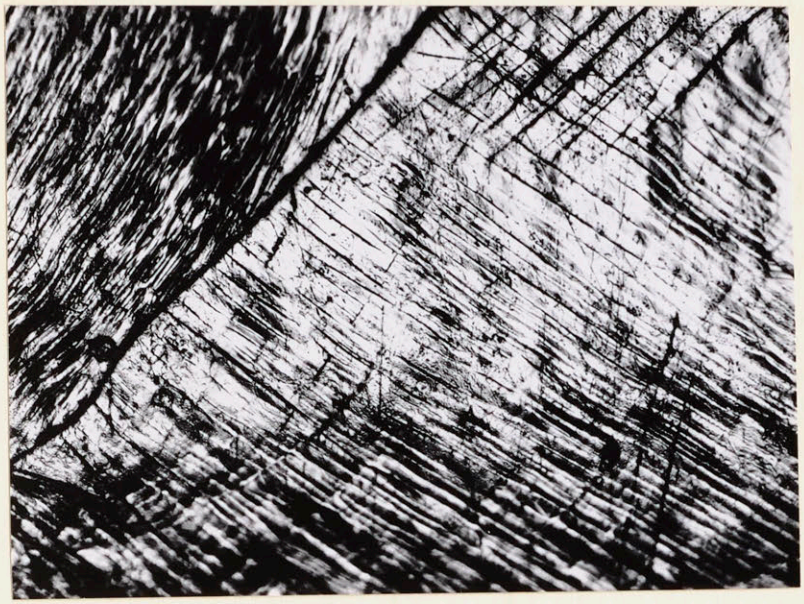

Figure 54. Specimen No. 63 (Point No. 16 of Figure 46). High Purity coarse grained aluminum. R. A. = 12 percent - 500° F, 0.05 hours rupture time. 150 ×.

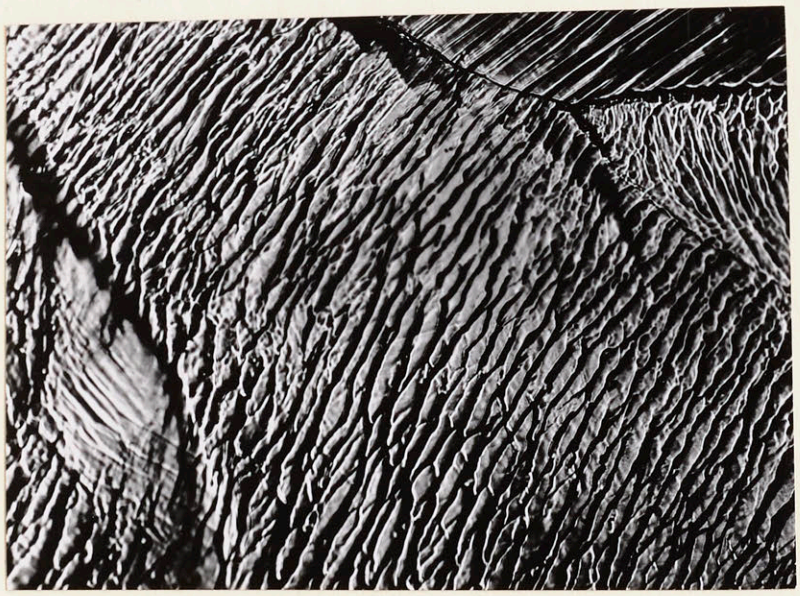

Figure 55. Specimen No. 35 (Point No. 17 of Figure 46). High Purity coarse grained aluminum. R. A. = 15 percent. 400 ° F, 1.54 hours rupture time, 150 × (oblique illumination).

Figure 56. Specimen No. 32 (Point No. 5 of Figure 46). High Purity coarse grained aluminum. R. A. = 35 percent. 500° F, 8.25 hours rupture time. 150 × (oblique illumination).

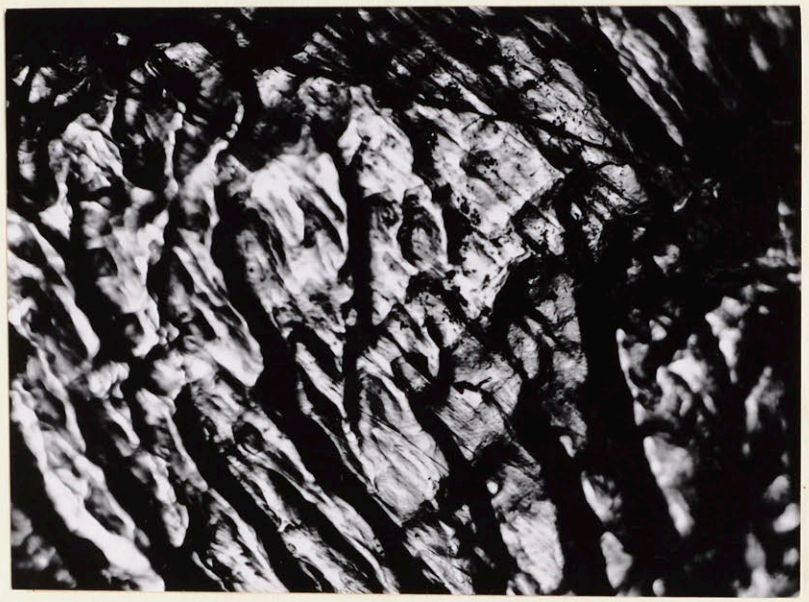

Figure 57. Specimen No. 89 (Point No. 6 of Figure 46). High Purity coarse grained aluminum. R. A. 40 percent. 700° F, 0.079 hours rupture time. 150 ×.

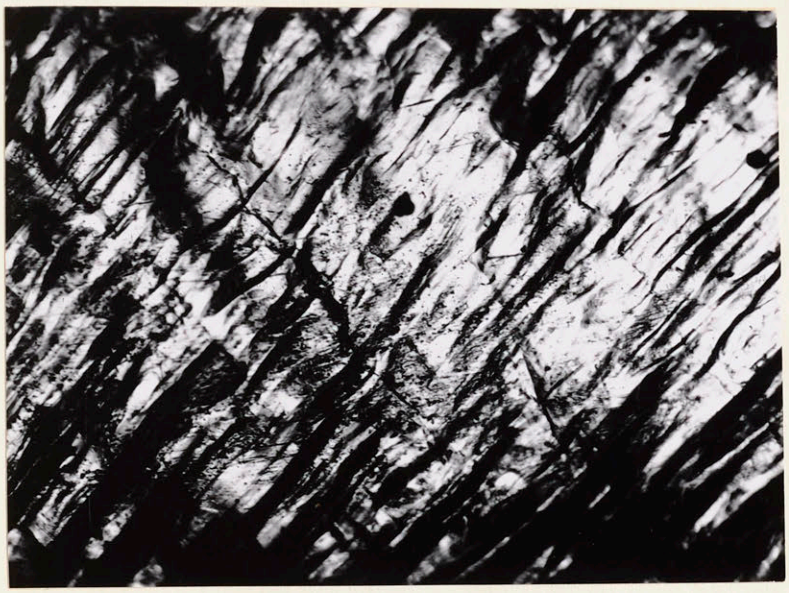

Figure 58. Specimen No. 89 (Point No. 6 of Figure 46). High Purity coarse grained aluminum. R. A. 40 percent. 700° F, 0.079 hours rupture time. 150 ×.

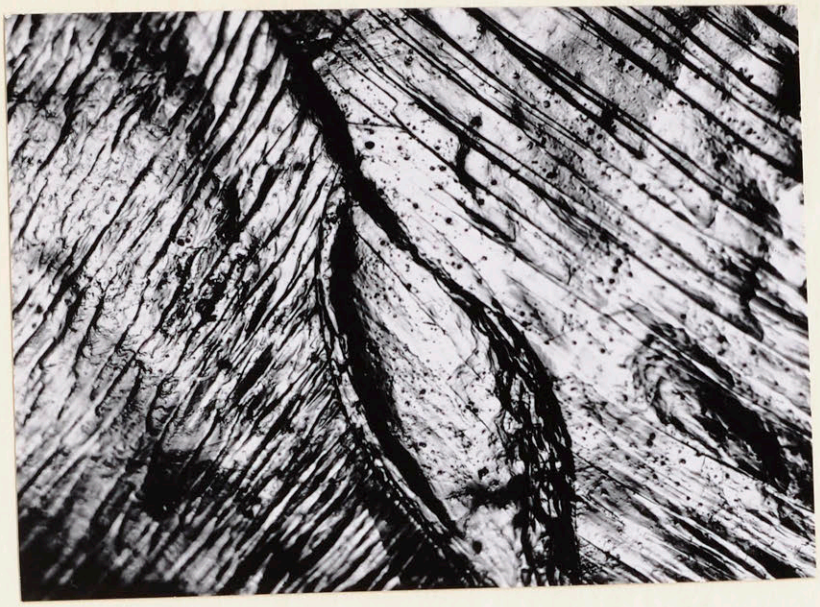

Figure 59. Specimen No. 66 (Point No. 7 of Figure 46). High Purity coarse grained aluminum. R. A. 18 percent - 400° F, 850 hours estimated rupture time. 150 ×.

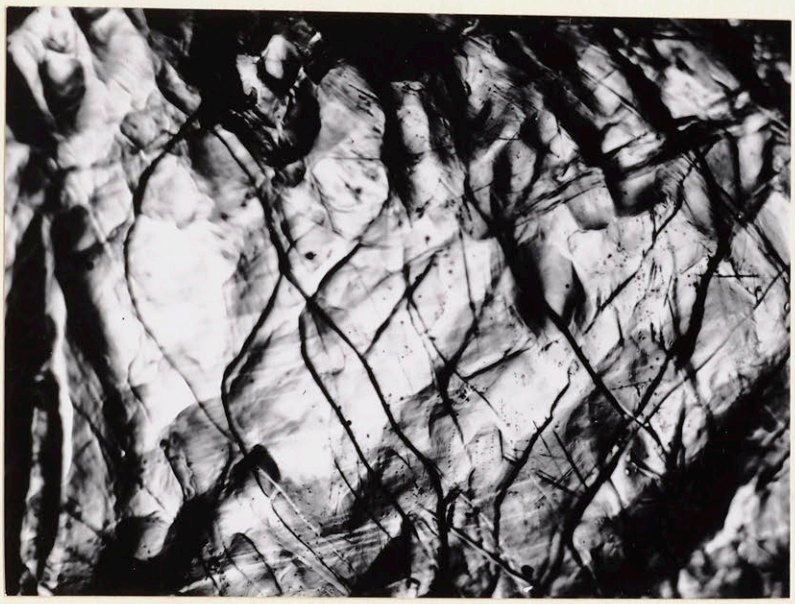

Figure 60. Specimen No. 66 (Point No. 7 of Figure 46). High Purity coarse grained aluminum. R. A. 18 percent. 400° F, 850 hours estimated rupture time. 150 ×.

Figure 61. Specimen No. 71 (Point No. 8 of Figure 46). High Purity coarse grained aluminum. R. A. 30 percent. 500° F, 140 hours estimated rupture time. 150 ×.

Figure 62. Specimen No. 71 (Point No. 8 of Figure 46). High Purity coarse grained aluminum. R. A. 30 percent. 500° F, 140 hours estimated rupture time. 150 ×.

Figure 63. Specimen No. 23 (Point No. 18 of Figure 46). High Purity coarse grained aluminum. R. A. 40 percent. 700° F, 13.5 hours estimated rupture time. 150 ×.

Figure 64. Specimen No. 47 (Point No. 19 of Figure 46). High Purity coarse grained aluminum. R. A. 30 percent. 900 ° F, 0.33 hours rupture time. 150 ×.

The metallographic evidence of a breakdown of the grains into "sub-grains" at elevated temperature is shown by Figure 60, Figure 62, Figure 63, and Figure 64. As the conditions are changed to "Higher Temperature", the size of each sub-grain increases. The size of the sub-grains in each sample is fairly constant and the distribution of the sub-grains in each grain is very regular.

Figure 62 shows that two rows of sub-grain boundaries form irregular lines, which are normal to the main system of slip bands. This fact was observed in other cases.

The striking similarity between rows of sub-grains and interslip spaces suggest that the sub-grain may be formed through a slip process. In this respect the sub-grains would be similar to Bragg's crystallites: however, the testing conditions are such that recovery is very active and therefore no strain can remain in the lattice after deformation. The slip spacing is very large and each slip band consists of a large number of slip planes: therefore, the appearance of the deformed surface is rather irregular.

A support to this hypothesis is given by the fact that the observed sub-grains have dimensions which are of the same order of magnitude of the slip spacing.

The average slip spacing was determined on the micrographs presented above, or directly on the sample where the spacing was larger than 0.1 millimiters. This spacing was determined on the surface of the specimen irrespective of the amount of total strain which varied between 10 percent

and 40 percent. The temperature was not regarded as a variable. Considering the method of determination of slip spacing, the values of average slip spacing are worthy only of indicating order of magnitude values.

The logarithm of the applied stress was plotted versus the logarithm of the average slip spacing in Figure 65: a linear relationship was obtained.

The average dimensions of the "cells" are also plotted in Figure 65 to show that the "cells" have dimensions which are similar to the average slip spacing. The solid line of Figure 65, which has a slope -1, indicates that the average slip spacing is inversely proportional to the applied stress, at least as a first approximation. This fact is in agreement with Orowan's formula (6.91): however, the average spacing was found to be 10 to 50 times larger than the minimum spacing predicted by Orowan's formula; but in closer agreement with the experimental values obtained by Yamaguchi[42]. The divergence between experiment and theory can be justified by assuming that a larger amount of strain is necessary to obtain the minimum slip spacing.

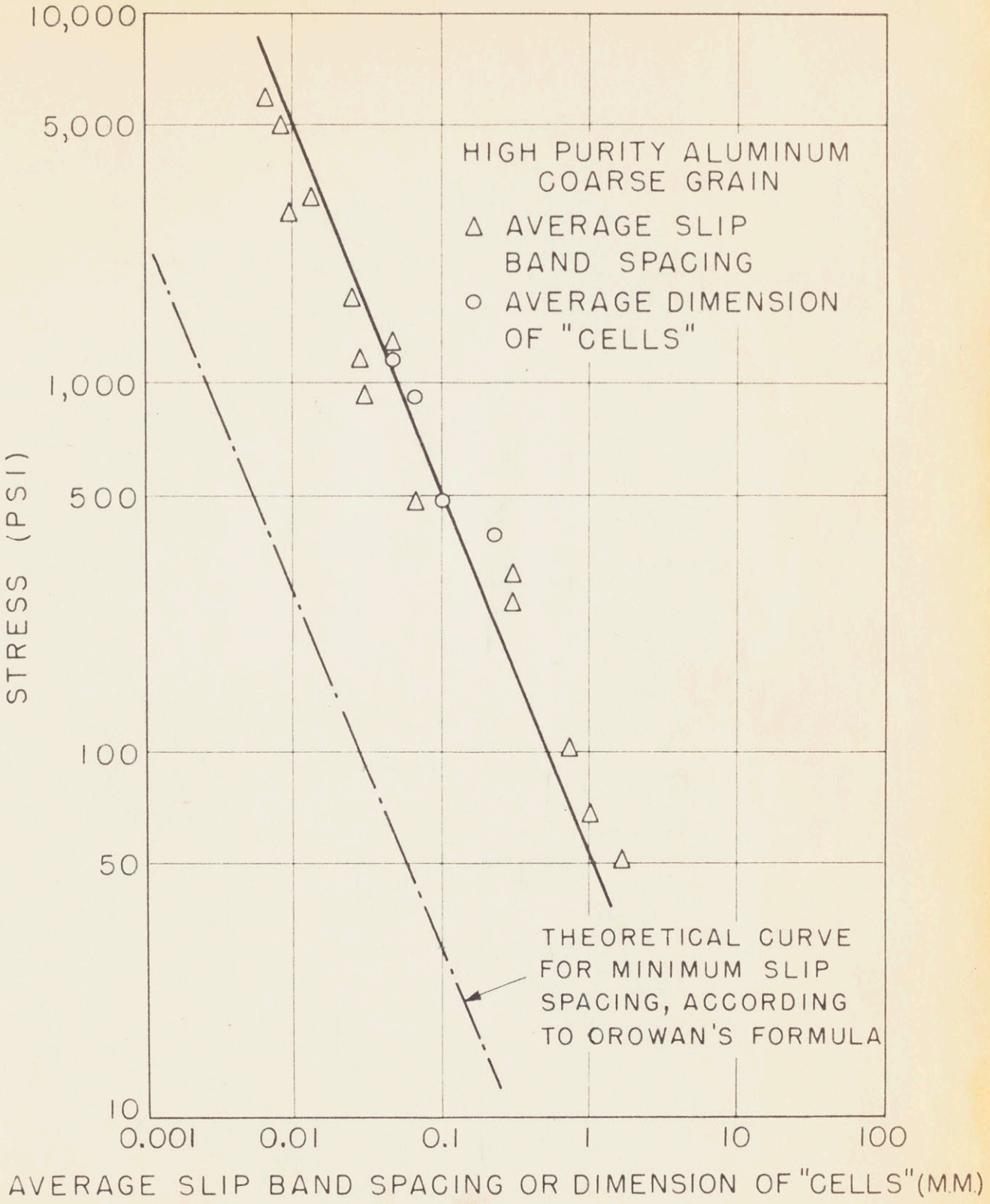

Figure 65. Log-log plot of stress versus average slip spacing and versus average dimensions of the sub-grains. High purity coarse grained aluminum.

Fine Grained Specimens

Similar conclusions are reached when the fine grain samples are observed. Figure 66 through Figure 69 show the micrographs of the surface of the samples tested at 500° F under different stress conditions. Figure 66 is from that part of the specimen which has a diameter of 0.25 inch. Here the applied stress was about 2.5 times smaller than the stress applied to the test portion of the sample. The micrograph shows an appreciable amount of grain boundary flow and very little deformation of the grains.

Figure 67 shows the typical aspect of a "High Temperature" sample; there is flow at the grain boundaries, and absence of slip bands in most of the grains, however, one wavy band crosses the largest grains.

When the "Low Temperature" conditions are applied to the specimen, the slip bands become more evident (Figure 68) and the slip spacing decreases as the stress increases (Figure 69).

In order to compare these results to the results obtained for coarse grained samples, the slip spacing was calculated from the plot of Figure 65, for the stresses applied to the fine grained samples. The calculated spacing was multiplied by the magnification of the micrographs (150 ×) and the following results were obtained:

for stress corresponding to Figure 67: spacing at 150 × = 7.5 mm.

for stress corresponding to Figure 68: spacing at 150 × = 3.9 mm.

for stress corresponding to Figure 69: spacing at 150 × = 1.8 mm.

The micrographs show that there is good agreement between the calculated and the observed spacings of Figure 68 and Figure 69.

Figure 66. Specimen No. 58 High Purity fine grained aluminum - 0.25-inch part of the specimen. 500° F - Calculated reduction of area= 0.5 percent. 150 ×.

Figure 67. Specimen No. 58 (Point No. 20 of Figure 46) High Purity fine grained aluminum. R.A. = 14 percent. 500° F, 28 hours rupture time. 150 ×.

Figure 68. Specimen No. 57 (Point No. 21 of Figure 46). High Purity fine grained aluminum. R. A. = 15 percent. 500° F, 5.43 hours rupture time. 150 × .

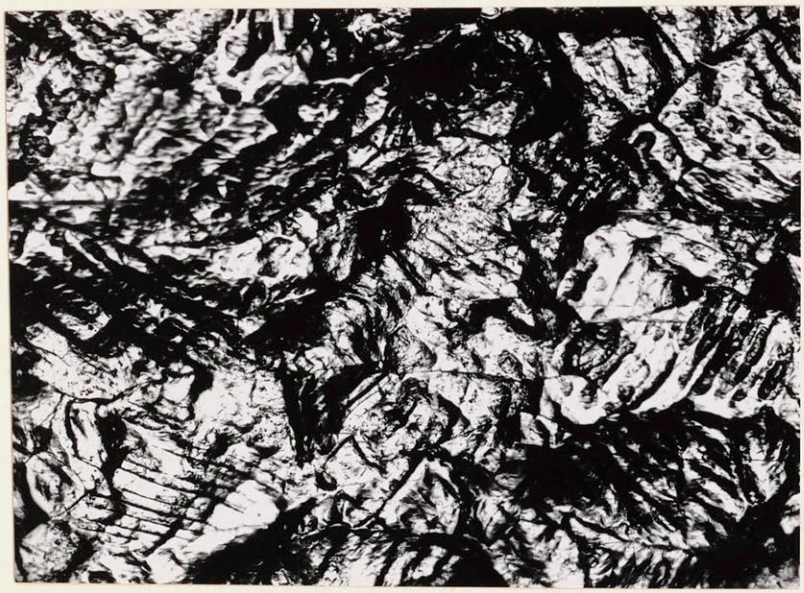

Figure 69. Specimen No. 56 (Point No. 22 of Figure 46) High Purity fine grained aluminum. R. A. = 17 percent. 500° F, 0.44 hour rupture time. 150 ×.

Figure 67 demonstrates a similar agreement if the spacing between the visible slip bands and the nearest grain boundary is measured. This fact suggests that the grain boundary inhibits the development of slip bands in a manner similar to the action of the neighboring slip bands. If this is true, slipless flow should be observed only if the grain size is fine enough for the applied stress. Under similar conditions a much coarser grained sample should show slip bands. A sample with mixed grain size should show slip bands only in grains which are larger than a critical size. The observations made on high purity and 2S aluminum support this hypothesis, but more critical experiments are needed to confirm these conclusions.

6.112 2S Aluminum

The curves "Log. Stress versus Log. Minimum Creep Rate" of Figure 17 for 2S aluminum have been replotted in Figure 70.

Photomicrographs of samples tested at the conditions indicated by the reference points of Figure 70 are presented in Figure 71 to Figure 74. These micrographs have been taken on the surface of the deformed samples. Since the grain size is very fine and because a heavy oxide film is formed on the surface of the specimen during testing, the micrographs are not as clear as the ones presented before for the high purity aluminum. However, the micrographs show a progressive change in the appearance of the sample as the testing conditions are changed from "Low Temperature" to "High Temperature" behavior.

There is no indication of grain boundary flow in Figure 71. Slip bands are visible in all of the grains. When the "transition" conditions are reached (Figure 72 and Figure 73) the slip bands are not present in all the grains: the slip spacing is larger and the grain

boundaries are "thicker". At "High Temperature" (Figure 74) no slip bands are visible; grain boundary flow and grain boundary migration occur; the grain boundary migration is not as pronounced as in the high purity aluminum. A few intercrystalline cracks were seen on the surface of the specimen.

The results concerning the stress dependence of the slip spacing for high purity aluminum are applicable to the 2S aluminum. This conclusion is only approximate, since a close evaluation of the slip spacing for 2S aluminum is not possible. However, it is worth mentioning that the slip spacing calculated from the plot of Figure 65 for the stress conditions of Figure 74 is 0.1 millimiters, which corresponds to 15 millimeters at a magnification of 150 ×. Figure 74 whows that no grain is larger than 15 mm.; this may be an explanation for the "slipless" appearance of the surface of this sample.

A few 2S aluminum samples were sectioned and examined after electrolytic polishing and electrolyting etching. Figure 75 and Figure 76 show typical appearances of samples deformed at "Low Temperature": the grains are elongated and the grain boundaries do not show any evidence of separation. These samples failed by drawing down to a point fracture. The longitudinal section near the fracture point shows a progressive elongation of the grains, with no indication of recrystallization.

Figure 77 is a longitudinal section of a sample tested at 1100° F under "Low Temperature" conditions. It was mentioned before that at 1100° F elongated coarse grains grow, especially along the surface of the specimen (see Figure 19 in Part A). Figure 77 reveals that the appearance of the

polycrystalline part of the section is similar to the appearance of Figure 75 and Figure 76: it is a typical "Low Temperature" behavior. Near the fracture point one or a few big grains are formed.

The presence of intercrystalline cracking at "High Temperature" is shown by Figure 78. It should be noticed that the electrolytic polish attacks sharp edges preferentially and makes the cracks deeper.

Another example of intercrystalline cracking is presented in Figure 79, where a big crystal is also visible along the surface of the sample. The formation of big crystals is characterisitc of testing at 1100° F.

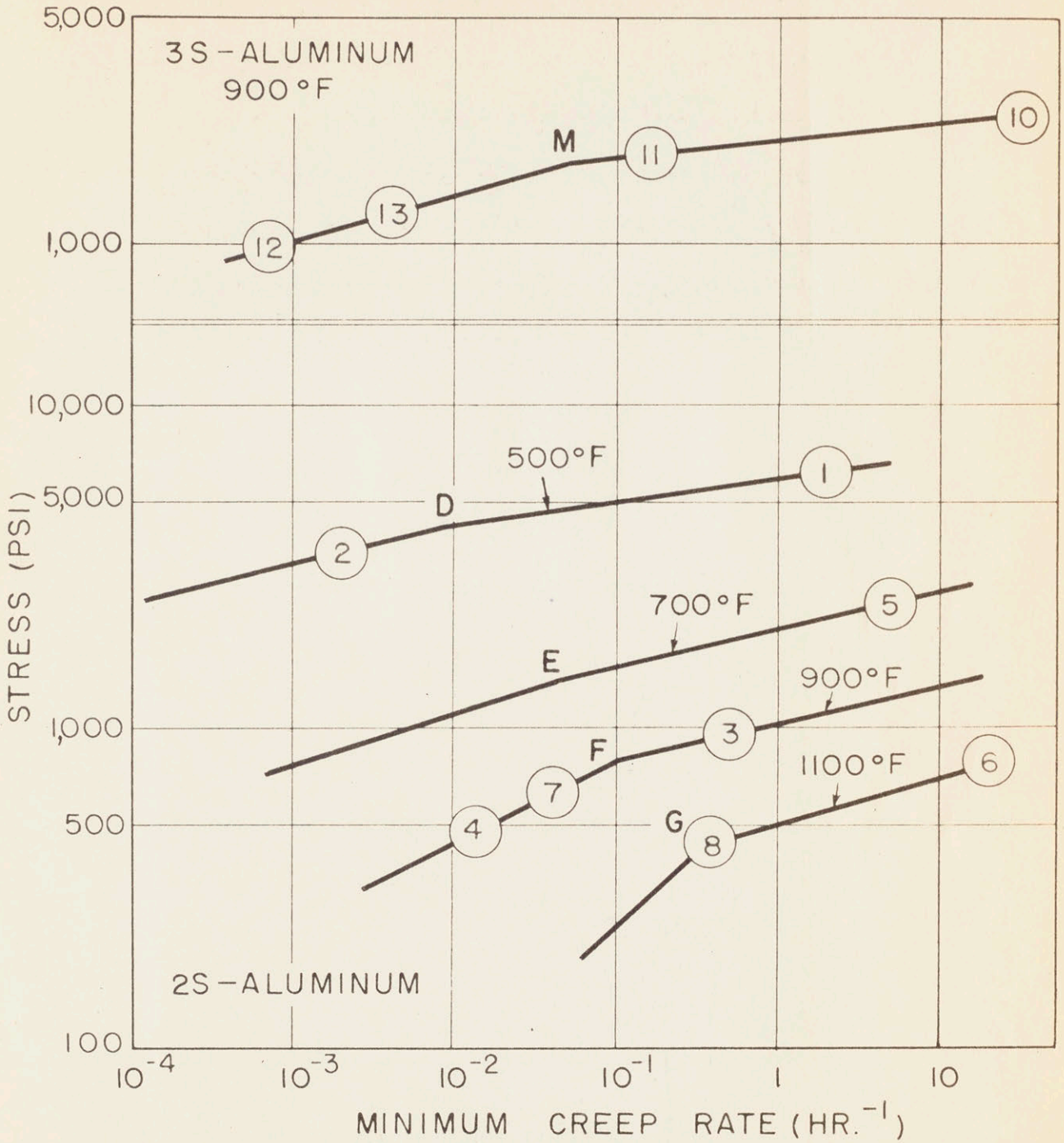

Figure 70. Log-log plot of stress versus minimum creep rate for 2S and 3S aluminum, replotted from Figure 17. The reference numbers refer to the micrographs of Figure 71 to Figure 85.

Figure 71. Specimen No. 204 (Point No. 1 of Figure 70). 2S aluminum 500° F, 0.11 hour rupture time. R.A. = 26 percent. 150 ×.

Figure 72. Specimen No. 203 (Point No. 2 of Figure 70). 2S aluminum. 500° F, 101 hours rupture time. R.A. = 16 percent. 150 ×.

Figure 73. Specimen No. 218 (Point No. 3 of Figure 70). 2S aluminum. 900° F, 0.95 hour rupture time. R. A. = 26 percent. 150 ×.

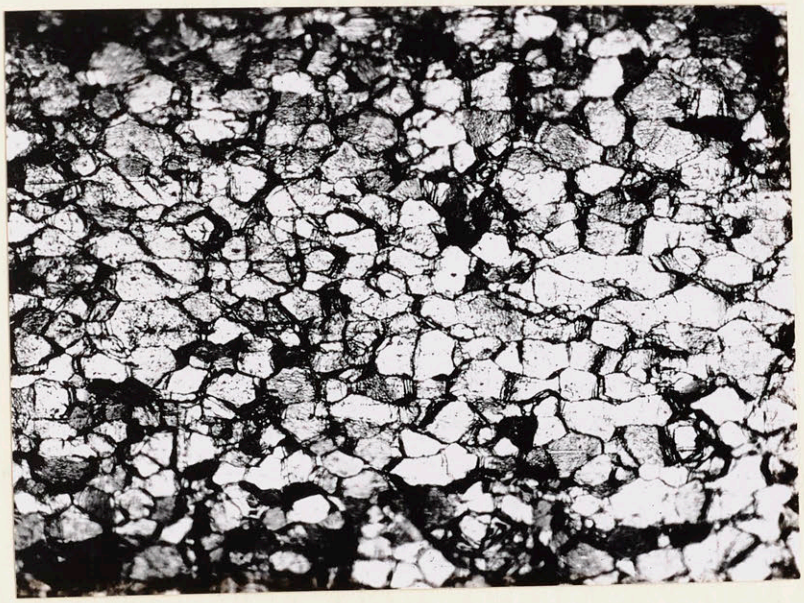

Figure 74. Specimen No. 221 (Point No. 4 of Figure 70). 2S aluminum. 900° F, 41.5 hours rupture time. R.A. = 31 percent. 150 ×.

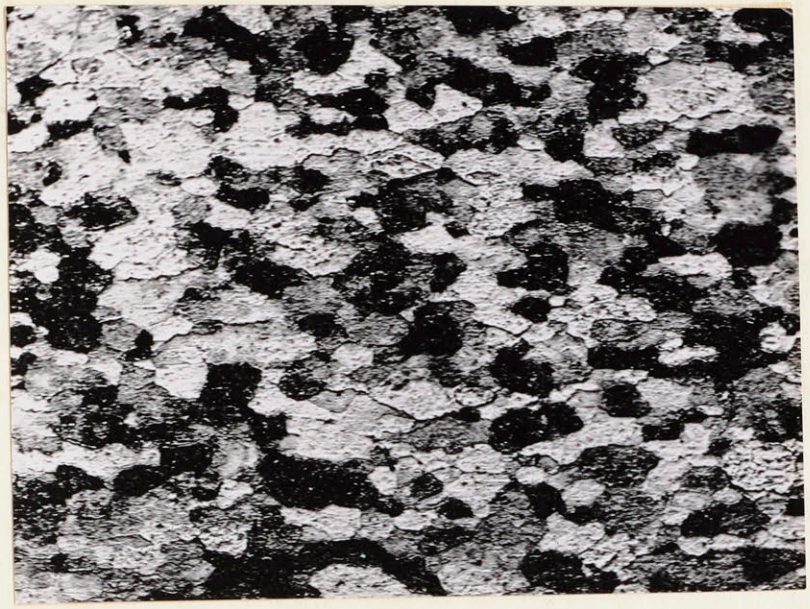

Figure 75. Longitudinal section of specimen No. 204 (point No. 1 of Figure 70) 2S aluminum. 500° F, 0.11 hour rupture time. R.A. = 25 percent. Electrolytic polish and etch. 150 × (oblique illumination)

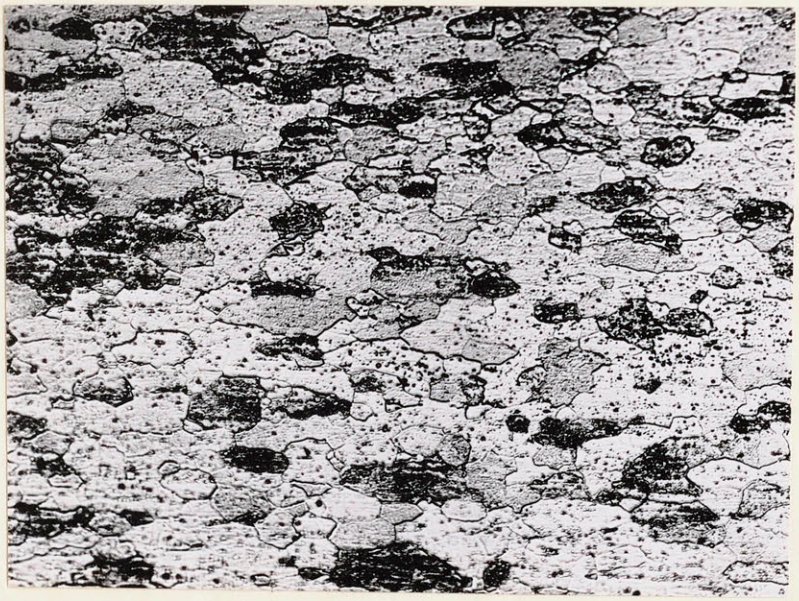

Figure 76. Longitudinal section of specimen No. 216 (Point No. 5 of Figure 70) 2S aluminum. 700° F, 0.09 hour rupture time. Near neck. Electrolytic polish and etch. 150 × (oblique illumination)

Figure 77. Longitudinal section of specimen No. 224 (Point No. 6 of Figure 70) 2S aluminum. 1100° F, 0.78 hour rupture time. Near neck. Electrolytic polish and etch. 50 ×.

Figure 78. Longitudinal section of specimen No. 207 (Point No. 7 of Figure 70). 2S aluminum. 900° F, 18.4 hour rupture time. Near fracture. Electrolytic polish and etch. 150 ×.

6.113 3S Aluminum

The curves "Log. Stress versus Log. Minimum Creep Rate" has been replotted in Figure 70 for 3S aluminum.

The micrographs of three deformed samples are presented in Figure 80 to Figure 82. The progressive increase of grain boundary flow is very marked. The slip spacing increases as the stress decreases: no slip bands are visible in Figure 82, which corresponds to "High Temperature" conditions.

The appearance of the 3S aluminum samples is quite similar to the appearance of the 2S aluminum samples. An estimation of the slip spacing does not lead to any satisfactory results, since the maximum reduction in area of the 3S aluminum samples at elevated temperatures is only 5 to 6 percent; therefore, a direct comparison to the behavior of 2S or high purity aluminum is not possible.

There is very little evidence of grain boundary migration in 3S aluminum. There is considerable oxidation, which makes the interpretation of the micrographs rather difficult.

The examination of longitudinal sections showed that at "Low Temperature" the grains deform and no grain boundary cracking occurs (Figure 83). Recrystallization was observed only near the fracture point in a few samples (Figure 84): in these cases, recrystallization may have occurred after the end of the test.

Under "High Temperature" conditions, intercrystalline cracking is visible and the failure occurs along the grain boundaries, as shown by Figure 85.

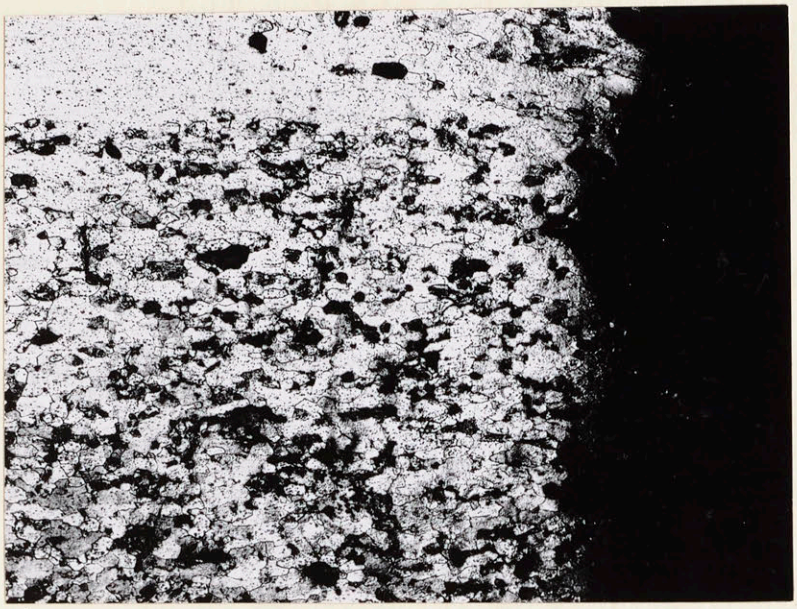

Figure 79. Longitudinal section of specimen No. 225 (Point No. 8 of Figure 70). 2S Aluminum. 1100° F, 0.93 hour rupture time. Near fracture. Electrolytic polish and etch.

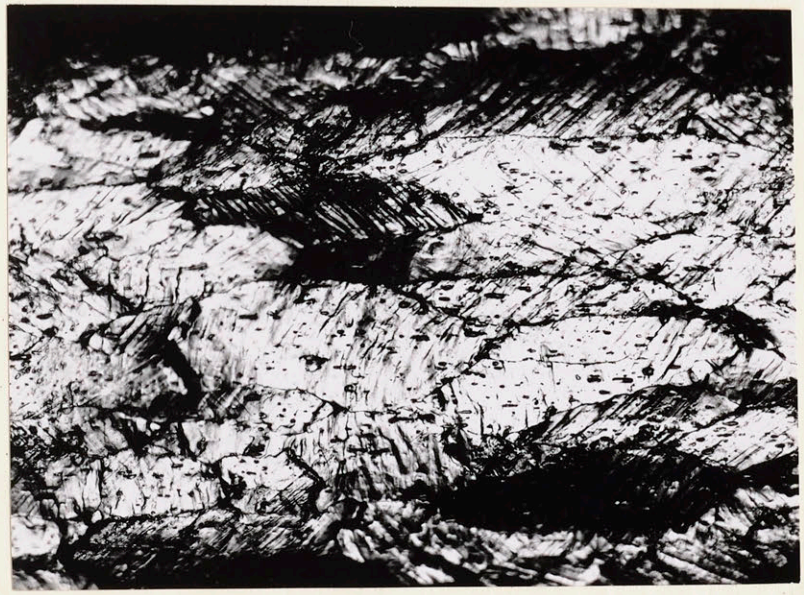

Figure 80. Specimen No. 301 (Point No. 10 of Figure 70). 3S aluminum. 900° F, 0.01 hour rupture time. R.A. = 23 percent. 150 x.

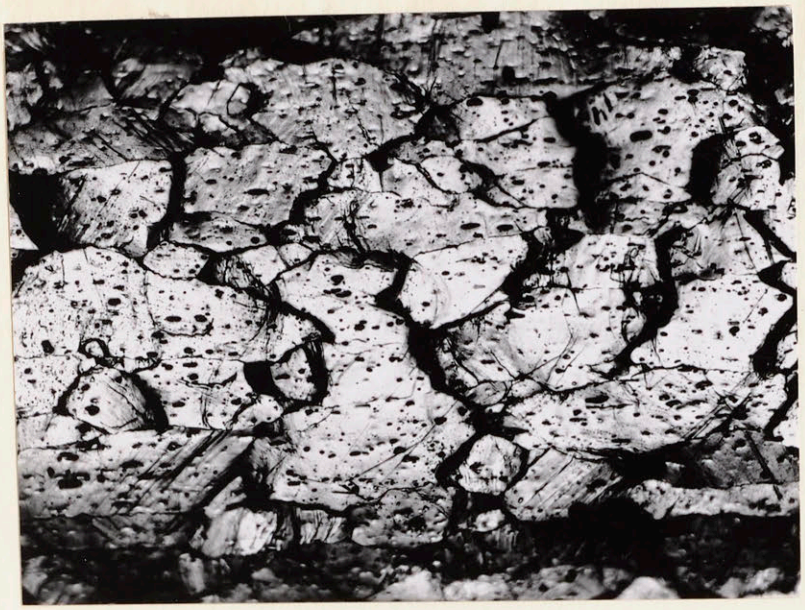

Figure 81. Specimen No. 307 (Point No. 11 of Figure 70). 3S aluminum. 900° F, 0.93 hour rupture time. R.A. = 6 percent. 150 ×.

Figure 82. Specimen No. 305 (Point No. 12 of Figure 70). 3S aluminum. 900° F, 58 hours rupture time. R.A. = 5 percent. 150 ×.

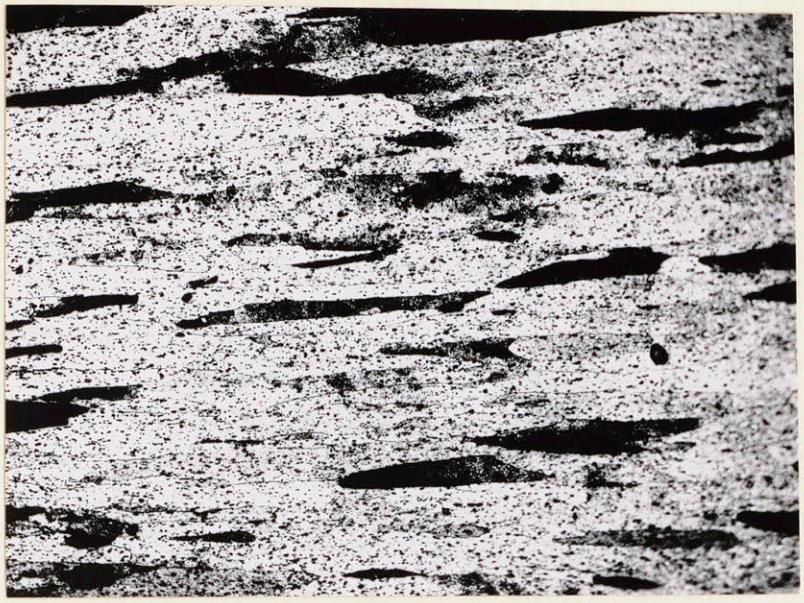

Figure 83. Longitudinal section of specimen No. 301 (Point No. 10 of Figure 70). 3S aluminum. 900° F, 0.01 hour rupture time. R.A. = 23 percent. Electrolytic polish and etch. 50 ×.

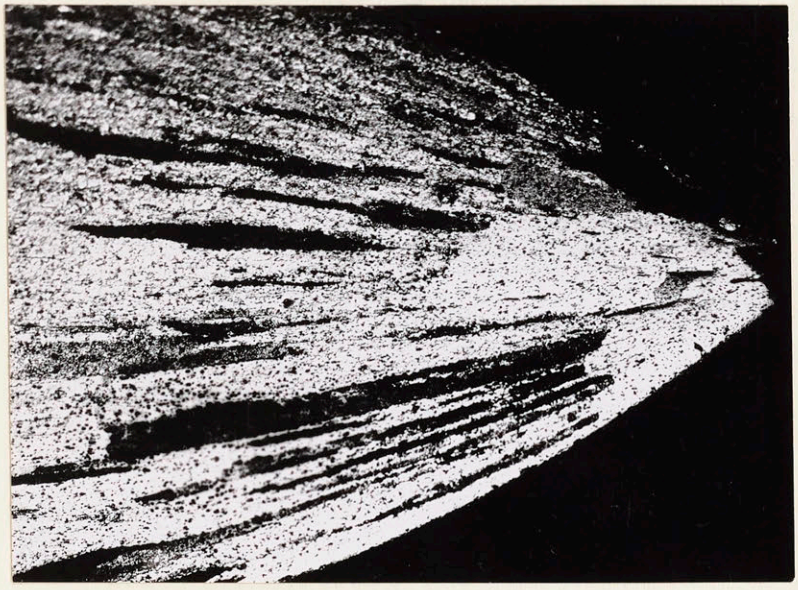

Figure 84. Longitudianl section of specimen No. 301 (Point No. 10 of Figure 70). 3S aluminum. 900° F, 0.01 hour rupture time. Fracture point. Electrolytic polish and etch. 50 ×.

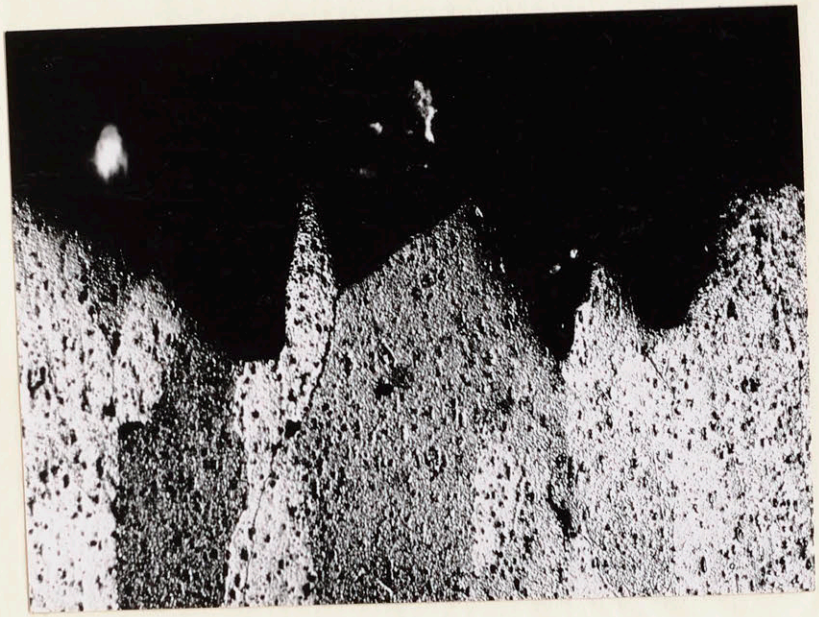

Figure 85. Longitudinal section of specimen No. 306 (Point No. 13 of Figure 70). 3S aluminum. 900° F, 11.3 hours rupture time. Fracture. Electrolytic polish and etch.

7. DISCUSSION OF THE RESULTS AND CONCLUSIONS

(a) The results of the present investigation confirm the existence of a transition from "low temperature" to "high temperature" behavior of metals. The transition occurs at higher temperature, the faster the strain rate.

Metallographic observations demonstrate that the transition corresponds to the beginning of grain boundary flow and therefore it has the same meaning as Jeffries' "equi-cohesion".

(b) The transition coincides with the change in slope of the straight lines which are obtained when the logarithm of the stress is plotted versus the logarithm of the minimum creep rate.

(c) When the test conditions change from "low temperature" to "high temperature" the type of fracture of impure aluminum (2S and 3S) changes from ductile to brittle and the ductility at the beginning of the third stage of creep decreases markedly. On the other hand, high purity aluminum shows no change in ductility or in type of failure.

(d) The effect of impurities on creep and rupture properties of metals and especially on the transition from "low temperature" to "high temperature" behavior can be interpreted by modifying the theory of equi-cohesion as follows: it is assumed that two intersecting lines are obtained when the hypothetical strength of the grain and of the grain boundaries are plotted versus the temperature (Figure 86). The difference in slope between the two lines is greater for an impure material (Figure 86 -B) than for a high purity material (Figure 86 -A).

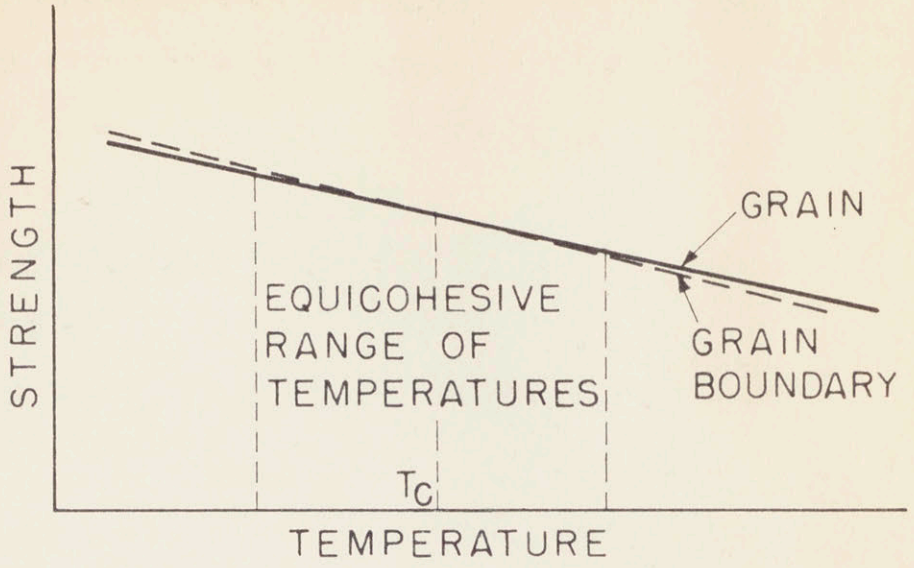

(A) HIGH PURITY METAL

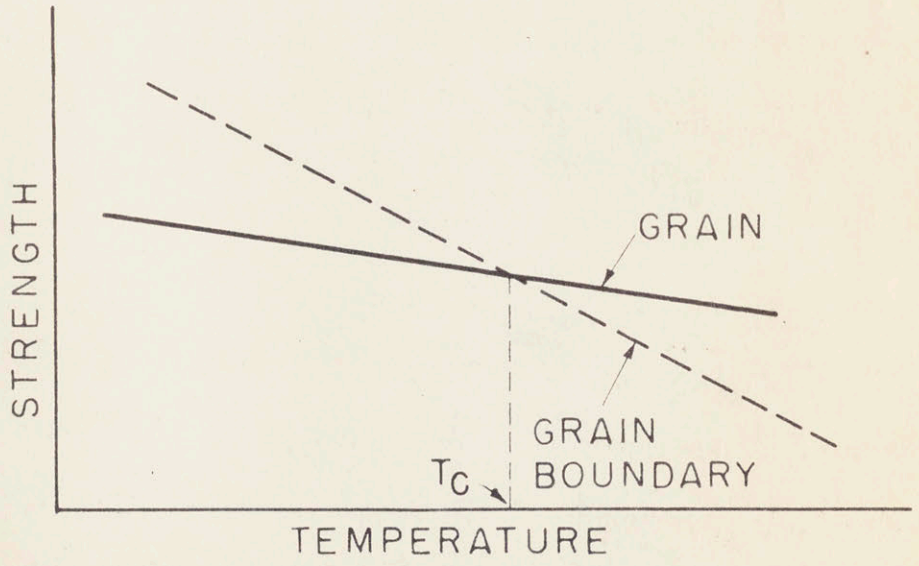

(B) IMPURE METAL

Figure 86. Strength of the grain and strength of the grain boundary as a function of temperature. High purity and impure metals.

Although in each case equal strength of grain and grain boundaries occurs at some critical temperature T_c, the high purity material has a wide range of temperatures within which the strength of the grain and the strength of the grain boundaries are not markedly different (equi-cohesive range of temperature).

If a specimen is tested below the critical temperature T_c grain boundary flow does not control the creep and rupture process. If a specimen is tested above the critical temperature T_c the grain boundaries flow, the grains are more free to deform and therefore the creep resistance of the material is lowered. The decrease in creep resistance of the grains and the contribution of the grain boundary flow to the elongation of the specimen explain the "breaks" observed in the log-log plot of stress versus minimum creep rate. This is true for both impure and high purity materials. Grain boundary flow cannot occur in a polycrystalline material unless either the grains deform or the grain boundaries crack. In the case of high purity aluminum grain boundary flow creates strains in the neighboring grains. This is to be expected since the difference in strength of grains and grain boundaries is very small (see Figure 86-A). Moreover local recovery and grain boundary migration are likely to occur since the impurity content is low. In such a way the material can undergo a large amount of deformation without formation of cracks along the grain boundaries. An impure material behaves in a different way. Possibly, even in this case grain boundary flow determines strains in the grains. Since there is a marked difference between the strength of the grains and of the grain boundaries (see Figure 86-B), and since the impurities hinder local recovery and grain boundary migration, cracks open along the grain boundaries.

Cracking at the grain boundaries gives origin to stress intensification, which starts the third stage of creep. This is the reason for a marked decrease in ductility at the transition from "low temperature" to "high temperature" behavior for impure aluminum. As the deformation proceeds, more and more cracks open along the grain boundaries until the specimen fails in a brittle manner. A comparison of the results obtained for 2S and 3S aluminum indicates that the change in creep and rupture behavior at the transition is sharper the larger the amount of impurities. This fact is in agreement with the hypothesis presented in Figure 86.

(e) The presence or absence of slip bands on the surface of the deformed specimens is not related to the transition from "low temperature" to "high temperature" behavior. There is indication that the change from slip to "slipless" flow is a function of the applied stress and of the grain size. The metallographic observations reveal that slip bands are present even at "high temperature" if the grains are large enough.

(f) "Sub-grain" formation was observed metallographically in a few cases; it appears that the sub-grains are closely related to the slip systems. Therefore, the sub-grains seem to be the effect and not the cause of plastic deformation at elevated temperature. It is true, that, as the temperature is increased, the deformation is less and less localized, the slip bands become wider, and assume a wavy appearance. However, the slip bands always retain a certain regularity, if the grain size is large enough.

(g) The experimental results did not help to interpret the mechanism of creep as operative on an atomic scale. A negative conclusion was reached, which consists of disproving the applicability of the Eyring theory of activated complex to the creep process. This theory is applicable at least as a first approximation only within a narrow range of creep rates.

(h) The experimental data are insufficient for a complete analysis of the temperature dependence of the creep rates. The analysis has been limited to a part of the data obtained for high purity aluminum. The analysis indicates that the temperature coefficient of creep rates, which may be regarded as an "activation energy", is a function of the applied stress. The uncertainty of the experimental data has a large effect on the computation of the activation energies for creep. This fact has been verified by making computations which were based on other published data as well as on data obtained during the present investigation. The calculations lead to the conclusion that the activation energies for creep can be determined only as far as their order of magnitude is concerned.

(i) The rupture time data indicate that, as a first approximation, the rupture time is inversely proportional to the minimum creep rate. Hence the creep behavior of a metal can be expressed in terms of minimum creep rates as well as in terms of rupture times. Short time tests may be sufficient to indicate the value of the constant of proportionality. Therefore, the rupture time of long time tests can be roughly predicted without bringing the test to completion. Only a few data concerning 3S aluminum do not agree with the simple relationship between rupture time and minimum creep rate which was mentioned above.

(l) The study of primary creep lead to the conclusion that the transient creep of aluminum is not of the "exhaustion" type, at least for the test conditions investigated. On the other hand, the data fit the

Andrade equation fairly well. The data support Andrade's theory, according to which the creep strain is due to the contribution of a transient ("beta") flow and of a steady state ("kappa") flow. A simple graphical method was used to determine the "beta" coefficient of primary creep. The computations were only approximate, but sufficient to indicate that the stress dependence of the "beta coefficient" at constant temperature is similar to the stress dependence of the minimum creep rate at constant temperatue.

8. SUGGESTIONS FOR FURTHER WORK

There are a great number of critical experiments which can be performed to confirm and expand the conclusions of the present research. A few suggestions are reported below:

(a) Creep and rupture testing with different grades of aluminum between 99.995 and 99.3 percent. Study of the effect of amount and type of impurities on the "transition" points, type of failure, and ductility.

(b) Direct observation of grain boundary migration during testing using a high temperature microscope.

(c) Systematic study of "slipless" flow, by observing the appearance of a mixed grain size sample. The study should be done in relation to the effect of total strain at constant stress.

(d) Determination of "beta" coefficients of primary creep from very accurate data. Study of the stress dependence of the "beta" coefficient.

(e) Study of sub-grain formation by X-ray diffraction and metallography.

9. ABSTRACT

Creep and stress rupture testing of high purity, 2S and 3S aluminum was done at constant stress from 200° F to 1100° F.

A transition in the creep and rupture behavior was established for the three materials at proper conditions of temperature and strain rate. This transition corresponds to the conditions at which the grain boundary start flowing under stress.

At temperatures higher, or strain rates slower than the transition conditions 2S and 3S aluminum fail by brittle failure. High purity aluminum shows a ductile failure under any testing conditions.

Grain boundary migration occurs in high purity aluminum during creep testing at high temperature.

The log-log method of plotting creep rate and rupture time data as a function of the applied stress has been found to be most suitable to express the creep and rupture behavior of the materials tested. A linear relationship was observed, but a change in slope was noticed at the transition points.

The mechanical testing has been supplemented by metallographic observations, which revealed facts concerning the mode of deformation and failure of aluminum under different testing conditions.

BIOGRAPHICAL NOTE

The writer, Italo Servi, was born in Gallarate, Italy, on October 3, 1922. He attended grade and junior high school in that city (1928 to 1938) and senior high school in Milan, Italy (1938 to 1941). He then matriculated at the University of Milan, Department of Industrial Chemistry, and after a five year course of study he received the degree of Dottore in Chimica Industriale in October 1946.

He enrolled at the Massachusetts Institute of Technology in 1947 and received a S.M. degree in Metallurgy in 1949. In February, 1948, he was appointed Research Assistant in the Department of Metallurgy, at the Massachusetts Institute of Technology.

The writer is a student member of the American Institute of Mining and Metallurgical Engineers, and a member of the American Society for Metals and of the Society of the Sigma Xi.

9. BIBLIOGRAPHY

1. R. H. Thurston: "Note relating to a peculiarity distinguishing annealed from unannealed iron" Science, 1st series, 1, (1883), page 418.

2. H. M. Howe: "The Patience of Copper and Silver as Affected by Annealing" Trans. A.I.M.E. 13 (1885), page 646.

3. F. T. Trouton and A. O. Rankine: "On the Stretching and Torsion of Lead Wires Beyond the Elastic Limit" Philos. Magazine, VI, 8, (1904), page 538.

4. P. Phillips: "The Slow Stretch in Indiarubber, Glass and Metal Wire when Subjected to a Constant Pull". Philos. Magazine, VI, 9, (1905) page 513.

5. E. N. daC. Andrade: "Plastic Flow at Constant Stress" Proc. Royal Society of London A-84, (1910) page 1, ibid. A-90 (1914) page 329.

6. P. G. McVetty: "The Interpretation of Creep Tests" Proc. A.S.T.M., Part II, 34, (1934), page 105.

7. S. Dushman, L.W. Dunbar and H. Huthsteiner: "Creep of Metals". Journ. Applied Physics 15 (1944), page 108.

8. O. D. Sherby: "The Effect of Grain Size on the Creep Properties of 2S-O aluminum." Univ. of California, Berkeley, Dept. of Engin., M. S. Thesis, 1949.

9. J. E. Dorn and T. E. Tietz: "Creep and Stress Rupture Investigations on Some Aluminum Alloy Sheet Metals". Trans. A.S.T.M., Part II, 49, (1949), page 815.

10. D. Hanson and M. A. Wheeler: "The Deformation of Metals under Prolonged Loading. I: Flow and Fracture of Aluminum". Journ. Inst. of Metals 45 (1931) page 229.

11. G. R. Wilms and W. A. Wood: "Mechanism of Creep in Metals" Journ. Inst. of Metals 75, (1949) page 693.

12. W. A. Wood and W. D. Rachinger: "The Mechanism of Deformation in Metals with Special Reference to Creep". Journ. Inst. of Metals 76 (1949) page 237.

13. W. A. Wood and R. F. Scrutton: "Mechanism of Primary Creep in Metals". Journ. Inst. of Metals 77 (1950) page 423.

14. T. S. Ke: "Experimental Evidence of the Viscous Behavior of Grain Boundaries in Metals". Physical Review 71 (1947) page 533.

15. R. D. Heidenreich and W. Shockley: "Study of Slip in Aluminum Crystals by Electron Microscope and Electron Diffraction Methods". Report of a conference on strength of solid, Bristol, 1948, page 57.

16. A. F. Brown: "Elementary Slip Process in Aluminum as Shown by the Electron Microscope". Metall. applications of the Electron microscope, Institute of Metals, London, 1950, page 103.

17. Z. Jeffries: "Effect of Temperature, Deformation and Grain size on the Mechanical Properties of Metals". Trans. A.I.M.E. 60 (1919), page 474.

18. C. L. Clark and A. E. White: "Influence of Recrystallization Temperature and Grain Size on the Creep Characteristics of Non-ferrous Alloys". Proc. A.S.T.M., Part II, 32 (1932) page 492.

19. K. V. Hanffstengel and H. Hanemann: "Der Kriechvorgang in Belasten Blei. Ein Beitrag zur Erforschung der Kriechvorgänge in Metallen". Zeit. Metallkunde 30 (1938), page 41.

20. D. Hanson: "The Creep of Metals". Trans. A.I.M.E. 133 (1939) page 15.

21. E. R. Parker and C. F. Riisness: "Effect of Grain Size and Bar Diameter on Creep Rate of Copper at 200° C". Trans. A.I.M.E. 156 (1944) page 117.

22. W. Siegfried: "Failure from Creep as Influenced by the State of Stress" Journ. of Applied Mechanics 10 (1943) page A-202.

23. A. H. Sully: "Metallic Creep" London, 1949.

24. J. McKeown: "Creep of Lead and Lead Alloys. Part I: Creep of Virgin Lead". Journ. Institute of Metals 60 (1937) page 201.

25. C. Crussard: "Influence du grain d'un métal sur la vitesse de fluage". Académie de France, Comptes Rendues 219 (1944) page 681.

26. N. J. Grant and A. G. Bucklin: "On the Extrapolation of Short-time Stress-rupture Data" Trans. A.S.M. 42 (1950) page 720.

27. R. P. Carreker and J. H. Hollomon: "Analysis of the Creep of Nickel" General Electric Company, Report RL-433. September 1950.

28. N. F. Mott and F. R. N. Nabarro: "Dislocation Theory and Transient Creep". Report of a conference on strength of solid, Bristol, 1948. page 1.

29. P. Ludwick: "Elements der technologische Mechanik" Berlin, 1908.

30. R. Bailey: "The Utilization of Creep-test Data in Engineering Design" Proc. Inst. Mechanical Engineers, 131, (1935) page 131.

31. H. Eyring: "Absolute Reaction Rates Equation Applied to Viscosity, Plasticity and Diffusion". Journ. of Chemical Physics 4, (1936) page 283.

32. W. Kauzmann: "Flow of Solid Metals From the Standpoint of Chemical-Rate Theory ". Trans. A.I.M.E. 143 (1941). page 57.

33. I. S. Servi and N. J. Grant: "Creep and Stress Rupture as Rate Processes" M.I.T. Metallurgy Department. Quarterly Report, January, 1951. (unpublished).

34. A. Gervais: Private communication.

35. N. J. Mott: "Mechanical Properties of Metals" Physica 15, (1949) page 119.

36. E. A. Calnan and B. D. Bruns: "Some X-ray Observations on the Nature of Creep Deformation in Polycrystalline Aluminum". Journ. Institute of Metals 77 (1950) page 445.

37. W. L. Bragg: "A Theory of the Strength of Metals". Nature 149, (1942), page 511.

38. P. Lacombe and L. Beaujard: "Sub-boundary and Boundary Structures in High Purity Aluminum". Report of a conference on strength of solid, Bristol, 1948. Page 91.

39. R. W. Cahn: Discussion on a paper by W. G. Burgers. Report of a conference on strength of solid, Bristol, 1948. page 136.

40. C. Crussard et al. Discussion on papers by Wilms and Wood, and by Wood and Rachinger. Journ. Institute of Metals 75 (1949) page 1125.

41. C. Crussard and G. Wyon: "Modification de structure de l'aluminium au cours du fluage". Journées Métallurgiques d'Automne de la Societé Francaise de Métallurgie. Paris 1950.

42. K. Yamaguchi: "The Slip-bands Produced when Crystals of Aluminum are Stretched". Sci. Papers of the Inst. of Phys. and Chem. Research Tokyo 8 (1928), page 289.

43. E. Orowan: "Origin and Spacing of Slip Bands" Nature 147 (1941) page 452.

44. R. King, R. W. Cahn and B. Chalmers: "Mechanical Behavior of Crystal Boundaries". Nature 161 (1948), page 682.

45. P. R. Sperry: "Grain Boundary Migration in Aluminum". Trans. A.I.M.E. 188 (1950) page 103.

46. P. A. Beck and P. R. Sperry: "Strain Induced Grain Boundary Migration in High Purity Aluminum". Journ. Applied Physics 21 (1950) page 150.

47. P. A. Beck and P. R. Sperry: "Two Types of Grain Boundary Migration in High Purity Aluminum". Journal of Metals 188 (1950) page 468 A.

48. G. B. Greenough and E. M. Smith: "The Mechanism of Creep as Revealed by X-ray Methods". Journ. Institute of Metals 77 (1950) page 435.

49. N. J. Mott: "Theories of the Mechanical Properties of Metals". Research 2 (1949) page 162.

50. E. N. daC. Andrade: "A New Device for Maintaining Constant Stress in a Rod Undergoing Plastic Extension". Proc. of the Physical Society, London, 60, (1948) page 304.

51. J. C. Fisher and R. P. Carreker: " A Simple Constant Stress Creep Test" Journal of Metals 1 (1949) page 178.

52. E. N. daC. Andrade and B. Chalmers: "The Resistivity of Polycrystalline Wires in Relation to Plastic Deformation, and the Mechanism of Plastic Flow". Proc. Royal Society, London, A-138, (1932) page 348.

53. C. E. Pearson: "The Viscous Properties of Extruded Eutectic Alloys of Lead-Tin and Bismuth-Tin". Journal Institute of Metals 54, (1934) page 111.

54. H. T. Tapsell and H. V. Pollard and W. A. Wood: " A Combined Creep Machine and X-ray Spectrometer". Journal of Scientific Instruments 25 (1948) page 198.

55. A. G. Ward and R. R. Marriott: "A Constant Stress Apparatus for the Study of the Creep Properties of Plastics". Journal of Scientific Instruments 25 (1948) page 147.

56. L.M.T. Hopkin: " A Simple Constant-Stress Apparatus for Creep Testing". Proc. Physical Society, London, 63-B (1950) page 346.

57. P. Jacquet: "Le polissage electrolytique des surfaces métalliques et ses applications". Paris, 1948.

58. I. S. Servi: "Galvanic Macro-etch for High Purity Aluminum". Metal Progress 58 (1950) page 732.

59. P. Lacombe and L. Beaujard: "The Applications of Etch Figures on Pure Aluminum to the Study of Some Metallographic Problems". Journ. Inst. of Metals 74 (1947) page 1.

60. C. Crussard: "Étude des glissements plastiques dans les cristaux d'aluminium". Revue de Métallurgie 42 (1945) pages 286 and 321.

APPENDIX I

APPENDIX I

Constant Stress Creep Testing

Constant stress creep testing up to rupture is not possible, since the deformation of the specimen is not uniform during the last part of the test. In fact, either a neck is formed (ductile specimen) or cracks open inside or at the surface of the sample (brittle specimen). In both cases there is a stress intensification, which is not the same in different parts of the specimens. Therefore, constant stress creep testing must be restricted to the condition of uniform deformation.

When the deformation is essentially uniform the stress can be kept constant if the load is decreased proportionally to the reduction of area of the specimen. Assuming that the volume is constant, since the change in density during deformation is negligible, the condition for constant stress is

$$w\,l = w_o\,l_o \qquad (I.1)$$

where w is the load applied when the length of the specimen is l;

w_o is the initial load and

l_o is the initial length of the specimen.

The conditions of equation (I.1) can be obtained experimentally in different ways. Andrade[5] used a load which sinks in water as the specimen elongates. Andrade[50] and Fisher and Carreker[51] used an apparatus based on the change of the resolved force acting on two arms when the angle between the two arms is changed. Andrade and Chalmers[52], Pearson[53], Tapsell, Pollard and Wood[54], Ward and Marriott[55] and Hopkin[56] designed different kinds of constant stress apparatus which were based on the change in a lever ratio as the specimen elongates.

The last method has been used in the present research. A cam of special design has been fastened to a pulley (Figure I.1). A steel cable has been attached to the pulley; another cable has been attached to the cam. The system was mounted on ball bearings and was able to rotate freely. The cable which was connected to the pulley was attached to the loading beam of the creep testing machine. The other cable was attached to the dead load. At the beginning of the test the system was in the position shown by Figure I.1. The two cables were aligned; therefore the full load was applied to the loading beam. As the specimen elongated, the system turned clockwise. The cable attached to the loading beam did not change position, while the point of application of the load moved toward the center of the pulley, as the system turned; therefore, the load applied to the loading beam decreased.

A quarter of a turn of the pulley corresponded to a decrease in applied load of 50 percent; and to an elongation of the specimen of 100 percent. The cam was designed graphically, according to the equation:

$$r = Ro \frac{\varrho}{\varrho_o + \varrho} \qquad (I.2)$$

where r = point of application of the dead load

ϱ = corresponding angle of rotation of the system

Ro = radius of the pulley

ϱ_o = angle of rotation of the system, which corresponds to 100 percent elongation of the specimen.

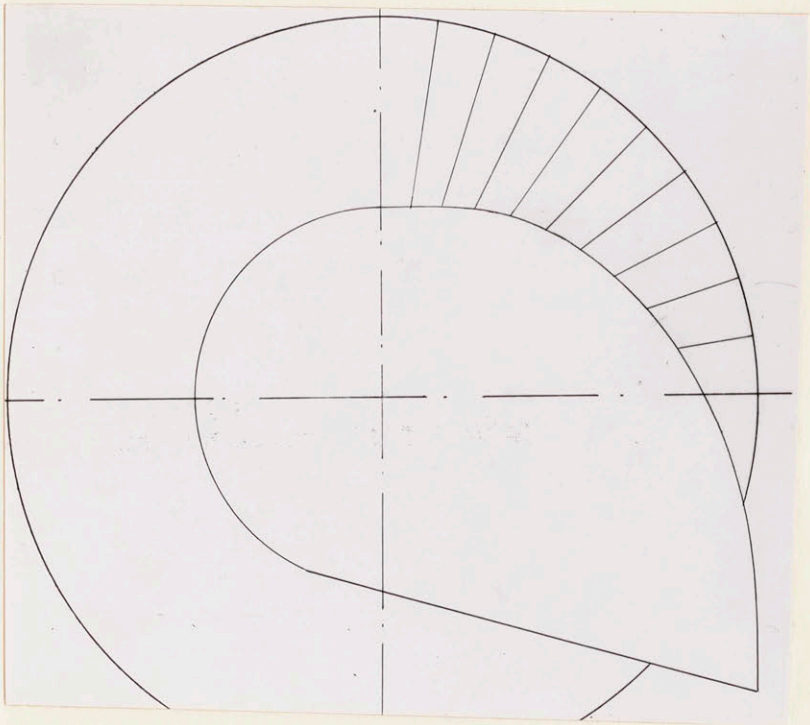

Figure I.1. Constant Stress Apparatus
To scale.

APPENDIX II

APPENDIX II

Calibration of Thermocouples - Testing for Temperature Gradient and Temperature Control

A chromel-alumel thermocouple was used as an arbitrary "standard". All the controlling thermocouples used for creep testing have been calibrated versus the "standard". For this purpose the hot junctions were placed in holes which have been drilled in a block of copper. This block of copper was kept at constant temperature by a photocell-type controller. After a few hours the electromotive forces of the thermocouples were read; a difference in temperature up to 3° F was found between each couple and the "standard".

Since this difference is too large to be neglected, a calibration of the controlling thermocouples was made before each series of tests; at the same time the temperature gradient was measured. The following technique was used: the "standard" and a thermocouple A were placed on the middle and lower parts of the specimen, respectively. The thermocouple A was connected to the temperature controller: the controller dial was set in order to read the wanted temperature on the "standard" thermocouple. The temperature gradient was reduced to a minimum by adjusting the voltage and the variable resistors of the electrical circuit.

This operation was repeated before each series of creep tests. The thermocouple A was used as the controlling thermocouple for creep testing at the temperature at which it has been calibrated.

APPENDIX III

APPENDIX III

Metallography of Aluminum

The metallographic preparation of aluminum samples is generally done by electrolytic polishing in order to avoid the deformation of the surface during polishing. Jacquet[57] presented an excellent review of the methods which have been suggested for best results.

New techniques have been developed during the course of the present investigation and shall be described in detail.

The "galvanic etching" technique[58] has been found very useful to reveal the structure of coarse grained, high purity aluminum. This technique consists of etching the sample in a solution of hydrochloric acid (10 to 20 percent). The sample is coupled to a more noble metal such as copper or stainless steel. Hydrochloric acid attacks aluminum along the (100) planes: after a short time several large and irregular etch pits are observed on the sample. After a long time the whole surface has been attacked, and a sharp macro-etching effect is obtained. The contrast is very high, as shown by Figure III.1. Careful preparation of the sample before etching is recommendable, but not necessary.

The "galvanic" attack is much faster than the chemical attack; this fact helps in the etching of high purity aluminum, which is attacked very slowly by hydrochloric acid.

The "galvanic" etching technique has been used as a microetch to reveal the position of the grain boundaries. Best results are obtained if the observation is done under polarized light; in fact, the unetched sample is optically inactive and does not reflect the light, whereas the

etched portion of the sample is optically active. The amount of reflected light depends on the orientation of the grain. Therefore a great contrast is obtained at the grain boundaries.

Figure III-2 shows a partially etched sample: the black background is the unetched part of the specimen, which was polished electrolytically before "galvanic" etching.

Similar results are obtained by observation in polarized light through a sensitive tint plate: in this case the unetched part has a magenta color; while the etched part has different colors from light green to dark brown. Color photographs of good color contrast have been taken. This technique has the advantage of permitting the observation of the unetched background. If a creep specimen is partially etched after deformation, the appearance of the surface of the specimen is not totally destroyed by the etching. The final structure can be determined by observing the color of the etched portions of the specimen, and can be compared to the appearance of the unetched surface. This technique gave excellent results for the determination of the direction of grain boundary migration under stress.

Electrolytic polishing has been done successfully by using the Jacquet[57] solution which consists of

1/3 perchloric acid

2/3 acetic anhydride.

Another solution gave good results for high purity aluminum. This solution consists of

5 ml. of perchloric acid (72percent) and

95 ml. of glacial acetic acid.

When this modified solution is used, the distance between cathod and anode should be kept constant: hence a cylindrical cathode is necessary to polish tensile specimens.

If the applied voltage is below 20 volts, a macro-etching effect occurs. Between 25 and 60 volts the specimen is polished. At higher voltage the polishing effect is spoiled by the formation of a film on the surface of the specimen. The polishing time, after preparation on 3/0 metallographic paper, is about two minutes.

The modified solution mentioned above is suitable for a rapid examination of the structure of coarse grained samples: this was done by polishing the sample at 25 volts and lowering the voltage to 10 volts for a few seconds. In these conditions the specimen is macro-etched. The macro-etched can be removed in less than thirty seconds by increasing the voltage to 25 volts.

The current is mainly a function of the resistance of the polishing solution: hence the current changes as the temperature changes. The temperature should be controlled between 20° C and 30° C; and should be kept as uniform as possible by continuous stirring.

The modified Jacquet solution does not give very good results for 2S and 3S aluminum; a fair polish can be obtained in two minutes if more than 100 volts is applied.

2S and 3S specimen have been polished in the Jacquet solution at 20° C to 30° C with an applied of 45 volts. Continuous stirring is necessary to keep the current to a minimum value. Five to ten minutes are sufficient for a good metallographic polish. Micro-etching is done by

lowering the voltage to 2 to 5 volts for five to ten minutes. The specimen should not be removed from the bath during the etching operation: if deeper etching is wanted, the specimen should be re-polished for a few minutes.

Micro-etching of high purity aluminum was not necessary, since the modified polishing solution attacks the grain boundaries. For higher contrast a saturated solution of ammonium fluoborate at 80° C has been successfully used. The etch was done electrolytically at 15-18 volts, for thirty minutes.

Etch pits have been very useful to reveal uncertain grain boundaries: Figure III-3 shows a section of a high-purity specimen near the fracture point. A few grain boundaries appear: however, the observation of the etch pits reveals that the central "grain" is actually fragmented into several parts, which have similar orientations. In fact, the orientation of the etch pits slightly changes inside that "grain".

The etch pits of Figure III-3 were developed by using the Lacombe and Beaujard [59] solution, which consists of:

47 ml. of fuming nitric acid
50 ml. of hydrochloric acid (37.5 percent)
3 ml. of hydrofluoric acid (48 percent)

This solution should be used below 10° C for 30 seconds. A modified solution gave similar or better results. This solution consists of:

70 ml. nitric acid (70 percent)
50 ml. hydrochloric acid (37.5 percent)
3 ml. hydrofluoric acid (48 percent)

Examples of etch pits obtained with the modified solution appear in Figure III-4 and Figure III-5. The polished and etched sample of Figure III-4 has been deformed by compression: the combination of etch pits and slip lines is useful to determine the approximate orientation of each grain.

A peculiar effect was obtained by observing etch pits in polarized light: a comparison of observation in normal light and in polarized light is shown in Figure III-6 and Figure III-7.

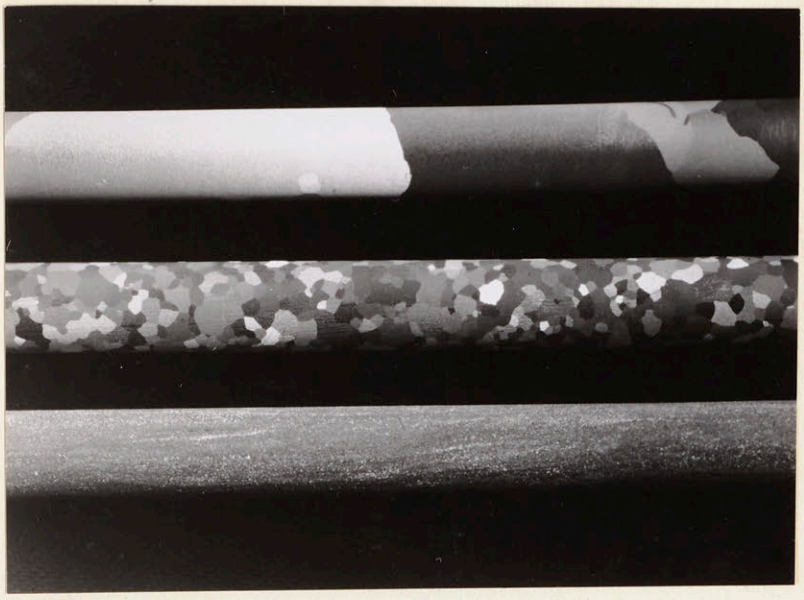

Figure III-1. Annealed 99.9 percent aluminum. "Galvanic" etch in HCl. 1.5 ×.

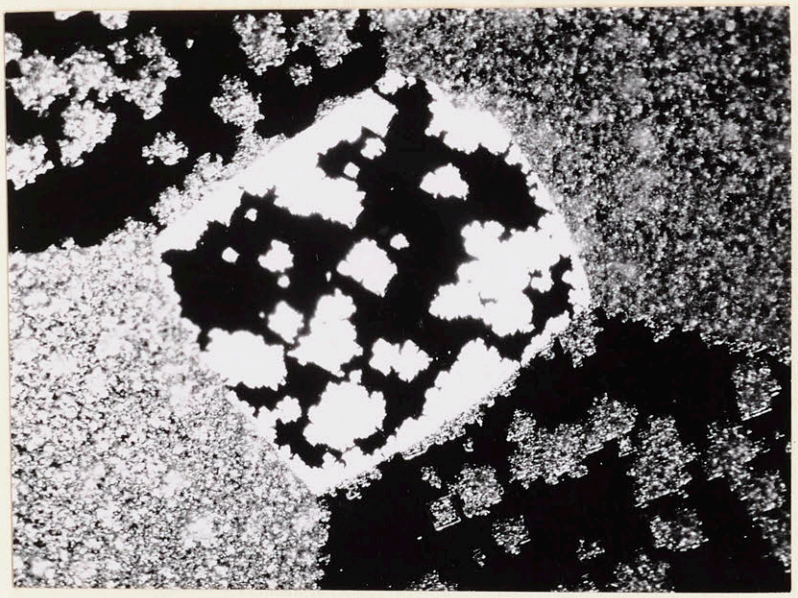

Figure III-2: High purity coarse grained aluminum specimen. Electrolytic polish, partial "galvanic" etch in HCl. 50 × (Polarized light).

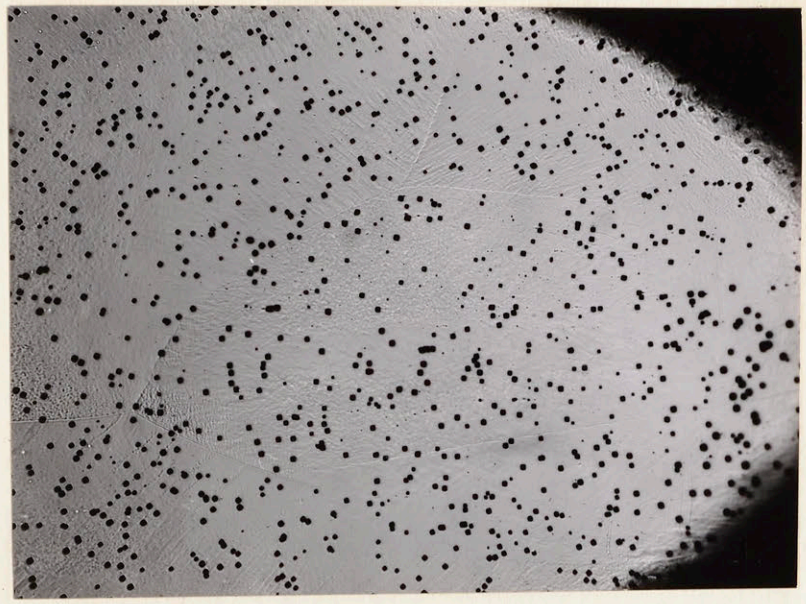

Figure III-3: High purity coarse grained specimen. Longitudinal section. Electrolytic polish. Etch pits. Developed by Lacombe reagent. 50 ×.

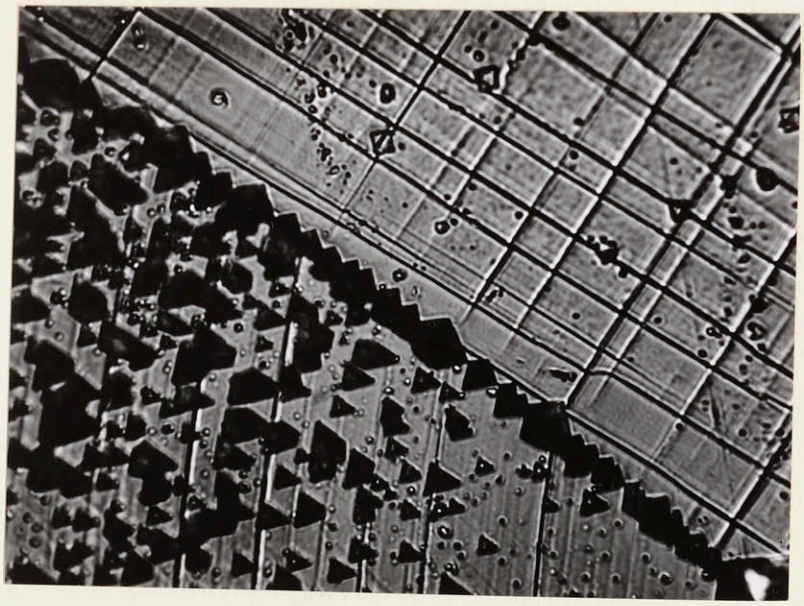

Figure III-4: High purity aluminum. Electrolytic polished. Etched in modified Lacombe reagent, deformed after etching. 1000 ×.

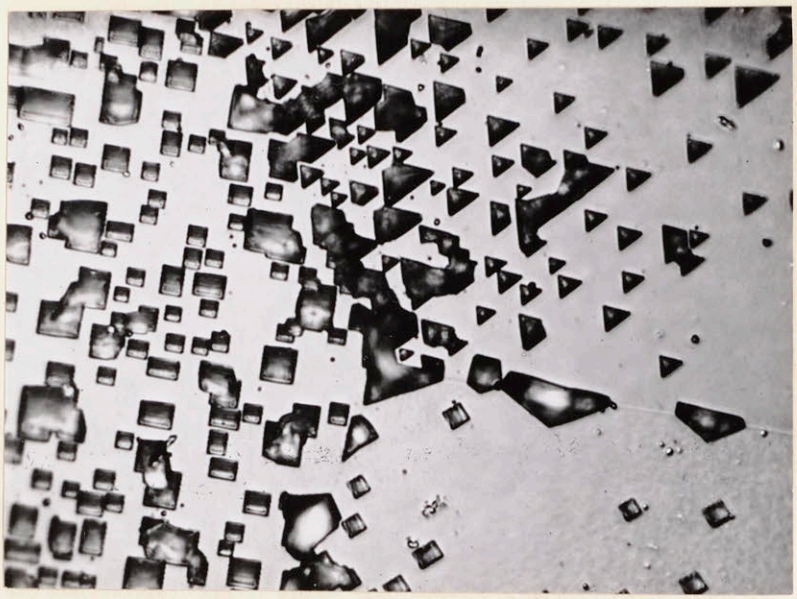

Figure III-5: High purity aluminum. Electrolytic polish. Etched in modified Lacombe reagent. 1000×.

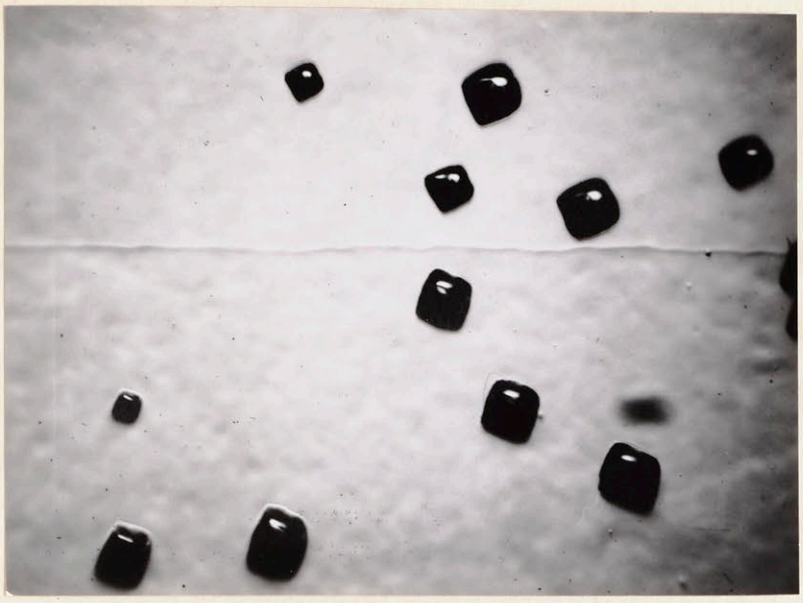

Figure III-6: High purity aluminum. Electrolytic polish. Etched in Lacombe reagent. 500 X.

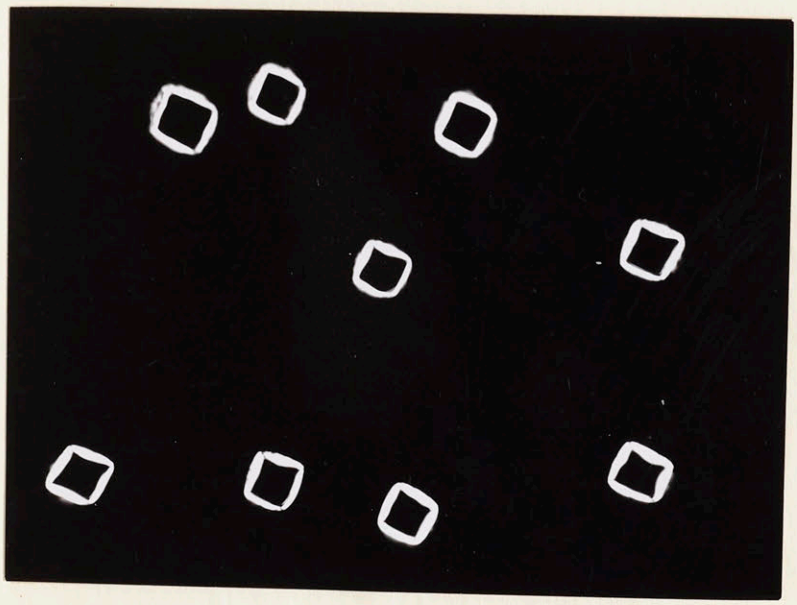

Figure III-7. High purity aluminum. Electrolytic polish. Etched in Lacombe reagent. (Polarized light) 500 X

APPENDIX IV

Tables of Experimental Data from Creep and Stress Rupture Tests

TABLE IV

Results of the Preliminary Tests for High Purity Aluminum

Test No.	Temp. ° F	Stress Psi	MCR $_{-1}$ Hr	R.T. Hr.	Total Elong. Inches	Remarks
1	700	650	~0.7	0.5	1.01	constant load
2	212	4000	~0.01	17	0.55	" "
3	1170	20-50	-	0.8	0.45	single crystal . C.L.
5	1000	50-100	-	48	0.68	very coarse, C. L.
7	700	630	0.28	1.3	0.85	constant stress
8	500	500	~0.001	450	1.00	constant load
12	700	325-650	0.785	1.3	1.08	load decreased during test
13	1000	200	-	0.33	0.97	constant load
14	1000	160	~0.9	0.5	0.81	constant load

TABLE V

Creep Test Results for High Purity Aluminum

Test No.	Temp. ° F.	Grain Size	Stress Psi	MCR Hr^{-1}	R. T. Hr	Total Elong. Inch	True Elong. Inch	Remarks
54	200	F	11,000	0.93	0.1*	-	0.38	Interrupted after 0.09 hrs.
52		F	8,050	0.02	6.25	0.46	0.31	
53		F	6,870	0.0043	39.3	0.54	0.37	
50		F	5,920	0.0009	177	0.49	0.32	
86		C	6,210	0.027				
84		C	5,890	0.038	3.4	0.52	0.35	
73		C	5,640	0.016	4.91	0.39	0.275	
72		C	5,100	0.003	29*	-	0.25	Interrupted after 27 hrs.
70		C	4,400	0.00045	324	0.52	0.41	
93	400	C	4,290	~11				
38		C	4,350	~2.1	0.075	0.54	0.51	
37		C	3,350	0.16	1.32	0.58	0.41	
35		C	3,479	0.099	1.54	0.50	0.38	
40		C	2,595	0.038	3.9	0.46	0.31	
43		C	2,210	0.013	24.64	0.60	0.475	
48		C	1,775	0.00295	102	0.60	0.39	
66		C	1,130	0.000255	850*	-	0.30	Interrupted after 736 hrs.
56	500	F	3,130	1.35	0.44	0.92	0.55	
55		F	2,415	0.394	1.57	0.94	0.45	
57		F	1,910	0.089	5.43	0.84	0.39	
58		F	1,200	0.013	28*	-		Interrupted after 24 hrs.
59		F	1,105	0.01	60*	-	0.40	Interrupted after 48 hrs.
97		F	750	0.00268	300*	-	0.30	Interrupted after 294 hrs.
87		C	3,400	~7	0.046	0.52	-	
85		C	3,000	2.25	0.08	0.48	0.30	
83		C	2,750	1.16	0.21	0.57	0.37	
28		C	2,320	0.35	0.74	0.60	0.35	

TABLE V (cont)

Test No.	Temp. °F	Grain Size	Stress Psi	MCR$_1$ Hr^{-1}	R.T. Hr	Total Elong. Inch	True Elong. Inch	Remarks
62	500	C	2,020	0.164	2.80	0.77	0.50	
32		C	1,660	0.051	8.25	0.66	0.40	
34		C	1,180	0.0089	56.25	0.81	0.48	
71		C	910	0.0031	140*	-	0.31	Interrupted after 96 hrs.
68		C	495	0.000222	550*	-	0.125	Interrupted after 500 hrs.
98	700	F	1,260	4.96	0.09	0.73	0.25	
96		F	765	0.605	0.92	0.89	0.35	
99		F	415	0.049	17.53	1.19	0.35	
89		C	1,260	7.5	0.079	0.83	0.50	
25		C	995	1.83	0.36	1.07	0.40	
21		C	920	1.12	0.47	0.75	0.40	
22		C	680	0.38	1.47	0.79	0.44	
23		C	450	0.05	13.5*	-	0.55	Interrupted after 12 hrs.
24		C	250	0.005	103.3	0.95	0.40	
45	900	C	445	4.35	0.11	0.73	0.425	
47		C	390	1.96	0.33	0.89	0.55	
41		C	355	1.53	0.24	0.54	0.30	
44		C	280	0.485	1.23	0.87	0.475	
42		C	170	0.0555	9.75	0.74	0.375	
74		C	120	0.009	67	0.54	0.20	
51	1100	F	170	1.54	0.366	0.72	0.35	
80		C	250	8.6	0.075	0.89	0.50	
76		C	170	1.54	0.317	0.70	0.30	
82		C	100	0.11	3.66	0.59	0.25	
81		C	85	0.038	10*	-	0.25	Interrupted after 8.2 hrs.

* Estimated values

TABLE VI

Creep Test Results for 2S Aluminum

Test No.	Temp. ° F	Stress Psi	MCR$_1$ Hr^{-1}	R. T. Hr	Total Elong. Inches	True Elong. Inches	Type of Fracture	Remarks
204	500	6525	2.28	0.11	0.52	0.375	Ductile	
205		6050	1.09	0.233	0.51	0.35	"	
202		5580	0.167	1.47	0.54	0.41	"	
206		5010	0.093	2.67	0.53	0.38	"	
201		4550	0.0285	10.28	0.53	0.30	"	
208		4175	0.0125	18	0.45	-	Intermediate	
203		3400	0.002	101.5	0.35	0.13	Brittle	
227		2540	~0.0001	-	-	-	"	Interrupted after 1000 hrs.
219	700	2575	5.35	0.12	1.10	0.30	Ductile	
216		2515	4.41	0.089	0.64	0.25	"	
209		2060	1.53	0.45	0.91	0.35	"	
211		1825	0.235	1.37	0.52	0.275	"	
210		1550	0.059	3.93	0.40	0.275	"	
223		1255	0.0215	20.6	0.49	-	Intermediate	
215		1095	0.0046	42.6	0.46	0.20	Ductile	
230		890	0.00065	224	0.22	0.18	Brittle	
212	900	1335	~22.5	0.02	0.64	0.32	Ductile	
231		1260	8.0	0.057	0.70	0.275	"	
217		1160	2.45	0.175	0.62	0.30	"	
218		975	0.493	0.95	0.55	0.35	"	
207		670	0.04	18.41	0.86	-	Intermediate	
221		500	0.0125	41.5	0.59	0.20	Brittle	
213		380	0.00535	81.5	0.64	0.20	"	
224	1100	800	21.2	0.0236	0.78	0.28	Ductile	
228	1100	650	4.75	0.12	0.84	0.29	"	
232		560	2.6	0.145	0.46	-	"	
225		460	0.54	0.93	0.62	0.25	Brittle	
235		320	0.12	3.66	0.60	0.20	"	
226		260	0.09	13	1.00	0.17	"	

TABLE VII

Creep Test Results for 3S Aluminum

Test No.	Temp. ° F	Stress Psi	MCR Hr^{-1}	R. T. Hr	Total Elong. Inches	True Elong. Inches	Type of Fracture	Remarks
301	900	2590	~ 30	0.01	0.54	0.30	Ductile	
303		2300	7.7	0.036	0.44	0.25	"	
304		1960	0.515	0.384	0.38	0.20	"	
307		1790	0.161	0.93	0.31	0.14	Intermediate	
302		1590	0.0285	4.1	0.22	0.055	Brittle	
306		1290	0.0039	11.3	0.11	0.015	"	
305		970	0.0007	58	0.12	0.01	"	